Arch. Comput. Meth. Engng.
Vol. **12, 4,** 391-478 (2005)

Archives of Computational Methods in Engineering
State of the art reviews

Computational Aspects of the Mechanics of Complex Materials

Paolo Maria Mariano
Università di Firenze, Firenze, Italy
paolo.mariano@dicea.unifi.it

Furio Lorenzo Stazi
Università di Roma "La Sapienza", Roma, Italy

Dedicated to Gianfranco Capriz on occasion of his eightieth birthday

Summary

Bodies with exotic properties display material substructural complexity from nano to meso-level. Various models have been built up in condensed matter physics to represent the behavior of special classes of complex bodies. In general, they fall within the setting of an abstract model building framework which is not only a unifying structure of existing models but - above all - a *tool* to construct special models of new exotic materials. We describe here basic elements of this framework, the one of *multifield theories*, trying to furnish a clear idea of the subtle theoretical and computational problems arising within it. We present the matter in a form that allows one to construct appropriate algorithms in special cases of physical interest. We discuss also issues related to the construction of compatible and mixed finite elements in linearized setting, the extension of extended finite element methods to analyze the influence of material substructures on crack growth, the evolution of sharp discontinuity surfaces in complex bodies. Concrete examples of complex bodies are also presented with a number of details.

1 INTRODUCTION

Technological demands of devices with sophisticated performances require, to be satisfied, the use of materials with exotic properties. We call *complex* such materials when their substructure from nano to meso-level influences drastically their gross behavior in a way in which interactions due to substructural changes are prominent and cannot be smeared out as in common homogenization procedures. Liquid crystals in nematic, smectic or cholesteric phase, quasicrystals, ferroelectrics, elastomers, fullerene-based composites even microcracked bodies and materials with strain gradient effects are prominent examples and constitute basic chapters of condensed matter physics.

Here, we review critically aspects of the mechanics of complex bodies, focusing the attention on the way in which theoretical instances need to be interpreted in constructing numerical algorithms. Some issues are emphasized as in the list below.

- There exists a general model building framework (the one of *multifield theories*) that unifies common models of complex materials and is also a theoretical tool to construct new special models for the behavior of new complex materials produced in the industrial practice. Such a framework is essentially the geometry and the mechanics associated with maps between manifolds.
- The construction of computational schemes for multifield models of condensed matter implies non-trivial aspects of interpolation over manifolds. Moreover, the treatment of boundary conditions in concrete cases is not immediate and require physical interpretations.
- Identification procedures from discrete models of prototype material elements may be a useful tool to get explicitly the values of constitutive coefficients in absence of adequate experimental data.

The number of explicit numerical simulations of the behavior of complex bodies in appropriate special cases is rather limited in the current scientific literature. From a computational

 ISSN: 1134–3060 Received: January 2005

point of view, the mechanics of complex materials appears as a rather unexplored land: the available results suggest that it deserves completely to be explored.

Our basic aim is to show how the general format of multifield theories can be arranged in a form in which well known reliable numerical techniques can be applied with appropriate modifications. In this way we try to suggest *a computational program* in the field.

1.1 The Point of View

When one analyzes the behavior of complex bodies, one faces situations that challenge in some sense the direct application of (even basic) aspects of standard continuum mechanics. The essential problem is that we are forced by physical evidences to try to describe the influence at a gross scale of minute events occurring at finer scales and altering the morphology of the body itself.

In the standard format of continuum mechanics, the one generated by Cauchy's work, a body is a collection of material elements whose morphology is identified just by their place in space: they are pictured as material points (see [146]). In this way, the geometrical description of the body skips details about the minute shape of molecular (or atomic) aggregates. However, when one looks to real bodies, one realizes that the material element is in fact not properly just a material point (an indistinct sphere, a 'monad' in Leibnitz's words), rather it is a *system* of (say) interacting molecules. To describe the morphology of this system, we introduce a *coarse grained morphological descriptor* ν. It may be an element of the unit sphere, a stretchable vector, a second-order tensor of various nature, a direction etc., depending on the physical conditions envisaged. Of course, we could develop models for each choice of the order parameter to describe different physical situations. Formally, all of them arise from the *same* general model-building framework, the one of multifield theories summarized here. Basically, we realize that to construct the formal structure of models of complex bodies we need just to require that ν be an element of an abstract manifold $\mathcal{M}$ of substructural shapes, endowed with 'minimal' geometrical properties. The choice of $\mathcal{M}$ is the first step toward the construction of each special model, thus it has a 'constitutive' nature, in a sense wider than usual.

The introduction of morphological descriptors - to represent details of the morphology of the body - allows us to account directly for interactions due to substructural events that may change, even drastically, stress distributions. In fact, interactions within a body are objects conjugated in the sense of power with the rates of its morphological descriptors. Here these rates are the standard velocity and the rate of change of ν. Standard tensions are associated with the former while micro-tensions with the latter. A new balance arises: the *local* balance of substructural interactions, the one that we call *Capriz balance*.

Really, such a balance is *not* necessarily a local (i.e. pointwise) version of a new integral balance assumed as a first principle. As we will show below, in general, an integral version of the balance of substructural interactions does not make sense unless $\mathcal{M}$ is (isometrically) embedded in a linear space so that one may freely move within it. In fact, the basic integral balance laws still remain the integral balance of forces and the one of couples. However, the latter is not standard and gives rise also to Capriz balance, but such a circumstance *does not mean* that substructural interactions are couples (or better, micro-couples): their geometrical nature is strictly determined by the nature of ν.

The isometric embedding of $\mathcal{M}$ in a linear space has a crucial role in constructing numerical schemes. In fact, the basic difficulty in managing multifield theories is that in general $\mathcal{M}$ *does not coincide with a linear space*. Then, interpolation over $\mathcal{M}$ by using the standard scheme based on the interplay between nodal values and shape functions could not make sense unless $\mathcal{M}$ is embedded in a linear space. However, although the embedding is always available when $\mathcal{M}$ has finite dimension, it is not unique and the choice of it is strict matter of physical modeling.

1.2 A Brief Historical Panorama on Multifield Theories

Since the character of this review is not historical, we do not account in detail for the wide list of contributions to special models of specific complex materials in an endless tedious way. Rather, we follow briefly here below just the historical path along which the ideas leading to the general model-building framework of multifield theories have been developed (for additional bibliography one may refer to [113], [119]).

The starting point were W. Voigt's suggestions [181], [182] that allowed in 1909 the brothers E. and F. Cosserat [42] to develop sistematically a theory of elasticity in which each material element is considered as a 'small' rigid body[1] able to rotate freely with respect to the neighboring material elements. This point of view constituted the first change of the traditional Cauchy's paradigm on the description of the morphology of deformable bodies. In 1958, J. L. Ericksen and C. A. Truesdell realized that Cosserat's ideas were a reliable framework for the construction of 'models' of elastic structures such as beams, plates, shells. Moreover, in their seminal paper [66] they developed further Cosserat's point of view by describing the 'internal' morphology of the material element by means of a *deformable* director (in Cosserat's scheme the director - or the triad - representing the material element can only rotate; thus it may be substituted by a proper orthogonal tensor, i.e. an arbitrary element of the Lie group $SO(3)$)[2].

Elements of the unit sphere with the identification of antipodes (i.e. elements of the projective plane P^2) were also used as morphological descriptors by J. L. Ericksen in 1960-1962 [60], [61], [63] to describe liquid crystals in nematic phase. Main developments of this special multifield theory can be found in [105], [50], [20], [65]. Scalar order parameters have been added later to account for layered structures characterizing liquid crystals in smectic phase [18], [58].

Along this path, in a 1964 paper, R. D. Mindlin considered the material element as a cell able to *deform* independently of the rest of the body [137] (in certain sense an abstract version of macromolecules considered previously by Ericksen just for establishing a rich kinematical description of them [62]). So that Mindlin introduced a second order symmetric tensor as morphological descriptor and developed the relevant elasticity theory in linear setting. Materials well described by Mindlin's proposal or deformable directors are called *micromorphic*. Such a scheme has been developed in higher order sense in [78] by exploiting the principle of virtual work and in complete non-local sense in [67], [68]. A review of this sub-area can be found in [69] (see also [100], [34]).

Scalar order parameters have been also used to describe solid-to-solid phase transitions in shape memory alloys [73], isotropic damage [75] and granular flows [79]. For the latter case, tensor order parameters provide a more detailed description [19], [24]. As regards damage, it has been shown that a multifield approach to the description of damaged (or, more precisely, microcracked) bodies may allow us to circumvent essential flaws of traditional internal variable models, above all in developing numerical schemes. Vector [108], [109], [124], [125] and second order tensors [128], [120], [4], [111] may allow one to get a rather careful description of the underlying physics. The difference with respect to analogous choices in internal variable models (see [102] for a thoroughly critical review) is that in multifield setting one accounts directly for true interactions of local (self-forces) and gradient (microstresses) nature –associated with the rate of the morphological descriptors– and this circumstance changes completely the stage.

The list of special multifield models could be enlarged for example by remembering

[1] The dimensions of such a rigid body become *internal lengths* in the continuum modeling.

[2] The literature about Cosserat's scheme is abundant. The reader may find theoretical results in [180],[1], [129], [153], [87], [59], [2], [3], [86], [84], [114], [99] and computational issues in [165], [168], [166], [167], [72], [164], [174], [155].

that vector order parameters have been also used to describe in a multifield setting the polarization state in ferroelectrics (see [45], [158], [46], [80], [81], [82]), micromagnetics (see [51], [77], [183], [11]), superconductivity (see [35] and also [92] for a different point of view), also the rearrangements of collective atomic modes in quasiperiodic alloys (see [118], [126], [98]).

Increasing furthermore the above sketched list with other examples of special cases, without going in details, could be only of taxonomical interest. On the contrary, the point that we find of crucial interest is that the cases listed above (together with other multifield approaches not quoted here) are special (although important) realizations of a unique theoretical structure.

A program of unification of existing multifield models was initiated by G. Capriz in the late 1970's. After a series of papers unifying different sub-areas (see [13], [14], [16], [25], [26], [27], [28], [29]), in the seminal works [15] and [17] –the latter a treatise– Capriz presented the first general formulation of multifield theories[3] in continuum mechanics, by accounting for abstract morphological descriptors. Really, abstract order parameters were introduced in 1950's in statistical physics by L. D. Landau and E. M. Lifshitz (see the treatise [104] or subsequent editions) as a tool to describe thermodynamical properties of phase transitions above all in complex bodies such as spin glasses or ferromagnetic alloys. Moreover, such a point of view allowed the topological classification of defects in complex bodies by exploiting the properties of the fundamental group of the manifold $\mathcal{M}$ of substructural shapes (the papers of N. D. Mermin [132] and L. Michel [133] furnish a complete critical review of the matter). However, it is with the above mentioned works [15] and [17] that we find the first construction of a general model-building framework able to describe the influence of substructural changes in complex bodies on the gross deformative behavior in the circumstances we know. In these two works, a general point of view was indicated and a lot of consequent basic questions (some of foundational nature) opened. Amid other things, crucial questions are the nature of the balance of substructural interactions, its origin and its invariance with respect to classes of changes in observers. In fact, in [17] such a balance is postulated in its pointwise form (in special cases it reduces to Ginzburg-Landau equation). Really, restricted to the special case of micromorphic bodies, P. Germain [78] derived the relevant special version of the balance of substructural interactions just by postulating an appropriate version of the principle of virtual work involving microstresses and self-forces. However, if one wants to follow this way, one is forced to postulate the structure of the internal power, thus (as it will be clear in the development of this paper) the existence of a self-force acting *within* each material element. A postulate of this type is also necessary when one derives local balances from the balance of energy as proposed in 1995 by A. E. Green and P. M. Naghdi in the special situation in which the morphological descriptor is a director (even deformable) [85] and in the general case by G. Capriz and E. G. Virga [31] in 1994. Really, the latter authors, derived in [30] an integral version of the balance of substructural interactions by developing appropriately the traditional algebra of bodies [179], but they were forced to embedd $\mathcal{M}$ in a linear space. As anticipated in Section 1.1, this is the sole case in which an integral version of Capriz's balance can be postulated (technical reasons shall be furnished later). However, as a matter of fact, the question of the embedding is not trivial, because, although it always exists when $\mathcal{M}$ has finite dimension, it is not unique, so when one uses it –for example as an essential tool to construct finite elements– its choice becomes a strict matter of modeling and has in a wide sense a constitutive nature.

The nature of the balance of substructural interactions was also investigated deeply by

[3]The term "multifield" for theories involving morphological descriptors of substructures was introduced later in 1998 by one of us in the title of [120], then it started to walk with its legs.

R. Segev in [156]. He showed how the geometrical properties of $\mathcal{M}$ influence the representation of substructural interactions and their meaning.

In two works developed independently, namely [23] and [113], it was shown at the end that the invariance requirement just of the external power with respect to the action of the special orthogonal group $SO(3)$ allows one to get as a consequence (i) the existence of the substructural self-force and (ii) the pointwise balance of substructural interactions. The procedure makes use of a notion of observer enlarged with respect to the traditional one. However, the sole requirement of $SO(3)$ invariance - that is invariance with respect to observers differing by rigid body motions - induces an indeterminacy in the substructural self-force. In Hamiltonian setting the problem has been eliminated in [21] by proving the *covariance* of Capriz's balance - that is its invariance with respect to observers differing in the evaluation of $\mathcal{M}$ by the action of arbitrary Lie groups.

The discussion about the nature of the balance of substructural interactions is just an example of the basic questions that one faces in managing multifield theories. The clarification of these theoretical points has concrete interest because they are crucial in constructing special models for specific classes of complex bodies and also to understand how one may build up appropriate numerical schemes. In other words, the clear knowledge of theoretical structures opens the way to clear computational paths.

To complete the tale, we mention a class of problems for which the set of available numerical examples is very narrow, but there are reasons that push to conjecture that it could be a fruitful area of numerical experiments. Namely, multifield theories allow us to describe the influence of diffuse interfaces or the branching of substructures on macroscopic sharp defects, such as (moving possibly) macroscopic discontinuity surfaces and their possible junctions. Such surfaces may be structured or unstructured. In the former case they are endowed by surface energy, in the latter they are free of such an energy. *Surface substructural interactions* accrue over structured surfaces in complex bodies. They have been introduced by one of us in [110], [113], [112]. Moreover, it has been proven in [49] that the related interfacial balances are still covariant. Such balances allow us to describe phenomena like the evolution of paraelectric-ferroelectric interfaces as well as interfaces between isotropic and nematic phases in liquid crystals, damage fronts etc. Over junctions, appropriate *line substructural interactions* may be accounted for [22]. Finally, cracks in complex bodies deserve to be mentioned a part because experimental results about the influence of the material substructure on crack evolution are available in many special cases and justify the construction of unified treatments [116].

1.3 Structure of the Paper

In Section 2 we introduce basic issues of the general format of multifield theories. The point of view adopted is the one of non-linear theory. The reason is that multifield theories are essentially non-linear. Linearization is in general not immediate (unless $\mathcal{M}$ coincides with a linear space) and requires the use of non-trivial geometrical tools.

In Section 3 a model of elastic microcracked bodies is discussed in detail as a paradigmatic example of multifield theory of complex bodies. Due to the particular choice of $\mathcal{M}$, such a model can be easily linearized. Elementary two-dimensional finite element simulations display the unusual richness of possible results. They deal with both the case in which the microcrack distribution is deterministic and the one in which it is random; in the latter case, the combined use of finite element and Monte Carlo techniques is necessary.

General issues about the linearization of multifield theories are presented in Section 4 with reference to the elastic behavior. In this setting, various finite element schemes are constructed: compatible models and mixed models.

Section 5 deals with the analysis of the interaction between diffuse interfaces and sharp macroscopic 'defects'. The treatment of both macroscopic discontinuity surfaces and cracks

in complex bodies is sketched. For macroscopic sharp defects like cracks, extended finite elements are a reliable tool to analyze their behavior. Their common formulation can be generalized to multifield theories: the way is shown with reference to the special case of the interaction between diffuse microcracking and a macroscopic crack.

1.4 Notations

Some standard notations used in the body of the paper are summarized here.

Let $\mathbf{A}$ and $\mathbf{B}$ be tensors of type (p,q). We denote with $\mathbf{A}\cdot\mathbf{B}$ the standard scalar product given by $A^{i_1\dots i_p}_{j_1\dots j_q}B^{i_1\dots i_p}_{j_1\dots j_q}$. In particular, if $\mathbf{A}$ and $\mathbf{B}$ are second order tensors, we denote with $\mathbf{AB}$ the product which contracts only one index and bears a second order tensor; for example, we have $(\mathbf{AB})_{ij}=A_{ik}B^k_j$. If $\mathbf{A}$ is a tensor of the type (p,q), with $p,q>0$, and $\mathbf{B}$ is another tensor of the type (r,s), with $r,s>0$ and $r<p$, $s<q$, or $(r=p, s<q)$ or $(r<p, s=q)$, we indicate by $\mathbf{AB}$ (with some slight abuse of notation with respect to the product between second order tensors) the product which contracts all the indices of $\mathbf{B}$; in particular, if $p=0$ or $q=0$ we take $r=0$ or $s=0$ respectively. Given two vectors $\mathbf{a}$ and $\mathbf{b}$, $\mathbf{a}\otimes\mathbf{b}$ denotes their tensor product. In particular, if $\mathbf{A}$ and $\mathbf{B}$ are second order tensors we have $\mathbf{AB}\cdot(\mathbf{a}\otimes\mathbf{b})=\mathbf{A}^T\mathbf{a}\cdot\mathbf{Bb}$. For any pair of vector spaces $\mathbb{A}$ and $\mathbb{B}$ (with duals $\mathbb{A}^*$ and $\mathbb{B}^*$), $Hom(\mathbb{A},\mathbb{B})$ is the space of linear maps from $\mathbb{A}$ to $\mathbb{B}$. For any manifold M, T_mM is the tangent space of M at $m\in M$, while T^*_mM the relevant cotangent space. We will make use of two different regular bounded regions of the three-dimensional Euclidean point space $\mathcal{E}^3$, namely $\mathcal{B}_0$ and $\mathcal{B}$ and of an abstract manifold $\mathcal{M}$. Capital letters $A,B,C...$ used as indices denote coordinates on $\mathcal{B}_0$, while $i,j,k...$ coordinates on $\mathcal{B}$; finally, $\alpha,\beta...$ indicate coordinates on $\mathcal{M}$. The differential operators Div and ∇ indicate respectively divergence and gradient calculated with respect to coordinates in $\mathcal{B}_0$ while div and $grad$ are their counterparts with respect to coordinates in $\mathcal{B}$. The superscript T means transposition. The symbol ∂_y means partial derivative with respect to the entry 'y'. We indicate by the term *part* any subset of $\mathcal{B}_0$ with non-vanishing volume and the same regularity properties of $\mathcal{B}_0$. For any region $\mathfrak{b}$ of the space, $\partial\mathfrak{b}$ represents its boundary. Let Σ be any smooth surface in $\mathcal{B}_0$ oriented by the normal $\mathbf{m}$ at each point, for any field $e(\cdot)$ defined on $\mathcal{B}_0$ and differentiable there, we indicate by ∇_Σ its surface gradient along Σ, namely $\nabla_\Sigma e(\mathbf{X})=\nabla e(\mathbf{X})(\mathbf{I}-\mathbf{m}\otimes\mathbf{m})$, with $\mathbf{I}$ the second-order unit tensor. The trace of $\nabla_\Sigma e$ is the surface divergence of e, namely $Div_\Sigma e$. Other notations shall be explained later.

2 ELEMENTS OF THE GENERAL FORMAT OF THE MECHANICS OF COMPLEX BODIES

2.1 Deformations and Morphological Descriptors of the Substructural Complexity

We indicate by $\mathcal{B}_0$ the regular[4] region of the three-dimensional Euclidean point space occupied by the body in its reference place. A mapping $\tilde{\mathbf{x}}$, acting as

$$\mathcal{B}_0\ni\mathbf{X}\overset{\tilde{\mathbf{x}}}{\longmapsto}\mathbf{x}=\tilde{\mathbf{x}}(\mathbf{X})\in\mathcal{E}^3, \tag{1}$$

[4]Regularity is here intended in the sense of D-regions (see [52]). Roughly speaking, $\mathcal{B}_0$ is regularly open, coincident with the interior of its closure and is endowed with a surface-like boundary where the outward unit normal is well defined everywhere, except a finite number of corners and edges. From one hand such requirements serve to guarantee the applicability of divergence theorem while from the other hand to cover a class of regions of space sufficiently large to include gross shapes of bodies that we encounter in the physical world, the ones that engineers would like to menage to construct objects of different type. In this sense, the origin of the requirements of regularity for $\mathcal{B}_0$ are of various nature. They are not only restricted to the technical need to menage the divergence theorem because such a theorem (expressed in a rather abstract form) holds also for more exotic regions like, e.g., fractals.

is a *deformation* (or better a *transplacement*) and indicates the current place $\mathbf{x}$ of a generic material element resting at $\mathbf{X}$ in $\mathcal{B}_0$. It is assumed to be one-to-one, continuous and piecewise continuously differentiable; at each $\mathbf{X}$, the gradient of $\tilde{\mathbf{x}}$ is indicated by $\mathbf{F}$, namely $\mathbf{F} := \nabla\tilde{\mathbf{x}}(\mathbf{X}) \in Hom(T_{\mathbf{X}}\mathcal{B}_0, T_{\mathbf{x}}\mathcal{B})$.

One presumes also that $\tilde{\mathbf{x}}$ be orientation preserving that is equivalent to prescribe $\det\mathbf{F} > 0$ at each $\mathbf{X}$. Such a inequality is the major source of analytical difficulties in standard non-linear elasticity (see related discussion in [129], [36]). This kind of picture is not always sufficient to account for the morphology of substructural shapes. For instance, when one considers the equilibrium of a non-linear elastic body and analyzes it through the relevant non-convex energy depending just on $\mathbf{F}$, one may find minimizers describing laminates [150] (as in some typologies of shape memory alloys) or, say, tent-like (or rouf-like) microstructures [101]. However, when the material can undergo polarization, just to speak about a special example, one should introduce directly a descriptor of the polarization state, namely the polarization vector at each $\mathbf{X}$ [47].

Different physical circumstances may then require different descriptors of various mathematical nature. Moreover, for the same material substructure different morphological descriptors can be chosen. Each choice allows one to account for some aspects of the morphology of the material substructure and not for others.

A list of possible examples of special choice of morphological descriptors is furnished later. Here, instead of selecting a specific order parameter, we remark once more the basic fact that, to construct the whole mechanical format for analyzing the behavior of complex bodies, one needs just to require that the morphological descriptor ν be an element of a (paracompact) differentiable manifold $\mathcal{M}$ that we presume here without boundary, so that we have a map $\tilde{\nu}$ given by

$$\mathcal{B}_0 \ni \mathbf{X} \overset{\tilde{\nu}}{\longmapsto} \nu = \tilde{\nu}(\mathbf{X}) \in \mathcal{M}, \tag{2}$$

that we presume here (for the sake of simplicity) to be continuous and piecewise continuously differentiable.

A question arises at this point: What is the necessity to consider a so general object like an abstract manifold as $\mathcal{M}$?

The answer has articulated aspects. First, physical circumstances impose often that at each point the morphological descriptor ν does not belong to a linear space. A common example is the one of magnetostrictive materials in which ν describes a local magnetic spin and is naturally an element of the sphere S^2. Of course S^2 is a non-linear space because the sum of two arbitrary elements of it does not belong to S^2 itself.

Moreover, the geometrical properties of $\mathcal{M}$ have often physical meaning and are related to specific circumstances envisaged. More precisely, when own kinetic energy can be attributed to the material substructure, the expression of such an energy induces a metric over $\mathcal{M}$ and, vice versa, the choice of a metric over $\mathcal{M}$ influences the representation of the kinetic energy. Moreover, a connection over $\mathcal{M}$ allow us to represent contact interactions (i.e. weakly non-local interactions of gradient nature) associated with the influence on the substructure in a given material element of substructural changes in the neighboring elements. Also, in going toward more subtle topological issues, one may note that the homotopy fundamental group of $\mathcal{M}$ allows us to 'classify' substructural defects (see the comprehensive review [132]).

So, to have a theoretical setting able not only to unify known models of condensed matter physics but, above all, to be a tool to describe new exotic materials (that industrial needs may push to produce), we should attribute to $\mathcal{M}$ geometrical structure as less as possible. However, we need to maintain the elements strictly necessary to build up the representation of interactions and their balance. The choice that $\mathcal{M}$ be a differentiable manifold, as required above, fits all these requirements.

2.1.1 Elementary notions about manifolds

The reader acquainted with primary notions of differential geometry may in principle skip this section in his reading. Here, some basic definition and elementary remarks are collected just to render the paper self-contained and to introduce clearly the reader to non-trivial aspects of the matter.

A *topological space* is a set $\mathfrak{M}$ together with a family τ of subsets of it (that we call *open sets* of $\mathfrak{M}$; their complements in $\mathfrak{M}$ are then *closed*) such that (*i*) the empty set $\varnothing$ and $\mathfrak{M}$ belong to τ, (*ii*) the union of any collection of elements of τ is also an element of τ, (*iii*) the intersection of any pair of elements of τ is also in τ. $\mathfrak{M}$ is also Housdorff if for any pair of distinct elements ν_1 and ν_2 of it one may find neighborhoods $\mathfrak{I}_{\nu_1}$ and $\mathfrak{I}_{\nu_2}$ of ν_1 and ν_2 (namely open sets containing respectively ν_1 and ν_2) which do not intersect each other.

A subclass τ_B of τ is called *basis* for the topology τ if any open set of $\mathfrak{M}$ (i.e. any element of τ) can be represented by means of the union or the finite intersection of elements of τ_B. Here we assume that each element of $\mathfrak{M}$ has a countable basis. We say that a topological space $\mathfrak{M}$ is *locally Euclidean* of dimension m if each point of it has a neighborhood $\mathcal{U}$ homeomorphic to an open subset $\mathcal{V}$ of $\mathbb{R}^m$. This means that, for any $\nu \in \mathfrak{M}$, there is $\mathcal{U} \subseteq \mathfrak{M}$ containing ν and a one-to-one mapping φ from $\mathcal{U}$ onto $\mathcal{V}$, namely $\varphi : \mathcal{U} \to \mathcal{V} \subseteq \mathbb{R}^m$. The map φ induces a *local coordinate system* on a piece of $\mathfrak{M}$ so that the pair $(\mathcal{U}, \varphi)$ is called *chart*. Precisely, $\nu^\alpha = \varphi^\alpha(\nu)$ is in this sense the α-th coordinate of ν, being $\varphi^\alpha(\nu)$ the α-th coordinate of the m-dimensional vector $\varphi(\nu) \in \mathbb{R}^m$. Roughly speaking, a topological space $\mathfrak{M}$ is locally Euclidean of dimension m when we may establish around each point of it a local Euclidean coordinate system. For different points the relevant coordinate systems are in principle different but they have the same dimension. In particular, let us consider a collection $\mathfrak{F} = \{(\mathcal{U}_i, \varphi_i)\}$ of coordinate systems (with i belonging to an index set I) such that the union of all $\mathcal{U}_i$ –that may partially overlap with each other– is a *cover* of $\mathfrak{M}$, i.e. $\bigcup_{i \in I} \mathcal{U}_i = \mathfrak{M}$. If for *all* i, $j \in I$, we get

(i) $\varphi_i \circ \varphi_j^{-1} : \mathcal{U}_i \cap \mathcal{U}_j \to \mathcal{V}_i \cap \mathcal{V}_j \subseteq \mathbb{R}^m$ is of class C^k with $1 \leq k \leq +\infty$, and

(ii) for any coordinate system $(\mathcal{U}\, \varphi)$ such that $\varphi_i \circ \varphi_j^{-1}$ and $\varphi_i \circ \varphi^{-1}$ are of class C^k for all $i \in I$, one gets $(\mathcal{U}, \varphi) \in \mathfrak{F}$,
then $\mathfrak{F}$ is called *differentiable structure* of class C^k over $\mathfrak{M}$.

In other words, we have a differentiable structure over $\mathfrak{M}$ when we may cover it with an atlas of charts and we may go from any local coordinate system to the neighboring one (when the 'passage' is defined, i.e. when item (*i*) above applies) with the same degree of regularity.

A differentiable manifold $\mathcal{M}$ of finite dimension m and class C^k is a locally Euclidean space of dimension m endowed with a m-dimensional differentiable structure of class C^k.

When the degree of regularity (i.e. the class) is not specified (as in the case we treat in this paper) it is intended that $\mathcal{M}$ is of class C^∞.

Figure 1 is a sketch of the situation described above.

Paracompactness of $\mathcal{M}$ (a property required just above (2)) means that every open cover of $\mathcal{M}$ has a locally finite open refinement (i.e. roughly speaking a subcover such that every point of $\mathcal{M}$ has a neighborhood that meets only a finite number of the elements of the subcover). This property assures that $\mathcal{M}$ admits partitions of unity for any open cover.

To think about more familiar things, commonly the region $\mathcal{B}_0$ occupied by the body in its reference place is a sub-manifold of the three-dimensional point space $\mathcal{E}^3$ and is

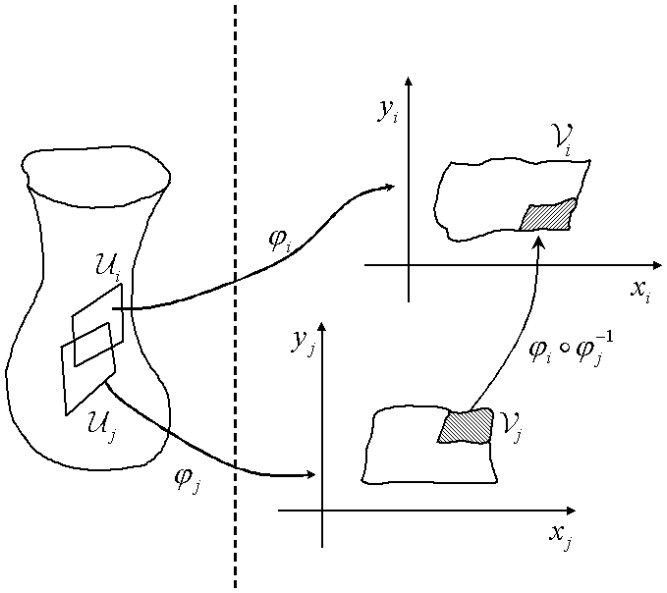

Figure 1. Local overlapping charts over a manifold. The dashed line means that $\mathcal{M}$ and its local representations in Euclidean space are in principle not parts of the same space

paracompact. So, the possibility to build up always over $\mathcal{B}_0$ a partition of unity is a crucial point, for example, to construct extended finite elements (see [5]).

A few additional notions complete this section. Let $f : [-\bar{s}, \bar{s}] \longmapsto \mathcal{M}$ be a not self-intersecting curve over $\mathcal{M}$, with $\bar{s}$ a positive real number, and indicate with ν the value $f(0)$. We say that f is *differentiable* if in some chart $(\mathcal{U}, \varphi)$ the map $\varphi \circ f$ is differentiable. If f_1, is another differentiable curve as f, we say that two curves are *equivalent* if $f(0) = f_1(0)$ and $\frac{d}{ds}(\varphi \circ f)\big|_{s=0} = \frac{d}{ds}(\varphi \circ f_1)\big|_{s=0}$. We call then *tangent* vector to $\mathcal{M}$ at ν the equivalence class of curves over $\mathcal{M}$ agreeing at ν up to the first order as defined just above and indicate with $\dot{\nu}$ such class. Of course $\dot{\nu}$ exists intrinsically because the equivalence relation is chart independent (see any standard textbook on differential geometry). The α-th component of $\dot{\nu}$ in the chart $(\mathcal{U}, \varphi)$ is given by $\dot{\nu}^\alpha = \frac{d}{ds}(\varphi^\alpha \circ f)\big|_{s=0}$. In other words we should imagine the counterpart of $\mathcal{U}$ in $\mathbb{R}^m$, namely $\mathcal{V} = \varphi(\mathcal{U})$, select over $\mathcal{V}$ the point $\varphi(\nu)$, evaluate the tangent vector to the curve $\varphi \circ f$ in $\mathcal{V}$ and consider it as the image in the coordinate system $(\mathcal{U}, \varphi)$ of $\dot{\nu}$. Of course, if $\dot{\nu}^\beta$ is the component of $\dot{\nu}$ at ν in another coordinate system, say $\left(\bar{\mathcal{U}}, \bar{\varphi}\right)$, the circumstance that $\mathcal{M}$ is endowed with a differentiable structure allows us to say that $\dot{\nu}^\beta = \frac{\partial \bar{\varphi}^\beta}{\partial \varphi^\alpha} \dot{\nu}^\alpha$ due to the change of coordinates from $(\mathcal{U}, \varphi)$ to $\left(\bar{\mathcal{U}}, \bar{\varphi}\right)$ in a neighborhood of ν. The components of $\dot{\nu}$ changes in such a way that $\dot{\nu}$ itself is left invariant. The set $T_\nu\mathcal{M}$ of all equivalent classes of curves at ν is the *tangent space* to $\mathcal{M}$ at ν. It is a linear space, the union $T\mathcal{M}$ of all tangent spaces to $\mathcal{M}$, namely $T\mathcal{M} = \bigcup_{\nu \in \mathcal{M}} T_\nu\mathcal{M}$, is the *tangent bundle* of $\mathcal{M}$. It has the natural structure of a differentiable manifold and its dimension is equal to $2m$: in fact, a generic element of $T\mathcal{M}$ is the pair $(\nu, \dot{\nu})$. $T\mathcal{M}$ does not coincides in general with a linear space although each $T_\nu\mathcal{M}$ is a linear space.

Each $\dot{\nu}$ cannot be separated by its pertinent ν unless a parallelism is defined over $\mathcal{M}$. Sometimes the choice of the parallelism (or better, the *connection*) over $\mathcal{M}$ implies subtle physical questions.

For each $T_\nu\mathcal{M}$, its dual counterpart is indicated by $T^*_\nu\mathcal{M}$ and called *cotangent space* of $\mathcal{M}$ at ν. It is a linear space with dimension equal to m. The union $T^*\mathcal{M}$ of all cotangent spaces of $\mathcal{M}$, namely $T^*\mathcal{M} = \bigcup_{\nu\in\mathcal{M}} T^*_\nu\mathcal{M}$, is the *cotangent bundle*, is naturally endowed with the structure of a differentiable manifold with dimension equal to $2m$ since the generic element of $T^*\mathcal{M}$ is the pair $(\nu, \mathbf{z})$ with $\mathbf{z} \in T^*_\nu\mathcal{M}$.

Notice that, if $\mathbf{z} \in T^*_\nu\mathcal{M}$ and $\dot\nu \in T_\nu\mathcal{M}$, the (scalar) product $\mathbf{z}\cdot\dot\nu$ is naturally defined (without adding additional algebraic structure) because it is the value of $\mathbf{z}$ at $\dot\nu$.

Notice that, although each $T^*_\nu\mathcal{M}$ is a linear space, the cotangent bundle $T^*\mathcal{M}$ does not coincide in general with a linear space.

2.1.2 Configuration space and motions

As remarked in defining (1) and (2), two sufficiently smooth maps characterize the morphology of the body, namely the transplacement map $\tilde{\mathbf{x}}$ and the morphological descriptor map $\tilde\nu$. So, the *configuration space* $\mathcal{C}$ of a complex body is the space of pairs $(\tilde{\mathbf{x}}, \tilde\nu)$. It is a product space of the type $\mathcal{C}_\mathbf{x} \times \mathcal{C}_\nu$ with $\tilde{\mathbf{x}}$ belonging to $\mathcal{C}_\mathbf{x}$ and $\tilde\nu$ to $\mathcal{C}_\nu$. The analytical properties[5] of $\mathcal{C}$ are essential in building up numerical schemes and in evaluating their convergence. In particular, $\mathcal{C}$ has a non-trivial structure that depends on the geometrical properties of $\mathcal{M}$ (that is on the special choice of $\mathcal{M}$ that physical circumstances impose in concrete cases). Examples of how the nature of $\mathcal{C}$ may be intricate are discussed in [49].

In our picture, *motions* are then sufficiently smooth time parametrized curves over $\mathcal{C}$. With reference to a given interval of time $[0, \bar t]$, we have then mappings

$$[0,\bar t] \ni t \longmapsto (\tilde{\mathbf{x}}_t, \tilde\nu_t) \in \mathcal{C} \tag{3}$$

and - with some slight abuse of notation - we indicate by $\mathbf{x} = \tilde{\mathbf{x}}(\mathbf{X}, t)$ the current place of a material element resting at $\mathbf{X}$ when $t = 0$ and with $\nu = \tilde\nu(\mathbf{X}, t)$ the value at the time t of the morphological descriptor.

Moreover, we denote with $\dot{\mathbf{x}}$ and $\dot\nu$ the rates given by

$$\dot{\mathbf{x}} = \frac{d\tilde{\mathbf{x}}}{dt}(\mathbf{X}, t), \qquad \dot\nu = \frac{d\tilde\nu}{dt}(\mathbf{X}, t). \tag{4}$$

Of course, at each $\mathbf{X}$ and t, $\dot{\mathbf{x}} \in T_\nu\mathcal{B}$, $\dot\nu \in T_\nu\mathcal{M}$.

This representation of the motion is Lagrangian in the sense that the rate fields considered just above are defined over $\mathcal{B}_0$. However, since $\tilde{\mathbf{x}}$ is assumed to be one-to-one everywhere in $\mathcal{B}_0$ (exception is for example the case in which macroscopic cracks are considered, a case that will be treated later), a complete spatial (Eulerian) representation of the motion is available.

A spatial field $\tilde\nu_a$ of morphological descriptors is then defined by $\tilde\nu_a = \tilde\nu \circ \tilde{\mathbf{x}}^{-1}$ so that $\nu_a = \tilde\nu_a(\mathbf{x},t)$. Correspondingly, we have the spatial counterparts of the rates $\dot{\mathbf{x}}$ and $\dot\nu$, indicated by $\mathbf{v}$ and υ: they are the values at $\mathbf{x}$ and t of fields $\tilde{\mathbf{v}}$ and $\tilde\upsilon$ defined formally by

$$\mathcal{B}\times[0,\bar t] \ni (\mathbf{x}, t) \overset{\tilde{\mathbf{v}}}{\longmapsto} \mathbf{v} = \tilde{\mathbf{v}}(\mathbf{x}, t) \in T_\mathbf{x}\mathcal{B}, \tag{5}$$

$$\mathcal{B}\times[0,\bar t] \ni (\mathbf{x}, t) \overset{\tilde\upsilon}{\longmapsto} \upsilon = \tilde\upsilon(\mathbf{x}, t) \in T_\nu\mathcal{M}. \tag{6}$$

[5]For example, as in standard non-linear elasticity, one may imagine that $\mathcal{C}_\mathbf{x} \subseteq W^{1,\,p}(\mathcal{B}_0, \mathcal{E}^3)$ for some $p \geq 1$, i.e. that $\tilde x$ be an element of the sobolev space $W^{1,p}(\mathcal{B}_0, \mathcal{E}^3)$ of point valued functions even if we might basically require in some circumstances that $\tilde{\mathbf{x}}$ be continuous and piecewise continuously differentiable (namely $PC^1(\mathcal{B}_0, \mathcal{E}^3)$)[36], [129], [163], a request that could apply also to $\mathcal{C}_\nu$ that we may consider thus coincident with $PC^1(\mathcal{B}_0, \mathcal{M})$.

We have

$$\dot{\mathbf{x}} = \mathbf{v} \qquad \text{and} \qquad \upsilon = \dot{\nu} + (grad\ \nu)\,\mathbf{v}. \tag{7}$$

We may write also

$$\upsilon = \dot{\nu} + (\nabla\nu)\,\mathbf{F}^{-1}\mathbf{v} \ = \dot{\nu} - (\nabla\nu)\,\dot{\mathbf{X}}, \tag{8}$$

where $\dot{\mathbf{X}}$ is the material velocity $-\mathbf{F}^{-1}\mathbf{v}$ derived from the inverse mapping $\mathbf{X} = \tilde{\mathbf{x}}^{-1}(\mathbf{x}, t)$ so that $\dot{\mathbf{X}} = \overline{(\tilde{\mathbf{x}}^{-1})}\,(\mathbf{x}, t)$.

2.1.3 Measures of deformations

At the beginning of Section 2 we have reminded that the requirement that $\tilde{\mathbf{x}}$ be orientation preserving is tantamount to prescribe that $\mathbf{F}$ has positive determinant everywhere. $\mathbf{F}$ is a part of the tangent map $T\tilde{\mathbf{x}} : T\mathcal{B}_0 \to T\mathcal{B}$ whose peculiar elements are pairs of the type $(\mathbf{x}, \mathbf{F})$; in other words, $T\tilde{\mathbf{x}}(\mathbf{X}) = \left(\tilde{\mathbf{x}}(\mathbf{X}), \tilde{\mathbf{F}}(\mathbf{X})\right) \equiv (\mathbf{x}, \mathbf{F})$. The reason for which we consider in common practice just $\mathbf{F}$ independently of the corrisponding $\mathbf{x}$ is that the geometry of the regions that the body may occupy is so 'nice' that allow us to separate invariantly[6] $\mathbf{x}$ from $\mathbf{F}$. It is not so for the tangent map $T\tilde{\nu} : T\mathcal{B}_0 \to T\mathcal{M}$ which is such that $T\tilde{\nu}(\mathbf{X}) = (\tilde{\nu}(\mathbf{X}), \nabla\tilde{\nu}(\mathbf{X})) \equiv (\nu, \nabla\nu)$. In this case, in principle, $\mathcal{M}$ may be so exotic that we cannot separate invariantly $\nabla\nu$ from its relevant ν. This is one of the reasons for which below we shall encounter in general the pair $(\nu,\nabla\nu)$ in the list of constitutive entries of the free energy unless some special cases may allow us to consider ν or $\nabla\nu$ separately. At each $\mathbf{X}$, we then get $\nabla\nu \in Hom(T_{\mathbf{x}}\mathcal{B}_0, T_{\nu}\mathcal{M})$, i.e. $\nabla\nu$ transforms linearly tangent vectors to $\mathcal{B}_0$ at $\mathbf{X}$ in tangent vectors to $\mathcal{M}$ at ν. We indicate with $\nabla\nu^*$ the adjoint of $\nabla\nu$. It is such that $\nabla\nu^* \in Hom(T^*_{\nu}\mathcal{M}, T^*_{\nu}\mathcal{B}_0)$. If we consider $\tilde{\nu}_a$, i.e. the counterpart of $\tilde{\nu}$ over $\mathcal{B}$, we have another tangent map $T\tilde{\nu}_a : T\mathcal{B} \to T\mathcal{M}$ such that $T\tilde{\nu}_a(\mathbf{x}) = (\nu_a, grad\ \nu_a)$.

It is easy to check by chain rule that $grad\ \nu_a = (\nabla\nu)\,\mathbf{F}^{-1}$.

The picture of the kinematics described up to here is summarized roughly in the diagram of Figure 2.

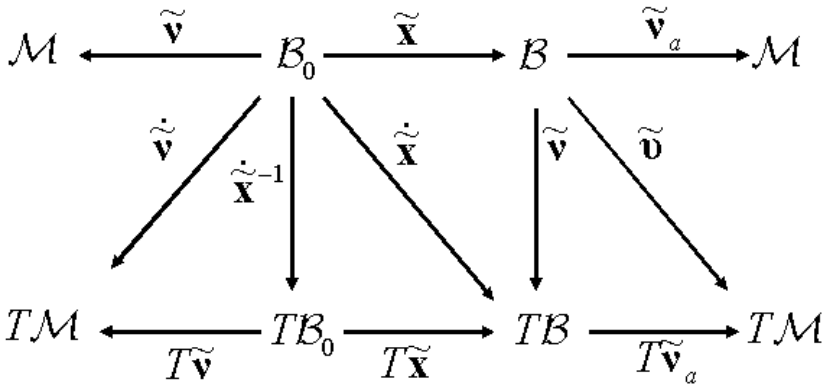

Figure 2. Summary of the description of body morphology

[6]Technically, one realizes that $T\mathcal{B}_0$ and $T\mathcal{B}$ are *trivial* bundles and a natural connection is available over them.

A few remarks about measures of deformations may clarify further the matter.

Let $\mathbf{g}$ be the matric in the ambient space (more properly in $\mathcal{B}$) and γ the material metric in $\mathcal{B}_0$. Both $\mathbf{g}$ and γ are symmetric, definite positive, second order tensors. These metrics may be even *flat*, i.e. they may coincide with the identity tensor $\mathbf{I}$. By indicating by $\mathbf{F}^T$ the transpose of $\mathbf{F}$, the mapping

$$\mathcal{B}_0 \ni \mathbf{X} \longmapsto \left(\mathbf{F}^T\mathbf{F}\right) \equiv \mathbf{C} \in Sym^+\left(T_{\mathbf{X}}\mathcal{B}_0, T^*_{\mathbf{x}}\mathcal{B}\right) \tag{9}$$

is the pull-back of $\mathbf{g}$ from $\mathcal{B}$ to $\mathcal{B}_0$ by means of the deformation $\tilde{\mathbf{x}}$ and in components we have $\mathbf{C}_{AB} = \left(\mathbf{F}^T\right)^i_{\ A}\mathbf{g}_{ij}\mathbf{F}^j_{\ B}$.

In standard continuum mechanics, at each $\mathbf{X}$, the difference $(\mathbf{C} - \gamma)$ is twice the non-linear deformation tensor $\mathbf{E}$ measuring relative changes of lengths by using $\mathcal{B}_0$ as paragon setting. In components we get $2E_{AB} = C_{AB} - \gamma_{AB}$ even if a more familiar expression is given by $2E^A_B = C^A_B - \delta^A_B$ with $C^A_B = \gamma^{AD}C_{DB}$ and $\delta^A_B = \gamma^{AD}\gamma_{DB}$ the Kronecker symbol.

In complex bodies, the special nature of the substructure (more specifically the choice of the morphological descriptor) may or may not influence directly the measures of deformation. In fact, when for example ν represents a microdisplacement, an indepenendent rotation or an independent deformation, its gradient may enter the expression of the measures of deformation together with ν itself. Cosserat and micromorphic materials are well-known special cases in which the order parameter and its gradient appear explicitly in the expression of measure of deformations (see all references about Cosserat and micromorphic materials quoted in the introduction). Other cases are microcracked bodies and quasiperiodic alloys: They will be treated explicitly in subsequent sections.

We could summarize in a unique statement the variety of situations envisaged by affirming that in general there is a map of the type

$$(\mathbf{F}, \mathbf{g}, \nu, \nabla\nu) \longmapsto \mathbf{G}\left(\mathbf{F}, \mathbf{g}, \nu, \nabla\nu\right) \in Sym^+\left(T_{\mathbf{X}}\mathcal{B}_0, T^*_{\mathbf{X}}\mathcal{B}_0\right) \tag{10}$$

with $\mathbf{G}$ a metric in $\mathcal{B}_0$ involving the pull-back of $\mathbf{g}$. Consequently, we could define an (extended) deformation tensor $\tilde{\mathbf{E}}$ by an expression of the type $\frac{1}{2}\left(\mathbf{G} - \gamma\right)$, erasing ν and/or $\nabla\nu$ in the list of entries of $\mathbf{G}$ each time in which the specific physical circumstances envisaged suggest such a cancellation. In particular, when the morphological descriptor represents aspects of the substructure not related directly to local - even microscopic - changes of lengths, standard $\mathbf{C}$ and $\mathbf{E}$, or their spatial counterparts, are sufficient to measure the macroscopic deformation. This is for example the case in which ν represents the volume fraction of a phase in two-component medium, the local orientation of stick molecules in nematic phase etc.

In any case, only specific physical circumstances may render concrete (10) that, on the contrary, would remain vague.

2.1.4 Observers and their classical changes

The notion of observer and the requirements of invariance of balance principles with respect to changes in observers are crucial points in mechanics: We need, in fact, that basic rules do not depend on any particular frame attached to some laboratory, but may be managed in all circumstances they may apply.

In classical mechanics, an observer is a slicing of space time, i.e. a *representation* of the interval of time and of the ambient space in which the motion of the body may develop (see [129] and [146] for a detailed treatment). It is essential to note that in standard context the interval of time and the ambient space are the *sole* geometrical ingredients necessary to describe the shape of the body and its motion. This remark is the starting point to formulate the more enlarged notion of observer necessary in the mechanics of complex

bodies. Here we follow strictly the point of view in [119] (see also [49], [21]) and state the following definition:

An observer $\mathcal{O}$ is a representation of all geometrical environments necessary to describe the morphology of a body and its motion.

In this sense, in our point of view an observer is a representation of (*i*) the interval of time, (*ii*) the ambient space, (*iii*) the manifold $\mathcal{M}$ of substructural shapes and (iv) the reference place $\mathcal{B}_0$. For the sake of simplicity, we deal with changes in observers agreeing about the measure of time and $\mathcal{B}_0$. However, the representation of the ambient space $\mathcal{E}^3$ and of $\mathcal{M}$ may be altered in different manners. In general (see [49]), we should consider the action over $\mathcal{E}^3$ of its group of authomorphisms[7] (i.e. changes in observers differing by arbitrary "deformations" of the ambient space itself) and the action over $\mathcal{M}$ of an arbitrary Lie group G. This would be the most general 'reasonable' family of changes in observers agreeing about the measure of time.

We consider here just *classical* changes in observers. For them, the ambient space undergoes only isometric changes ruled by $SO(3)$ and the same copy of the special orthogonal group $SO(3)$ acts also over $\mathcal{M}$. In other words we are describing in our enlarged setting the counterpart of the common motion of 'observers differing by rigid body motions'.

Let $t \longmapsto \mathbf{Q}(t) \in SO(3)$ be a one parameter family (smooth with respect to the parameter that we may identify with time) of elements of $SO(3)$ altering isometrically the ambient space $\mathcal{E}^3$ with $\mathbf{Q}(0)$ coincident with the identity in $SO(3)$. If $\dot{\mathbf{x}}^*$ is the value of velocity $\dot{\mathbf{x}}$ *after* a change in observer ruled by $\mathbf{Q}(t)$, we have

$$\dot{\mathbf{x}}^* = \dot{\mathbf{x}} + \mathbf{c}(t) + \dot{\mathbf{q}} \times (\mathbf{x} - \mathbf{x}_0) \tag{11}$$

where[8] $\mathbf{c}(t)$ is the translational velocity - constant in space - of one observer with respect to the other, $\dot{\mathbf{q}}$ the relevant rotational velocity and $\mathbf{x}_0$ a point chosen arbitrarily in $\mathcal{E}^3$. Moreover, if we consider that $SO(3)$ itself acts also over $\mathcal{M}$ and indicate with $\dot{\nu}^*$ the image of the rate $\dot{\nu}$ of the morphological descriptor *after* the change in observer induced by $\mathbf{Q}(t)$, we get

$$\dot{\nu}^* = \dot{\nu} + \mathcal{A}\dot{\mathbf{q}} \tag{12}$$

where, at each $\nu \in \mathcal{M}$, the linear operator $\mathcal{A}(\nu)$ belongs to $Hom\left(\mathbb{R}^3, T_\nu\mathcal{M}\right)$, i.e. it maps linearly vectors into elements of the tangent space $T_\nu\mathcal{M}$. At each ν, $\mathcal{A}(\nu)$ is represented by a matrix with three columns and a number of lines equal to $\dim \mathcal{M}$. In particular, if $\nu_{\mathbf{q}}$ indicates the value of ν after the rigid action of $SO(3)$ over $\mathcal{M}$, we have $\mathcal{A} = \left.\frac{d\nu_{\mathbf{q}}}{d\mathbf{q}}\right|_{\mathbf{q}=\mathbf{0}}$, where the vector $\mathbf{q}$ is associated with $\mathbf{Q} \in SO(3)$ by the exponential map and we have $\mathbf{Q} = \exp(-\mathsf{e}\mathbf{q})$, with e the Ricci's permutation index.

[7] The same reasonings apply when the ambient space is $\mathcal{E}^2$ or $\mathcal{E}^1$.

[8] Consider as above a smooth curve $[0, \bar{t}] \ni t \longmapsto \mathbf{Q}(t) \in SO(3)$ starting from the identity, i.e. $\mathbf{Q}(0) = \mathrm{Id}_{SO(3)}$. Let $\mathcal{O}$ be a given representation of $\mathcal{E}^3$ at $t = 0$. By means of $\mathbf{Q}(t)$ we may associate to any t an observer $\mathcal{O}'_t$ isometrically related to $\mathcal{O}$. The map from $\mathcal{O}$ onto $\mathcal{O}'_t$ is such that any generic point $\mathbf{x}$ in $\mathcal{O}$ is mapped in a point $\mathbf{x}' = \mathbf{w}(t) + \mathbf{Q}(t)(\mathbf{x} - \mathbf{x}_0)$ in $\mathcal{O}'_t$, where $\mathbf{w}(t)$ is the value of an arbitrary point-valued function smooth in time and $\mathbf{x}_0$ an arbitrary point. If we calculate the rate of $\mathbf{x}'$, namely $\dot{\mathbf{x}}'$, and pull-back it in $\mathcal{O}$ by means of the inverse transformation $\mathbf{Q}^T(t)$, by putting $\mathbf{c} = \mathbf{Q}^T\dot{\mathbf{w}}$ and $\dot{\mathbf{x}}^* = \mathbf{Q}^T\dot{\mathbf{x}}'$, we get (11).

In particular, for any vector d, we have also $\mathbf{Q}^T\dot{\mathbf{Q}}\mathsf{d} = \dot{\mathbf{q}} \times \mathsf{d}$ because $\mathbf{Q}^T\dot{\mathbf{Q}}$ is a skew-symmetric tensor. Roughly speaking, $\mathbf{c} + \dot{\mathbf{q}} \times (\mathbf{x} - \mathbf{x}_0)$ is the rigid body motion of the observer $\mathcal{O}'$ with respect to $\mathcal{O}$ superposed to $\dot{\mathbf{x}}$.

2.2 Balances of Standard and Substructural Interactions

In standard continuum mechanics we make distinction between *bulk* and *contact* forces in representing interactions. These forces are defined to be objects conjugated in terms of power with the standard velocity, i.e. with the rate of the sole morphological descriptor involved, namely the placement of each material element. When multiplied by the velocity (even virtual) they furnish the power developed along a certain mechanical process at a given time. In the case of complex bodies, even if a material element is at rest, the substructure *inside* it may undergo changes measured by the rate $\dot{\nu}$. So that interactions of substructural nature arise. We assume that they are of bulk and contact nature as in the standard case and are defined by objects conjugated in the sense of power with $\dot{\nu}$. As a consequence, since $\dot{\nu}$ belongs to the tangent space $T_\nu\mathcal{M}$ to $\mathcal{M}$ at ν, we should select elements (indicated by letters μ, β or $\mathbf{z}$ indifferently) of the cotangent space $T^*_\nu\mathcal{M}$ in order the product by $\dot{\nu}$ be defined.

Previous remarks summarize roughly the line of reasoning we follow below to represent the external power of *all* interactions over a generic part of the body and to derive related integral and pointwise balances.

As usual, we call *part* any subset $\mathfrak{b}$ of $\mathcal{B}_0$ with the same regularity properties of $\mathcal{B}_0$ itself. Moreover, we indicate by $\mathfrak{P}(\mathcal{B}_0)$ the set of all parts of $\mathcal{B}_0$ and by $vel_c(\mathcal{B}_0)$ the set of pairs of velocity fields, namely $\left(\dot{\tilde{\mathbf{x}}},\dot{\tilde{\nu}}\right)$ with compact support in $\mathcal{B}_0$.

We call then *power* a map

$$P : \mathfrak{P}(\mathcal{B}) \times Vel_c(\mathcal{B}_0) \to \mathbb{R} \tag{13}$$

such that

(i) $P(\cdot, \dot{\mathbf{x}}, \dot{\nu})$ is *additive* and

(ii) both $P(\mathfrak{b}, \dot{\mathbf{x}}, \cdot)$ and $P(\mathfrak{b}, \cdot, \dot{\nu})$ are *linear*.

For any fixed part $\mathfrak{b}$ chosen arbitrarily in $\mathcal{B}_0$, we indicate by $\mathcal{P}^{ext}_{\mathfrak{b}}(\dot{\mathbf{x}}, \dot{\nu})$ the power of all *external* actions over $\mathcal{B}$. To represent explicitly $\mathcal{P}^{ext}_{\mathfrak{b}}(\dot{\mathbf{x}}, \dot{\nu})$ in Lagrangian setting (all fields are in fact defined over $\mathcal{B}_0$), we distinguish bulk and surface contributions and write

$$\mathcal{P}^{ext}_{\mathfrak{b}}(\dot{\mathbf{x}}, \dot{\nu}) = \int_{\mathfrak{b}} \left(\bar{\mathbf{b}} \cdot \dot{\mathbf{x}} + \bar{\beta} \cdot \dot{\nu}\right) d^3\mathbf{X} + \int_{\partial\mathfrak{b}} (\mathbf{P}\mathbf{n} \cdot \dot{\mathbf{x}} + \mathcal{S}\mathbf{n} \cdot \dot{\nu})\, d\mathcal{H}^2 \tag{14}$$

where $\mathbf{n}$ is the outward unit normal to the boundary $\partial\mathfrak{b}$ of $\mathfrak{b}$, $d^3\mathbf{X}$ the usual volume measure and $d\mathcal{H}^2$ the two-dimensional Haussdorff measure over $\partial\mathfrak{b}$. Standard interactions are measured by the vector of bulk forces $\bar{\mathbf{b}}$ and the first Piola-Kirchhoff stress $\mathbf{P}$.

(a) $\bar{\mathbf{b}}$ includes inertial (*in*) and non-inertial (*ni*) effects in additive way so that $\bar{\mathbf{b}} = \mathbf{b}^{in} + \mathbf{b}^{ni}$ and we shall write just $\mathbf{b}$ instead of $\mathbf{b}^{ni}$ to simplify notations. At each $\mathbf{X}$ we get $\bar{\mathbf{b}} \in T^*_{\mathbf{x}}\mathcal{B}$, and $T_{\mathbf{x}}\mathcal{B}$ is isomorphic to $\mathbb{R}^3$.

(b) At each $\mathbf{X}$, the tensor $\mathbf{P}$ belongs to $Hom(T^*_{\mathbf{X}}\mathcal{B}_0, T^*_{\mathbf{x}}\mathcal{B})$, which is isomorphic to $\mathbb{R}^3 \otimes \mathbb{R}^3$. In other words, $\mathbf{P}$ maps normals to ideal surfaces in $\mathcal{B}_0$ into tensions placed at the actual counterpart $\mathbf{x}$ of $\mathbf{X}$.

Substructural interactions are measured by $\bar{\beta}$ and the microstress by $\mathcal{S}$.

(c) $\bar{\beta}$ accounts for external bulk agencies acting directly on the substructure as in the case in which external electromagnetic fields alter the polarization state in ferroelectrics. Moreover $\bar{\beta}$ includes also inertial effects when they can be attributed to the substructure in a way independent of the bulk inertia. At each $\mathbf{X}$, we realize that $\bar{\beta}$ is an element of $T^*_\nu\mathcal{M}$.

(d) At each $\mathbf{X}$, the *microstress* $\mathcal{S}$ maps linearly vectors of $\mathbb{R}^3$ (normals to virtual surfaces in $\mathcal{B}_0$) in elements of $T^*_\nu\mathcal{M}$, i.e. $\mathcal{S}$ belongs to $Hom\left(T^*_{\mathbf{X}}\mathcal{B}_0, T^*_\nu\mathcal{M}\right) \cong Hom\left(\mathbb{R}^3, T^*_\nu\mathcal{M}\right)$. More precisely, consider a smooth virtual surface in $\mathcal{B}_0$ containing $\mathbf{X}$ and oriented there by the normal $\mathbf{n}$. The product $\mathcal{S}\mathbf{n}$ is a 'generalized traction': $\mathcal{S}\mathbf{n}\cdot\dot{\nu}$, in fact, measures the power exchanged between two adjacent material elements through the surface of normal $\mathbf{n}$ as a consequence of substructural changes.

Remark 1. The proof of the existence of $\mathbf{P}$ is classical and available in very weak conditions (see [162]). Moreover in standard continuum mechanics, the addition of a few analytical conditions to the definition of the power indicated above may allow one to obtain directly a representation of $\mathcal{P}^{ext}$ in terms of $\mathbf{P}$ without resorting directly to Cauchy theorem (see [142]) but making use of techniques of geometric measure theory. As regards the microstress, a Cauchy-like theorem cannot be obtained in the standard way (tetrahedron and so on), in general, because $\mathcal{M}$ does not coincide with a linear space. The usual procedure can be applied only by assuming that $\mathcal{M}$ is embedded in an appropriate linear space (see [30]). The embedding is always available (by Whitney theorem) because $\mathcal{M}$ is finite dimensional; the embedding can be also isometric (by Nash theorems) but it is not unique. An intrinsic explicit proof of the existence of $\mathcal{S}$ without resorting to the embedding of $\mathcal{M}$ is not yet available. Techniques proposed in [157] indicate a way of reasoning. Here we just claim the existence of the microstress. In any case we note that in Lagrangian-Hamiltonian setting it arises naturally by exploiting the principle of least action on a total energy depending on $\nabla\nu$. However, in this case constitutive issues would be involved while here, in this section, we are treating the matter without resorting to them. The representation of interactions, in fact, belongs to a family of classes of materials while the specification of constitutive issues selects just a specific class.

Balance equations follow from a basic axiom of invariance of the power with respect to classical changes in observers. The way of reasoning follows the standard path [146], differences are (i) the presence of measures of substructural interactions and (ii) the enlarged notion of observer that we have introduced above.

Axiom. *$\mathcal{P}^{ext}_{\mathfrak{b}}(\dot{\mathbf{x}}, \dot{\nu})$ is invariant with respect to classical changes in observers for any $\mathfrak{b}$, i.e.*

$$\mathcal{P}^{ext}_{\mathfrak{b}}(\dot{\mathbf{x}}^*, \dot{\nu}^*) = \mathcal{P}^{ext}_{\mathfrak{b}}(\dot{\mathbf{x}}, \dot{\nu}) \tag{15}$$

for any choice of $\mathbf{c}$, $\dot{\mathbf{q}}$, $\mathfrak{b}$.

By introducing the relations (11) and (12), in the explicit expression of $\mathcal{P}^{ext}_{\mathfrak{b}}(\dot{\mathbf{x}}^*, \dot{\nu}^*)$, the arbitrariness of $\mathbf{c}(t)$ and $\dot{\mathbf{q}}(t)$ allows us to obtain the *standard integral balance of forces*

$$\int_{\mathfrak{b}} \bar{\mathbf{b}}\, d^3\mathbf{X} + \int_{\partial\mathfrak{b}} \mathbf{P}\mathbf{n}\, d\mathcal{H}^2 = 0 \tag{16}$$

and a *generalized integral balance of moments*, namely

$$\int_{\mathfrak{b}} \left((\mathbf{x}-\mathbf{x}_0)\times\bar{\mathbf{b}} + \mathcal{A}^*\bar{\beta}\right) d^3\mathbf{X} + \int_{\partial\mathfrak{b}} \left((\mathbf{x}-\mathbf{x}_0)\times\mathbf{P}\mathbf{n} + \mathcal{A}^*\mathcal{S}\right) d\mathcal{H}^2 = 0, \tag{17}$$

where $\mathcal{A}^*$ is the adjoint of $\mathcal{A}$ and at each ν we get $\mathcal{A}^*(\nu) \in Hom\left(T^*_\nu\mathcal{M}, \mathbb{R}^3\right)$, i.e. $\mathcal{A}^*$ maps linearly co-vectors over $\mathcal{M}$ into three-dimensional vectors (see [113]). Notice that measures of substructural interaction do not appear in (16). In fact, a "translational velocity" does not appear in (12) because the translation group does not act transitively over $\mathcal{M}$ as it acts over the point space $\mathcal{E}^3$. Moreover, the arbitrariness of $\mathfrak{b}$ allows us to obtain pointwise balances. In fact, we get from (16) the standard pointwise balance of forces (*Cauchy balance*)

$$\bar{\mathbf{b}}+Div\mathbf{P} = \mathbf{0} \tag{18}$$

and from (17) the equation

$$\mathcal{A}^*\left(\bar{\beta}+Div\mathcal{S}\right) = \mathsf{e}\mathbf{P}\mathbf{F}^T - (\nabla\mathcal{A}^*)\,\mathcal{S} \tag{19}$$

with e Ricci's alternating index. Since at each $\mathbf{X}$ the sum $\bar{\beta}+Div\mathcal{S}$ is an element of $T^*_\nu\mathcal{M}$, i.e. it is co-vector of $\mathcal{M}$ at $\nu = \tilde{\nu}(\mathbf{X})$ (that is a linear form over the tangent space $T_\nu\mathcal{M}$) we see from (19) that the vector $\mathsf{e}\mathbf{P}\mathbf{F}^T - (\nabla\mathcal{A}^*)\,\mathcal{S}$ belongs to the range of $\mathcal{A}^*$. We find then two information from (19):

(i) There exists an element of the cotangent space of $\mathcal{M}$ at ν, say $\mathbf{z}$, such that

$$\mathcal{A}^*\mathbf{z} = \mathsf{e}\mathbf{P}\mathbf{F}^T - (\nabla\mathcal{A}^*)\,\mathcal{S} \tag{20}$$

(ii) The co-vector $\mathbf{z}$ (called *self-force*) is just equal to $\bar{\beta}+Div\mathcal{S}$, i.e.

$$\bar{\beta} - \mathbf{z}+Div\mathcal{S} = \mathbf{0}. \tag{21}$$

This last equation represents the *pointwise balance of substructural interactions* (*Capriz balance*). It is invariant with respect to changes in observer governed by $SO(3)$ because we have required exactly this kind of invariance to derive it. However, this requirement alone introduces a form of indeterminacy in the self-force because if we add to $\mathbf{z}$ any element of the null space of $\mathcal{A}^*$ - that is any co-vector $\bar{\mathbf{z}}$ such that $\mathcal{A}^*\bar{\mathbf{z}} = \mathbf{0}$ - the sum $\mathbf{z}+\bar{\mathbf{z}}$ satisfies also (20), then (21). Such an indeterminacy is eliminated by a stronger requirement of invariance, namely *covariance*, i.e. invariance with respect to the action of arbitrary Lie groups over $\mathcal{M}$. The covariance of the balance of substructural interactions can be proven in Lagrangian-Hemiltonian setting by making use of an appropriate version of Noether theorem (the proof can be found in [21]). We remind that in the same setting one may prove that also Cauchy balance of forces is covariant, where covariance means in this case invariance with respect to the action of the group of automorphisms of the ambient space. Roughly speaking we may say that observers deforming one with respect to the other read the same structure of the balance of forces.

As regards equation (20), if we premultiply it by Ricci's alternating symbol e, we get

$$skew\mathbf{P}\mathbf{F}^T = \frac{1}{2}\mathsf{e}\left(\mathcal{A}^*\mathbf{z}+(\nabla\mathcal{A}^*)\,\mathcal{S}\right). \tag{22}$$

Remark 2. The balance of substructural interactions (21) has a rather subtle nature. Its physical interpretation is as follows: locally (i.e. at each point) to sustain external bulk and contact substructural actions, the latter induced by neighboring matter, a self-force is generated in principle *within* each material element.

We may ask whether (21) is a *localized version* of an integral balance principle. In other words, may we postulate the integral version of (21) on any arbitrary part $\mathfrak{b}$ of $\mathcal{B}_0$ and

assume it as a *primitive* integral balance of substructural interaction? The answer is in general *negative*. To explain clearly the reason we need a brief digression.

Really, when we write the integral over A of a certain map ξ, two geometrical environments are involved: the domain A of ξ and its co-domain B. Although A could be even a manifold, B should be a linear space in order the integral be defined. When we consider for example the map $\mathbf{X} \longmapsto \left(\bar{\beta}(\mathbf{X}) - \mathbf{z}(\mathbf{X})\right)$, we see that it takes values in $T^*\mathcal{M}$; precisely, at each $\mathbf{X}$ we find $\left(\bar{\beta}(\mathbf{X}) - \mathbf{z}(\mathbf{X})\right) \in T^*_\nu\mathcal{M}$ and for each pair of points $\mathbf{X}_1$ and $\mathbf{X}_2$ the corresponding morphological descriptors ν_1 and ν_2 differ in general each other, so $\left(\bar{\beta}(\mathbf{X}_1) - \mathbf{z}(\mathbf{X}_1)\right)$ and $\left(\bar{\beta}(\mathbf{X}_2) - \mathbf{z}(\mathbf{X}_2)\right)$ belong to *different* linear spaces, namely $T^*_{\nu_1}\mathcal{M}$ and $T^*_{\nu_2}\mathcal{M}$. The cotangent space $T^*\mathcal{M}$ does not coincides with a linear space unless special circumstances occur. As a consequences the integral of $\bar{\beta} - \mathbf{z}$ over $\mathfrak{b}$ is in general not defined. Really one could propose to make use in the same sense of a connection over $\mathcal{M}$ to 'transfer' all values of $\bar{\beta} - \mathbf{z}$ from their relevant cotangent space to a given $T^*_\nu\mathcal{M}$ selected as ambient for the integration. However, unless physical circumstances impose a specific connection, the choice of it is in certain sense of constitutive nature. An integral balance of substructural interactions (if we were able to think of it) should be intrinsic, i.e. independent on the choice of the connection over $\mathcal{M}$. The connection itself would induce a parallel transport that would be in general not bounded or, if bounded, not uniformly bounded and, above all, not isometric. So that the possible choice of a certain $T^*_\nu\mathcal{M}$ would be not invariant. The Riemannian connection would assure an isometric parallel transport over $\mathcal{M}$ but there is no physical reason to prefer the Riemannian connection to others. In summary, we cannot assume an integral version of the balance of substructural interactions as primitive principle unless $\mathcal{M}$ coincides with a linear space (see also [119]).

By making use of balance equations (18), (21) and Gauss theorem we get

$$\mathcal{P}^{ext}_{\mathfrak{b}}(\dot{\mathbf{x}}, \dot{\nu}) = \mathcal{P}^{int}_{\mathfrak{b}}(\dot{\mathbf{x}}, \dot{\nu}), \tag{23}$$

where

$$\mathcal{P}^{int}_{\mathfrak{b}}(\dot{\mathbf{x}}, \dot{\nu}) = \int_{\mathfrak{b}} \left(\mathbf{P} \cdot \dot{\mathbf{F}} + \mathbf{z} \cdot \dot{\nu} + \mathcal{S} \cdot \nabla\dot{\nu}\right) d^3\mathbf{X} \tag{24}$$

for differentiable rate fields.

Remark 3. If we consider $\dot{\mathbf{x}}$ and $\dot{\nu}$ as 'virtual' velocity fields, (23) takes the role of a version of the principle of virtual work, which is valid for multifield theories of complex bodies. In this way, (23) is a basic ingredient to construct appropriate finite element schemes for multifield theories as we shall see later. Really, one could assume in principle the relation (23) as a primary balance principle, by assuming it valid for *any choice* of velocity fields. Balance equations of standard and substructural interactions would follow as a consequence (see [78] for the exploitation of this point of view in the case of micromorphic bodies). In standard continuum mechanics this procedure is basically equivalent to the requirement of invariance with respect to classical changes in observer (the ones ruled by the action of $SO(3)$) of the sole external power of bulk and surface interactions. In the case of the mechanics of complex bodies, in the multifield sense described here, it is not so. The reason is that, if we postulate (23) as a primary principle, we must assume the existence of a self-force $\mathbf{z}$, while, if we require just $SO(3)$ invariance of the external power, we obtain the need of the existence of $\mathbf{z}$ as a consequence.

2.2.1 Inertial effects

Special physical circumstances may allow us to attribute to the material substructure own kinetic energy. A paradigmatic example is the case of incommensurate intergrowth com-

pounds, that are quasiperiodic alloy characterized by the presence of incommensurate sublattices that may displace one with respect to the other in a way such that kinetic energy may be associated with this special micro-displacement process [118].

In general, to indicate the substructural kinetic energy we make use of a function

$$\mathcal{K} : T^*\mathcal{M} \to \mathbb{R}^+ \tag{25}$$

such that

1. $\mathcal{K}(\nu, \mu)$ is equal to zero only when $\mu = \mathbf{0}$,
2. $\mathcal{K}(\nu, \lambda\mu) = \lambda^2 \mathcal{K}(\nu, \mu)$ with $\lambda \in \mathbb{R}$, i.e. $\mathcal{K}(\nu, \cdot)$ is of degree 2 in μ,
3. the second derivative $\partial^2_{\mu\mu}\mathcal{K}$ exists and is positive definite.

The *total kinetic energy* of an arbitrary part $\mathfrak{b}$ of the body is given by

$$\{\textit{kinetic energy of } \mathfrak{b}\} = \int_{\mathfrak{b}} \left(\frac{1}{2}\rho_0 \dot{\mathbf{x}} \cdot \dot{\mathbf{x}} + \mathcal{K}(\nu, \mu) \right) d^3\mathbf{X} \tag{26}$$

where ρ_0 is the referential density of mass.

Remark 4. The choice of a rather abstract function $\mathcal{K}(\cdot,\cdot)$ has defined above to represent the substructural kinetic energy is not due to a pure taste for abstract formalism. Really, the standard kinetic energy $\frac{1}{2}\rho_0 \dot{\mathbf{x}} \cdot \dot{\mathbf{x}}$ has the same properties of $\mathcal{K}(\cdot,\cdot)$. However, $T\mathcal{B}$ is a trivial bundle so that we may separate invariantly the velocity $\dot{\mathbf{x}}$ from the point $\mathbf{x}$ where it is attached. On the contrary, in general $T^*\mathcal{M}$ is not a trivial bundle so that we cannot separate ν from μ unless special physical circumstances (as in the case of incommensurate undergrowth compounds) allow us to think of μ independently of ν.

As anticipated above, both $\bar{\mathbf{b}}$ and $\bar{\beta}$ contain inertial contributions in additive manner so that we have

$$\bar{\mathbf{b}} = \mathbf{b} + \mathbf{b}^{(in)} \quad \text{and} \quad \bar{\beta} = \beta + \beta^{(in)} \tag{27}$$

where $\mathbf{b}^{(in)}$ and $\beta^{(in)}$ are the inertial components.

To identify them, we assume as a postulate that the rate of the total kinetic energy of any arbitrary part $\mathfrak{b}$ of the body in $\mathcal{B}_0$ equals the opposite of the power of inertial bulk interactions $\mathbf{b}^{(in)}$ and $\beta^{(in)}$ for any choice of the velocity fields, namely we assume that

$$\frac{d}{dt}\int_{\mathfrak{b}} \left(\frac{1}{2}\rho_0 \dot{\mathbf{x}} \cdot \dot{\mathbf{x}} + \mathcal{K}(\nu, \mu) \right) d^3\mathbf{X} + \int_{\mathfrak{b}} \left(\mathbf{b}^{(in)} \cdot \dot{\mathbf{x}} + \beta^{(in)} \cdot \dot{\nu} \right) d^3\mathbf{X} = \mathbf{0} \tag{28}$$

for *any* choice of $\dot{\mathbf{x}}$ and $\dot{\nu}$.

By developing the time derivative of the first addendum of (28), thanks to the arbitrariness of $\mathfrak{b}$ we find [17]

$$\mathbf{b}^{(in)} = -\rho_0 \ddot{\mathbf{x}}, \tag{29}$$

and

$$\beta^{(in)} = -\frac{d}{dt}\partial_{\dot{\nu}}\mathcal{X}(\nu, \dot{\nu}) + \partial_{\nu}\mathcal{X}(\nu, \dot{\nu}) \tag{30}$$

The function $\mathcal{X}$ is called *kinetic co-energy* and has the properties listed in what follows.

(i) Its Legendre transform $\sup_{\dot{\nu}\in T_\nu\mathcal{M}} \left(\partial_{\dot{\nu}}\mathcal{X}\cdot\dot{\nu}-\mathcal{X}\left(\nu,\dot{\nu}\right)\right)$ with respect to $\dot{\nu}$ is such that the sup is attained at a *unique* point in $T_\nu\mathcal{M}$.

(ii) Where the sup is attained, it coincides with the substructural kinetic energy, namely

$$\mathcal{K}\left(\nu,\mu\right)=\partial_{\dot{\nu}}\mathcal{X}\cdot\dot{\nu}-\mathcal{X},\quad \mu=\partial_{\dot{\nu}}\mathcal{X}. \tag{31}$$

Roughly speaking, the identification of $\beta^{(in)}$ by means of (28) is possible in terms of a function, namely $\mathcal{X}\left(\nu,\dot{\nu}\right)$, which is such that its Legendre transform coincides with the kinetic energy. This situation is not so exotic as it appears. Really, the same route is followed in identifying $\mathbf{b}^{(in)}$ but, since the standard kinetic energy is quadratic, it coincides with its Legendre transform. In other words, the interplay between $\mathcal{X}$ and $\mathcal{K}$ is the same interplay between Lagrangian and Hamiltonian densities.

After the identifications of the inertial terms $\mathbf{b}^{(in)}$ and $\beta^{(in)}$, the balance equations become

$$\mathbf{b}+Div\mathbf{P}=\rho_0\ddot{\mathbf{x}}, \tag{32}$$

$$\beta-\mathbf{z}+Div\mathcal{S}=\frac{d}{dt}\partial_{\dot{\nu}}\mathcal{X}\left(\nu,\dot{\nu}\right)-\partial_{\nu}\mathcal{X}\left(\nu,\dot{\nu}\right). \tag{33}$$

2.2.2 Eulerian representation of balance equations

Up to this point we have developed a Lagrangian picture of standard and substructural interactions. In other words, fields have been considered defined over $\mathcal{B}_0$ so that (32) and (33) hold pointwise in $\mathcal{B}_0$.

An actual (Eulerian) description of interactions is available by pushing forward the relevant quantities from $\mathcal{B}_0$ on $\mathcal{B}$. More specifically, in $\mathcal{B}$, the counterparts of (32) and (33) read

$$\mathbf{b}_a+div\sigma=\rho\dot{\mathbf{v}}, \tag{34}$$

$$\beta_a-\mathbf{z}_a+div\mathcal{S}_a=\frac{d}{dt}\partial_{v}\mathcal{X}\left(\nu_a,v\right)-\partial_{\nu_a}\mathcal{X}\left(\nu_a,v\right), \tag{35}$$

moreover (22) becomes

$$skew\sigma=\frac{1}{2}\mathsf{e}\left(\mathcal{A}^*\mathbf{z}_a+\left(grad\mathcal{A}^*\right)\mathcal{S}_a\right). \tag{36}$$

Here, σ denotes Cauchy stress and the subscript "a" means that the relevant quantities are the 'actual' counterpart of the original ones. More precisely, by means of inverse Piola's transform, one obtains

$$\sigma=\left(\det\mathbf{F}\right)^{-1}\mathbf{P}\mathbf{F}^T,\qquad \mathcal{S}_a=\left(\det\mathbf{F}\right)^{-1}\mathcal{S}\mathbf{F}^T, \tag{37}$$

$$\mathbf{b}_a=\left(\det\mathbf{F}\right)^{-1}\mathbf{b},\quad \mathbf{z}_a=\left(\det\mathbf{F}\right)^{-1}\mathbf{z},\qquad \beta_a=\left(\det\mathbf{F}\right)^{-1}\beta \tag{38}$$

In this way, we may recognize that at each $\mathbf{x}$ we have $\sigma\in Hom\left(T^*_{\mathbf{x}}\mathcal{B},T^*_{\mathbf{x}}\mathcal{B}\right)$ and $\mathcal{S}_a\in Hom\left(T^*_{\mathbf{x}}\mathcal{B},T^*_{\nu}\mathcal{M}\right)$. Moreover, $\mathbf{b}_a\in T^*_{\mathbf{x}}\mathcal{B}$ and $\mathbf{z}_a$, $\beta_a\in T^*_{\nu}\mathcal{M}$ exactly like $\mathbf{b}$, $\mathbf{z}$ and β. The way in which σ and $\mathcal{S}_a$ act is represented in Figure 3 where $\boldsymbol{\tau}$ represents here the *microtraction* (i.e. the contact interaction that we have represented with $\mathcal{S}\mathbf{n}$ in the expression of the external power) and $\mathbf{t}$ the standard traction (the one given by $\mathbf{P}\mathbf{n}$ in $\mathcal{P}^{ext}_{\mathfrak{b}}\left(\dot{\mathbf{x}},\dot{\nu}\right)$).

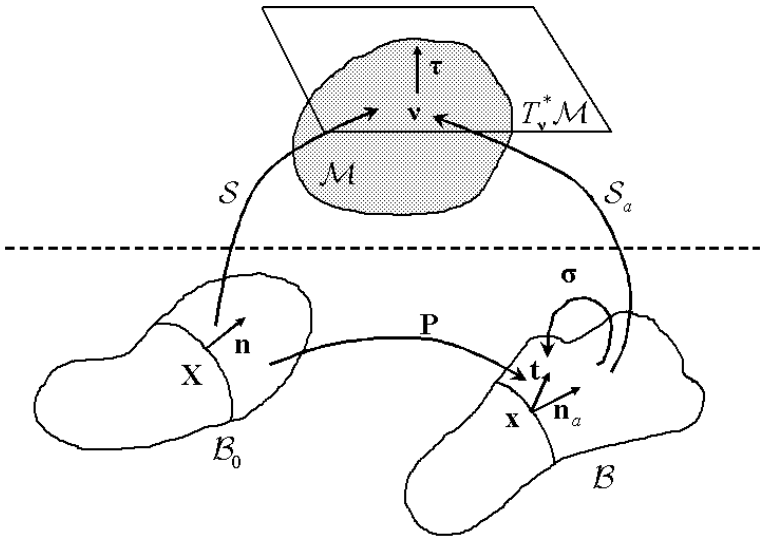

Figure 3. Scheme of the 'action' of stress measures

2.3 Constitutive Restrictions

The format developed in previous sections is common to all materials for which multifield representation of the morphology is necessary to account for prominent aspects of the substructural morphology even at 'minute' scales. Constitutive prescriptions select subclasses of complex materials (even before specifying the nature of $\mathcal{M}$). However, such (general) prescriptions cannot be selected at will. In fact, for the materials they characterize, all possible mechanical processes must satisfy the laws of thermodynamics, in particular the second law (see [39]). Here, for the sake of simplicity we restrict our treatment to the case of isothermal processes so that we make use of an isothermal version of the second law prescribing that the rate of free energy[9] of an arbitrary part $\mathfrak{b}$ minus the power of all external actions over $\mathfrak{b}$ is less or equal to zero for any choice of the velocity fields, namely

$$\frac{d}{dt}\int_{\mathfrak{b}} \psi d^3\mathbf{X} - P^{ext}_{\mathfrak{b}}\left(\dot{\mathbf{x}}, \dot{\nu}\right) \leq 0 \tag{39}$$

for any choice of $\dot{\mathbf{x}}$, $\dot{\nu}$ and $\mathfrak{b}$. In (39), ψ is the free energy density.

Notice that we are not considering possible migration of substructures from one material element to another[10].

Here, substructures remain always *within* the pertinent material element although they may undergo changes there even of irreversible nature.

By developing the time derivative in the first addendum of (39), since $\mathfrak{b}$ is fixed in time, thanks to the arbitrariness of $\mathfrak{b}$, the use of (23), from (39) we get

$$\dot{\psi} - \mathbf{P}\cdot\dot{\mathbf{F}} - \mathbf{z}\cdot\dot{\nu} - \mathcal{S}\cdot\nabla\dot{\nu} \leq \mathbf{0} \tag{40}$$

We treat first the case of elastic complex bodies. For them we assume constitutive structures of the type

$$\psi = \tilde{\psi}\left(\mathbf{F}, \nu, \nabla\nu\right), \tag{41}$$

[9]The existence of the free energy for a complex body can be proven by using the abstract thermodynamic formalism developed in [40].

[10]See [117] for a general treatment of migration, also [91] and [122] for special cases.

$$\mathbf{P} = \tilde{\mathbf{P}}\left(\mathbf{F}, \nu, \nabla\nu\right), \tag{42}$$

$$\mathbf{z} = \tilde{\mathbf{z}}\left(\mathbf{F}, \nu, \nabla\nu\right), \tag{43}$$

$$\mathcal{S} = \tilde{\mathcal{S}}\left(\mathbf{F}, \nu, \nabla\nu\right), \tag{44}$$

where we have omitted an *explicit* dependence on $\mathbf{X}$ for the sake of simplicity. $\nabla\nu$ accounts for weakly non-local effects of gradient type. When ν describes a multi-phase material structure (as in the case of two-phase materials in which the morphological descriptor is the volume fraction of one phase), $\nabla\nu$ allows us to spread over the bulk effects of minute diffused interfaces - a sort of regularization.

Moreover, once we have decided to account for the presence of $\nabla\nu$ in the constitutive list of entries of the free energy and the measures of interactions, the contemporary presence of ν is due to the circumstances that, in general, we cannot decompose invariantly $\nabla\nu$ from the pertinent ν. By developing the time derivative of ψ we get

$$\left(\partial_{\mathbf{F}}\psi - \mathbf{P}\right) \cdot \dot{\mathbf{F}} + \left(\partial_{\nu}\psi - \mathbf{z}\right) \cdot \dot{\nu} + \left(\partial_{\nabla\nu}\psi - \mathcal{S}\right) \cdot \nabla\dot{\nu} \leq 0, \tag{45}$$

for any choice of the rates involved. Really, for any choice of the state $(\mathbf{F}, \nu, \nabla\nu)$ we may select arbitrarily[11] the rates $\dot{\mathbf{F}}$, $\dot{\nu}$, $\nabla\dot{\nu}$, so that the validity of (45) implies

$$\mathbf{P} = \partial_{\mathbf{F}}\tilde{\psi}\left(\mathbf{F}, \nu, \nabla\nu\right), \tag{46}$$

$$\mathbf{z} = \partial_{\nu}\tilde{\psi}\left(\mathbf{F}, \nu, \nabla\nu\right), \tag{47}$$

$$\mathcal{S} = \partial_{\nabla\nu}\tilde{\psi}\left(\mathbf{F}, \nu, \nabla\nu\right). \tag{48}$$

Remark 5. In seeing (46)-(48), one realizes straight away that, in the *static* case (i.e. when inertial effects are neglected) and in presence of *conservative* standard and substructural *bulk* actions, the balances of standard and substructural interactions are the Euler-Lagrange equations associated with the energy functional

$$\int_{\mathcal{B}_0} \tilde{\psi}\left(\mathbf{F}, \nu, \nabla\nu\right) d^3\mathbf{X} - \int_{\mathcal{B}_0} \tilde{U}\left(\mathbf{x}, \nu\right) d^3\mathbf{X}, \tag{49}$$

where $\tilde{U}$ is the potential of conservative standard and substructural interactions, under suitable regularity conditions for ψ. Moreover, in this setting, by substituting (46)-(48) in (22) we realized that (22) itself is nothing but the condition assuring $SO\left(3\right)$ invariance of ψ (see [17]).

Special expressions of ψ are generalizations of Ginzburg-Landau energies so that we may have for example structures of the type

$$\psi = \tilde{\psi}\left(\mathbf{F}, \nu\right) + \frac{1}{2}\mathfrak{a}\left\|\nabla\nu\right\|^2 \tag{50}$$

[11] In fact, $\left(\dot{\mathbf{F}}, \dot{\nu}, \nabla\dot{\nu}\right)$ can be selected in an open set because no constraint are imposed.

where[12]

(i) $\tilde{\psi}(\cdot,\nu)$ is polyconvex in $\mathbf{F}$ and the dependence on ν may be of various nature;

(ii) $\mathfrak{a}$ is a constitutive constant;

(iii) $\|\nabla\nu\|$ indicates in a concise way $\|\nabla\nu\|^2_{Hom(T_{\mathbf{X}}\mathcal{B}_0,T_\nu\mathcal{M})}$.

Expressions of the type (50) appear in the case of two-phase materials, ferroelectrics, magnetoelastic bodies. The term $\frac{1}{2}\mathfrak{a}\|\nabla\nu\|^2$ is due to the spatial variation of the morphological descriptors implied by non-uniform distributions of substructures. It disappears in 'large body limit' that is when the effect of inhomogeneities or domain branching is negligible. Moreover, as mentioned previously, the term $\frac{1}{2}\mathfrak{a}\|\nabla\nu\|^2$ accounts also in a smeared sense for possible surface energy between phases.

As a further special case, if $\tilde{\psi}(\mathbf{F},\nu)$ satisfies the additive decomposition $\tilde{\psi}(\mathbf{F},\nu) = \tilde{\psi}_1(\mathbf{F}) + \tilde{\psi}_2(\nu)$, we may extract an immediate physical interpretation: $\tilde{\psi}_1(\mathbf{F})$ is the free energy associated with the relative change of place of neighboring material elements; $\tilde{\psi}_2(\nu)$ is the additional energetic contribution of substructural events occurring *within* the material element.

As a matter of fact, the free energy density ψ *cannot* depend on the rate of deformation and the rates of the morphological descriptor and its gradient.

To prove this statement, let us admit for a while that ψ could depend, say, on the rate of ν in a generalized way, namely $\psi = \tilde{\psi}(\mathbf{F},\nu,\nabla\nu,\dot{\nu})$. If so, by calculating the time derivative of ψ, we would obtain an inequality given by (45) with the left-hand side term augmented by an addendum of the type $\partial_{\dot{\nu}}\psi\cdot\ddot{\nu}$. As a consequence, since no measure of interaction is associated with $\ddot{\nu}$ in terms of power, the validity of the inequality for any choice of the velocity fields implies $\partial_{\dot{\nu}}\psi = 0$, which completes the proof.

However, when viscous effects occur at gross and substructural level, the Piola-Kirchhoff stress $\mathbf{P}$, the microstress $\mathcal{S}$ and the self-force $\mathbf{z}$ do depend on the rates $\dot{\mathbf{F}}$, $\dot{\nu}$, $\nabla\dot{\nu}$ which measure the 'removal' from 'thermodynamical equilibrium' where (46)-(48) hold.

The simplest case occur when just substructural viscosity occur *within* each material element in a way such that just the self-force $\mathbf{z}$ depends on $\dot{\nu}$ in addition to $\mathbf{F}$, ν, $\nabla\nu$. We follow the same way of reasoning adopted for standard viscosity in [39] and [163]. In this way we assume first that $\mathbf{z}$ be decomposed *additively* in its viscous and non-viscous components, namely

$$\mathbf{z} = \mathbf{z}^v + \mathbf{z}^{nv} \tag{51}$$

with

$$\mathbf{z}^{nv} = \tilde{\mathbf{z}}^{nv}(\mathbf{F},\nu,\nabla\nu), \tag{52}$$

$$\mathbf{z}^{v} = \tilde{\mathbf{z}}^{v}(\mathbf{F},\nu,\nabla\nu;\dot{\nu}), \tag{53}$$

with the restriction $\tilde{\mathbf{z}}^v(\mathbf{F},\nu,\nabla\nu;\mathbf{0}) = 0$.

Then we assume also that (41), (42) and (44) hold. In this way the point of view of our picture is that the free energy rules only the non-viscous parts of the stress measures. The local dissipation inequality (40) then becomes

$$(\partial_{\mathbf{F}}\psi - \mathbf{P})\cdot\dot{\mathbf{F}} + (\partial_\nu\psi - \mathbf{z}^{nv})\cdot\dot{\nu} + (\partial_{\nabla\nu}\psi - \mathcal{S})\cdot\nabla\dot{\nu} - \mathbf{z}^v\cdot\dot{\nu} \leq 0 \tag{54}$$

[12]Of course we may have cases in which the explicit dependence on $\mathbf{X}$ is necessary (as we will see later), so that we could have $\tilde{\psi}(\mathbf{X},\mathbf{F},\nu)$ and $\mathfrak{a}(\mathbf{X})$ [116].

and is valid for any choice of the velocity fields involved, so that we get (46)-(48) and

$$\mathbf{z}^v \cdot \dot{\nu} \geq 0 \tag{55}$$

which declares the purely dissipative nature of $\mathbf{z}^v$.

A solution of previous inequality is given by

$$\mathbf{z}^v = \lambda \dot{\nu} \tag{56}$$

with $\lambda = \tilde{\lambda}\left(\mathbf{F}, \nu, \nabla\nu\right)$, $\tilde{\lambda}$ a *scalar* definite positive function in some cases depending also on $\dot{\nu}$. As a consequence, in this case the balance of substructural interactions becomes

$$\beta - \mathbf{z}^{nv} + Div\mathcal{S} - \lambda\dot{\nu} = \frac{d}{dt}\partial_{\dot{\nu}}\mathcal{X} - \partial_{\nu}\mathcal{X} \tag{57}$$

Of course, another solution to (55) is given by $\mathbf{z}^v = \mathsf{A}\dot{\nu}$ with $\mathsf{A} \in Hom\left(T_\nu\mathcal{M}, T^*_\nu\mathcal{M}\right)$, at each $\mathbf{X}$, or, in components over $\mathcal{M}$, $\left(\mathbf{z}^v\right)_\alpha = \mathsf{A}_{\alpha\beta}\dot{\nu}^\beta$ with A definite positive, i.e. $\mathsf{A}_{\alpha\beta}\dot{\nu}^\alpha\dot{\nu}^\beta \geq 0$ for any choice of $\dot{\nu}$, the equality sign holding when $\dot{\nu} = \mathbf{0}$. The solution $\mathbf{z}^v = \mathsf{A}\dot{\nu}$ reduces to (56) when $\mathsf{A}_{\alpha\beta} = \lambda\delta_{\alpha\beta}$. Finally, we may consider $\mathbf{z}^v$ as the derivative with respect to $\dot{\nu}$ of the dissipation potential given by $\frac{1}{2}\mathsf{A}_{\alpha\beta}\dot{\nu}^\alpha\dot{\nu}^\beta$, a sort of Rayleigh function over $\mathcal{M}$.

In this special case $\mathbf{z}^v \cdot \dot{\nu}$ is the substructural (mechanical) production of entropy.

The issue becomes more complicated when additional gradient substructural viscosity and gross viscosity - i.e. friction between adjacent material elements - occur. In this case, decompositions of $\mathbf{P}$ and $\mathcal{S}$ in their viscous and non-viscous components are necessary in addition to (51). They read

$$\mathbf{P} = \mathbf{P}^{nv} + \mathbf{P}^v \tag{58}$$

$$\mathcal{S} = \mathcal{S}^{nv} + \mathcal{S}^v \tag{59}$$

Now we have

$$\mathbf{P}^v = \tilde{\mathbf{P}}^v\left(\mathbf{F}, \nu, \nabla\nu; \dot{\mathbf{F}}, \dot{\nu}, \nabla\dot{\nu}\right), \tag{60}$$

$$\mathcal{S}^v = \tilde{\mathcal{S}}^v\left(\mathbf{F}, \nu, \nabla\nu; \dot{\mathbf{F}}, \dot{\nu}, \nabla\dot{\nu}\right), \tag{61}$$

$$\mathbf{z}^v = \tilde{\mathbf{z}}^v\left(\mathbf{F}, \nu, \nabla\nu; \dot{\mathbf{F}}, \dot{\nu}, \nabla\dot{\nu}\right), \tag{62}$$

while the non-viscous components still satisfy (42)-(44) and the constitutive structure of the free energy is given by (41).

The viscous parts of the stress measures satisfy also the restrictions

$$\tilde{\mathbf{P}}^v\left(\mathbf{F}, \nu, \nabla\nu; \mathbf{0}, \mathbf{0}, \mathbf{0}\right) = \mathbf{0}, \tag{63}$$

$$\tilde{\mathcal{S}}^v\left(\mathbf{F}, \nu, \nabla\nu; \mathbf{0}, \mathbf{0}, \mathbf{0}\right) = \mathbf{0}, \tag{64}$$

$$\tilde{\mathbf{z}}^v\left(\mathbf{F}, \nu, \nabla\nu; \mathbf{0}, \mathbf{0}, \mathbf{0}\right) = \mathbf{0} \tag{65}$$

In this case, if we follow the same path leading to (55), we obtain instead of (55) itself its counterpart given by

$$\mathbf{P}^v \cdot \dot{\mathbf{F}} + \mathcal{S}^v \cdot \nabla\dot{\nu} + \mathbf{z}^v \cdot \dot{\nu} \geq 0 \tag{66}$$

As solution to (66) we find $\mathbf{P}^v$, $\mathcal{S}^v$ and $\mathbf{z}^v$ as linear functions of $\dot{\mathbf{F}}$, $\nabla\dot{\nu}$ and $\dot{\nu}$ with tensor coefficients depending on $\mathbf{F}$, $\nabla\nu$ and ν, namely

$$\begin{aligned} \tilde{\mathbf{P}}^v &= \mathsf{A}_1^{(\mathbf{P})}\dot{\mathbf{F}} + \mathsf{A}_{\mathbf{2}}^{(\mathbf{P})}\dot{\nu} + \mathsf{A}_3^{(\mathbf{P})}\nabla\dot{\nu}, \\ \tilde{\mathcal{S}}^v &= \mathsf{A}_1^{(\mathcal{S})}\dot{\mathbf{F}} + \mathsf{A}_{\mathbf{2}}^{(\mathcal{S})}\dot{\nu} + \mathsf{A}_3^{(\mathcal{S})}\nabla\dot{\nu}, \\ \tilde{\mathbf{z}}^v &= \mathsf{A}_1^{(\mathbf{z})}\dot{\mathbf{F}} + \mathsf{A}_{\mathbf{2}}^{(\mathbf{z})}\dot{\nu} + \mathsf{A}_3^{(\mathbf{z})}\nabla\dot{\nu}. \end{aligned} \tag{67}$$

Of course, the linear operator represented by

$$\begin{pmatrix} \mathsf{A}_1^{(\mathbf{P})} & \mathsf{A}_2^{(\mathbf{P})} & \mathsf{A}_3^{(\mathbf{P})} \\ \mathsf{A}_1^{(\mathcal{S})} & \mathsf{A}_2^{(\mathcal{S})} & \mathsf{A}_3^{(\mathcal{S})} \\ \mathsf{A}_1^{(\mathbf{z})} & \mathsf{A}_2^{(\mathbf{z})} & \mathsf{A}_3^{(\mathbf{z})} \end{pmatrix} \tag{68}$$

must be *definite positive* at each $\mathbf{X}$ (see the analogous case of thermoelastic simple bodies with viscosity effects discussed in [163]). However, the reduced dissipation inequality (66) does not imply that each single addendum be semi-positive definite. On the other hand, if we prescribe (in certain sense as *additional* dissipation inequalities) that each viscosity mechanism be intrinsically dissipative, i.e. that

$$\begin{aligned} \mathbf{P} \cdot \dot{\mathbf{F}} &\geq 0, \\ \mathcal{S} \cdot \nabla\dot{\nu} &\geq 0, \\ \mathbf{z} \cdot \dot{\nu} &\geq 0. \end{aligned} \tag{69}$$

independently, then (68) becomes diagonal.

Remark 6 We know that the dependence on the rates is just the simplest way to account for viscous effects. The theory of standard materials with memory would deserve to be extended to the multifield setting treated here. Concrete examples such as *relaxor ferroelectrics* - for which vanishing memory effects are prominent - suggest the need of this kind of development of the general theory. Really, when $\dot{\mathbf{F}}$, $\dot{\nu}$, and $\nabla\dot{\nu}$ are present in the list of constitutive entries, we are dealing with complex materials of "differential" type, a special class of complex materials with memory.

Once (46)-(48) have been derived, it is immediate to obtain the constitutive structures of the spatial counterparts of the measures of interactions by using (37) and (38).

2.3.1 A generalized Doyle-Ericksen formula

A purely spatial description of the mechanism of complex body is available (see [21], [97]). With the words "purely spatial" we indicate that no reference configuration $\mathcal{B}_0$ is considered and used as a paragon setting for lengths or as domain of definition of various fields. The body occupies only the region $\mathcal{B}$ 'here and now', all fields are defined just over $\mathcal{B}$.

In the elastic case, in which the body is characterized by the elastic energy $e(\cdot)$ and we consider the velocity fields (5) and (6) over $\mathcal{B}$, the conservation of energy in a part $\mathfrak{b}_a$ of $\mathcal{B}$ reads

$$\delta\left(\int_{\mathfrak{b}_a} e d^3\mathbf{x}\right) - P^{int}_{\mathfrak{b}_a}(\mathbf{v}, v) = 0 \tag{70}$$

where δ indicates the variation of the total elastic energy in $\mathfrak{b}_a$, namely $\int_{\mathfrak{b}_a} ed^3\mathbf{x}$; and

$$P^{int}_{\mathfrak{b}_a}(\mathbf{v}, \upsilon) = \int_{\mathfrak{b}_a} (\sigma \cdot grad\mathbf{v} + \mathbf{z}_a \cdot \upsilon + \mathcal{S}_a \cdot grad\upsilon)\, d^3\mathbf{x} \tag{71}$$

The velocity $\mathbf{v}$ and the actual rate υ of the morphological descriptor are chosen as *virtual* fields. In particular, we presume that $\mathbf{v}(\cdot,\cdot)$ be of pure deformative nature, i.e. $skew\,(grad\mathbf{v}) = \mathbf{0}$.

We assume that $e\,(\cdot)$ admits constitutive structure of the type

$$e = \tilde{e}\,(\mathbf{g}, \nu_a, grad\nu_a)\,, \tag{72}$$

where $\mathbf{g}$ is the metric in space, so that

$$\delta e = \partial_{\mathbf{g}} e \cdot \delta\mathbf{g} + \partial_{\nu_a} e \cdot \delta\nu_a + \partial_{grad\nu_a} e \cdot \delta grad\nu_a. \tag{73}$$

Analogous constitutive structures are presumed for σ, $\mathbf{z}_a$, and $\mathcal{S}_a$. Notice that no reference to $\mathcal{B}_0$ is made. The deformation is only accounted for by means of the dependence of the energy on the metric in space.

To specify the nature of the variations involved, we first consider $\mathbf{g}$ dragged along the flow $\mathbf{v}$ so that $\delta\mathbf{g}$ coincides with the autonomous Lie derivative $L_{\mathbf{v}}\mathbf{g}$ of $\mathbf{g}$ along $\mathbf{v}$ ($\mathbf{g}$ does not depend explicitly on time) and we have

$$\delta\mathbf{g} = L_{\mathbf{v}}\mathbf{g} = 2sym\,(grad\mathbf{v}) = 2grad\mathbf{v} \tag{74}$$

The last equality holds because we have assumed $skwgrad\mathbf{v} = \mathbf{0}$.

Moreover, we put

$$\delta\nu = \upsilon, \tag{75}$$

$$\delta grad\nu = grad\upsilon + (grad\nu)\, grad\mathbf{v}. \tag{76}$$

By substituting (74)-(76) in (70), the arbitrariness of $\mathbf{v}$ and υ allows us to get

$$\mathbf{z}_a = \partial_{\nu_a} e, \tag{77}$$

$$\mathcal{S}_a = \partial_{grad\nu_a} e, \tag{78}$$

$$\sigma = \mathbf{2}\partial_{\mathbf{g}} e - (grad\nu_a)^*\, \mathcal{S}_a. \tag{79}$$

The last identity is a generalized version of Doyle-Ericksen formula [21]. With respect to the case of standard elasticity (see [56], [129]) the new additional term $-(grad\nu_a)^*\,\mathcal{S}_a$ governs the transfer of energy from the substructural level to the macroscopic level. Its contribution appears evident in complex fluids where it governs strictly the possibility of topological transitions that may develop along flows [115].

2.4 Differences and Analogies with Internal Variable Models

After having displayed the essential elements of the mechanics of complex bodies, it is natural to underline analogies and differences with internal variable models that are largely used to describe microstructural effects in various circumstances. To clarify the issue one should come back to the 1967 paper [38] where the format of internal variable models is

first presented in the realm of the continuum mechanics of deformable bodies (see also [160], [134], [135], [136] for basic results on this matter). Roughly speaking, one imagines to have a list of variables, collected in a vector $\alpha \in \mathbb{R}^n$, describing the 'internal' state of each material element and satisfying a general evolution law of the type[13]

$$\dot{\alpha} = \bar{\omega}\,(\mathbf{F}, \alpha) \tag{80}$$

postulated *a priori*.

Both the first Piola-Kirchhoff stress $\mathbf{P}$ and the free energy depend on α, namely

$$\mathbf{P} = \tilde{\mathbf{P}}\,(\mathbf{F}, \alpha) \qquad , \qquad \psi = \tilde{\psi}\,(\mathbf{F}\,\alpha)\,. \tag{81}$$

Moreover, as usual, $\mathbf{P}$ is given by

$$\mathbf{P} = \partial_{\mathbf{F}}\psi, \tag{82}$$

and satisfies the standard Cauchy balance (18). The reduced dissipation inequality reads

$$\partial_\alpha \psi \cdot \dot{\alpha} \geq \mathbf{0} \tag{83}$$

However, (83) does not mean that ψ cannot depend on α, because $\dot{\alpha}$ cannot be selected at will since it is ruled by (80) so that (83) becomes

$$\partial_\alpha \psi \cdot \bar{\omega} \geq \mathbf{0} \tag{84}$$

which is a restriction on the possible structures of ψ and $\bar{\omega}$.

Differences and analogies appear then evident.

1. In internal variable models, α measures exclusively the removal from thermodynamic equilibrium by means of irreversible processes 'ruled' by (80) and (84). When conservative processes develop, internal variable models reduce to *standard* elasticity and α plays just a parametric role. When, in fact, $\dot{\alpha} = 0$ in the scheme above there is no production of entropy because $\partial_\alpha \psi \cdot \bar{\omega} = 0$ and (80) reduces to a sort of internal 'constraint' $\bar{\omega}\,(\mathbf{F}, \alpha) = 0$.

2. On the contrary, in the setting of multifield theories, the one described in previous sections, when mechanical process are conservative and the range is elastic, a *non-standard* elasticity occur and may allow us to obtain unusual results as we shall see later in developing concrete examples.

3. No crude interactions are associated with α in a direct sense. The expression of the external power includes just standard forces. The derivative of the free energy with respect to α represents only an affinity quantifying the sole production of entropy by means of (84).

4. A direct action on the material texture of possible external actions such as electromagnetic fields is not accounted for in (80).

5. Formally, we may link models with internal variables with the multifield setting described here. Let the following hypotheses apply:

   (i) There aren't external bulk actions over the substructure, i.e. $\beta = 0$.

[13] The temperature and its gradient may be added in the list of entries of $\bar{\omega}$ in non-isothermal problem.

(ii) Substructural inertia is absent.

(iii) Substructural actions of contact nature are absent. Each material element is a solitary individual that does not interact with its neighboring fellows. The microstress $\mathcal{S}$ is then completely absent (as it occurs for example in dilute solutions of bubbles).

(iv) The rate of the morphological descriptor is associated with substructural viscous effects *within* each material element.

With these assumptions, the free energy density ψ has a constitutive structure of the type $\psi = \tilde{\psi}(\mathbf{F}, \nu)$ and the balance of substructural interactions reduces to

$$\mathbf{z} = \mathbf{0}. \tag{85}$$

However, since substructural inertia occurs, $\mathbf{z}$ can be decomposed in its irreversible and reversible components so that (85) becomes

$$\mathbf{z}^v = -\mathbf{z}^{nv}, \tag{86}$$

with $\mathbf{z}^v$ given by (56). As a consequence, (86) reduces to

$$\dot{\nu} = -\frac{1}{\lambda}\partial_\nu \psi(\mathbf{F}, \nu) \tag{87}$$

which coincides formally with (80) when we put

$$\bar{\omega}(\cdot, \cdot) = -\frac{1}{\lambda}\partial_\nu \psi(\cdot, \cdot) \tag{88}$$

with λ the second derivative with respect to $\dot{\nu}$ of a Rayleigh function over $\mathcal{M}$ as recalled above.

In this way, in the sense summarized above, internal variable models may be considered as special cases of multifield theories. The description of specific physical circumstances may suggest us the appropriate point of view.

2.5 Some Example of Complex Materials

Below we indicate a first list of special cases of complex bodies. However, before going in details, we recall briefly our *familiar lexicon*.

$\mathcal{M}$ is the *manifold of substructural shapes*, while each element ν of it is a *morphological descriptor* of the substructure within the material element 'collapsed' at $\mathbf{X}$. The rate $\dot{\nu} \in T_\nu\mathcal{M}$ is the *rate of change* (even of virtual nature) of the substructure at $\mathbf{X}$. *Substructural interactions* are actions *within* each material element ($\mathbf{z}$) and *between* neighboring material elements ($\mathcal{S}$), due to substructural rearrangements.

To construct any special model of a complex material in the *general model building framework* described above, we need first to have a sort of ideal picture of the material element and to select consequently the morphological descriptor and the nature of $\mathcal{M}$. Once the morphology of the material substructure has been described geometrically, one should select an appropriate explicit form of the free energy and possible dissipation potentials or - more simply - viscous coefficients. Symmetry requirements, experimental data and identification from ideal lattice models of the material element may help in selecting the form of the energy and, in general, in determining the values of constitutive coefficients.

2.5.1 Porous and multi-phase bodies

When pores are finely distributed throughout a body, we may imagine that each material element be a patch of matter with spherical voids and select the morphological descriptor as a scalar indicating the *void volume fraction* of the material patch at $\mathbf{X}$. In this case $\mathcal{M}$ reduces to the interval of the real axis $[0,1]$ and $\mathcal{A}$ vanishes identically. Substructural bulk measures of interaction β and $\mathbf{z}$ reduce to scalars β and z, while the microstress $\mathcal{S}$ is a vector (see [148], [44], [43], [121]). Since $\mathcal{A}$ vanishes identically, the procedure based on the invariance of external power fails and this special case seems to be pathological with respect to it. Formally, one may circumvent the problem by using as a morphological descriptor a spherical second order tensor. In this way one may obtain the balance of substructural interactions as in previous sections, then, since one may select ν as $a\mathbf{I}$, with $\mathbf{I}$ the second order unit tensor and $a = \tilde{a}\,(\mathbf{X}, t)$, one may reduce to the scalar case straight away.

In the case of *linear elastic materials with voids*, by indicating with ε the infinitesimal strain tensor $\varepsilon = \mathrm{sym}\nabla\mathbf{u}$ ($\mathbf{u}$ is the displacement), linear constitutive equations are associated with the free energy ψ coincident with a quadratic form in ε, ν and $\nabla\nu$ (ν is now a scalar). Additionally, one can take into account viscous effects due to the surface tension at pores by using the procedure described in Section 2.3. Then, one obtains for elastic porous materials the following constitutive relations with damping:

$$\sigma_{ij} = C_{ijhk}\varepsilon_{hk} + C^{(1)}_{ijk}\nu_{,k} + C^{(2)}_{ij}\nu, \tag{89}$$

$$z = C^{(3)}\dot{\nu} - C^{(4)}\nu - C^{(5)}_{ij}\varepsilon_{ij} - C^{(6)}_{i}\nu_{,i}, \tag{90}$$

$$\mathcal{S}_i = C^{(7)}_{ij}\nu_{,j} + C^{(8)}_{ijk}\varepsilon_{jk} + C^{(9)}_{i}\nu, \tag{91}$$

where C_{ijhk} is the usual stiffness tensor and $C^{(i)}$ are appropriate constitutive tensors, vectors or scalars (the tensor order is indicated in the formulas above). As usual, $\nu_{,i}$ denotes the derivative $\partial_{x^i}\nu$.

In the isotropic case, previous relations reduce to

$$\sigma_{ij} = \lambda\delta_{ij}\varepsilon_{hh} + 2\mu\varepsilon_{ij} + \xi^{(1)}\nu\delta_{ij}, \tag{92}$$

$$z = -\xi^{(2)}\dot{\nu} - \xi^{(3)}\nu - \xi^{(1)}\varepsilon_{hh}, \tag{93}$$

$$\mathcal{S}_i = \xi^{(4)}_{i}\nu_{,i}, \tag{94}$$

where δ_{ij} is the unit tensor, λ and μ are the standard Lamé constants. The inequalities

$$\mu > 0\ ,\ \xi^{(4)} \geqslant 0\ ,\ \xi^{(3)} \geqslant 0 \tag{95}$$

$$3\lambda + 2\mu \geqslant 0\ ,\ \ (3\lambda + 2\mu)\,\xi^{(3)} \geqslant 12\xi^{(1)} \tag{96}$$

apply. They assure uniqueness and weak stability of solution to the balance equations.

The scheme described above can be used also for granular matter [79], [149] and for two-phase materials. In the latter case, ν represents the volume fraction of one phase or

may be the indicator function of some phase, i.e. ν is zero if there one of the two phases is absent and is equal to 1 when only that phase is present.

Transition layers are identified throughout the body as the thin layers where $\nabla\nu$ undergoes large oscillations. During the evolution of phase transitions, the order parameter is governed by the balance of substructural interactions where terms like $\mathbf{z}^v$ are accounted for (see [151], [41], [73], [74]).

In the case of multi-phase materials one may choose as order parameter a list

$$\nu = (\nu_1, ..., \nu_N)\,, \tag{97}$$

whose entries take values on $[0, 1]$ and are subjected to the constraint

$$\sum_{i=1}^{N} \nu_i = 1, \tag{98}$$

thus only N-1 entries are independent.

In this case $\mathcal{M}$ becomes the cube

$$[0, 1] \times ... \times [0, 1] \quad N \textit{ times.} \tag{99}$$

If we look just to standard non-linear elasticity, in the case of multi-phase materials we have non-convex multi-well potentials. The scheme described above allows one to 'approximate' such a potential.

Solid-to-solid phase transitions in shape memory alloys may be also described by combining scalar and second-order tensor valued morphological descriptors, the latter allow us to account for the re-orientation of martensitic variants, as proposed in [8].

2.5.2 Ferroelectrics

Barium Titanate $BaTiO_3$ and the large family of PZT perovskite are examples of materials experiencing spontaneous polarization associated with crystalline rearrangements at a critical temperature called *Curie temperature*. Also, applied strain and external electric fields influence the local polarization state. Such materials are called *ferroelectrics*. They are used for various sophisticated devices and the literature about them is abundant (see, e.g., [80], [81], [158], [186], [187], [45], [46], [47]). For them the material element is just the crystalline cell and we describe the polarization state *within* it by means of a vector.

At each $\mathbf{X}$ we indicate the polarization vector by p, take it as *morphological descriptor* and assume that $0 \leq |\mathsf{p}| \leq p_m$, with p_m a material constant. Then $\mathcal{M}$ is the ball of radius p_m in $\mathbb{R}^3$. We also consider the body subjected to an external electric field $\mathfrak{E}$.

Balance equations are formally identical to (18), (21) and (22). $\mathcal{A}$ is the second order tensor $-\mathsf{p}\times$ (in components $(-\mathsf{p}\times)_{ij} = \mathsf{e}_{ijk}\mathsf{p}_k$, with e_{ijk} the alternating symbol). As a consequence, the relation (12) becomes $\dot{\mathsf{p}}^* = \dot{\mathsf{p}} + \mathsf{p} \times \dot{\mathbf{q}}$. Here, the microstress $\mathcal{S}$ accounts for interactions between neighboring crystals with different polarizations; $\mathbf{z}$ measures self-interactions within each polarized crystal. To include the effects of the applied electric field in the balance equations, we assume that the bulk interactions $\bar{\mathbf{b}}$ and $\bar{\beta}$ and the boundary 'tractions' $\mathbf{t} = \mathbf{P}\mathbf{n}$ and $\tau = \mathcal{S}\mathbf{n}$ can be decomposed additively in electromechanical (em) and purely electric parts (el), namely

$$\bar{\mathbf{b}} = \mathbf{b}_{em} + \mathbf{b}_{el}, \tag{100}$$

$$\bar{\beta} = \beta_{em} + \beta_{el}, \tag{101}$$

$$\mathbf{t} = \mathbf{t}_{em} + \mathbf{t}_{el}, \tag{102}$$

$$\tau = \tau_{em} + \tau_{el}. \tag{103}$$

For any arbitrary part $\mathfrak{b}$ of $\mathcal{B}$, the purely electric parts are defined by assuming that their power on any part $\mathfrak{b}$ equals the rate of electric energy in $\mathfrak{b}$. In other words, one postulates the validity of the balance

$$\frac{d}{dt} D(\mathfrak{b}) + \int_{\mathfrak{b}} (\mathbf{b}_{el} \cdot \dot{\mathbf{x}} + \beta_{el} \cdot \dot{\mathsf{p}})\, d^3\mathbf{X} + \int_{\partial\mathfrak{b}} (\mathbf{t}_{el} \cdot \dot{\mathbf{x}} + \tau_{el} \cdot \dot{\mathsf{p}})\, d\mathcal{H}^2 = 0, \tag{104}$$

where

$$D(\mathfrak{b}) = -\frac{1}{2} \int_{\mathfrak{b}} \rho \mathfrak{E} \cdot \mathsf{p} d^3\mathbf{X} \tag{105}$$

is the *electric energy* in $\mathfrak{b}$, associated with the local polarization state. We assume that such a balance holds (within classical limits) for any choice of the rates $\dot{\mathbf{x}}$ and $\dot{\mathsf{p}}$ involved.

A theorem of Tiersten [178] give us the explicit expression of the rate of D in the current configuration. We write the Lagrangian version of Tiersten's formula by pulling it back in the reference configuration so that we get

$$\frac{d}{dt} D(\mathfrak{b}) = -\int_{\mathfrak{b}} \rho\, (grad \mathfrak{E})\, \mathsf{p} \cdot \dot{\mathbf{x}} d^3\mathbf{X} - \int_{\partial\mathfrak{b}} \frac{1}{2} (\det \mathbf{F})\, p_n^2 \mathbf{F}^{-T} \mathbf{n} \cdot \dot{\mathbf{x}} d\mathcal{H}^2 - \int_{\mathfrak{b}} \rho \mathfrak{E} \cdot \dot{\mathsf{p}} d^3\mathbf{X}, \tag{106}$$

where p_n is the normal component of p. The arbitrariness of the rates $\dot{\mathbf{x}}$ and $\dot{\mathsf{p}}$ and the validity of (104) allow us to identify corresponding terms, namely

$$\mathbf{b}_{el} = \rho\, (grad \mathfrak{E})\, \mathsf{p}, \tag{107}$$

$$\beta_{el} = \rho \mathfrak{E}, \tag{108}$$

$$\mathbf{t}_{el} = \frac{1}{2} (\det \mathbf{F})\, p_n^2 \mathbf{F}^{-T} \mathbf{n}, \tag{109}$$

$$\tau_{el} = 0, \tag{110}$$

where $p_n = \mathsf{p} \cdot \mathbf{n}$. Consequently, the balance equations (18) and (21) become

$$\mathbf{b}_{em} + Div \mathbf{P} + \rho\, (grad \mathfrak{E})\, \mathsf{p} = 0, \tag{111}$$

$$\beta_{em} - \mathbf{z} + Div \mathcal{S} + \rho \mathfrak{E} = 0, \tag{112}$$

where $\mathbf{b}_{em}$ and β_{em} include the inertial terms as ever.

2.5.3 Cosserat materials

The scheme of Cosserat materials is a special case of multifield theories often used for *direct models of structural elements* like *beams*, *plates* or *shells* [66], [3] or to model *composites reinforced with diffused small rigid fibers*. Each material element is considered as a *rigid body* which can rotate independently of the neighboring fellows. In this way, ν can be naturally chosen as a proper orthogonal tensor $\mathbf{Q}$ (thus, an orthogonal matrix with determinant equal to 1) describing the independent rigid rotation of the material element and $\mathcal{M}$ coincides with the special orthogonal group $SO(3)$.

More simply, it is also possible to describe the independent rigid rotation of each material element by means of vector-valued order parameters ω (see [17] for the connection between the tensor representation and the vectorial representation of Cosserat materials; see also [87] and [147]).

Contact interactions are then the traction $\mathbf{t}$ and a contact couple $\mathfrak{m}$. This couple develops power in the rate of rigid independent rotation of each material element. At each virtual surface 'cut' in $\mathcal{B}_0$, $\mathfrak{m}$ is considered a function of the place, possibly of the time and of the normal to the surface 'cut' itself: $\mathfrak{m} = \hat{\mathfrak{m}}(\mathbf{X}, t, \mathbf{n})$. An analogous of Cauchy's theorem holds and it is possible to prove the existence of a second order tensor $\mathbb{M}$ such that

$$\mathbb{M}\mathbf{n} = \mathfrak{m} \tag{113}$$

The tensor $\mathbb{M}$ is a linear transformation from $\Re^3$ into itself: thus it is an element of $Hom\left(\mathbb{R}^3, \mathbb{R}^3\right)$. The couple $\mathfrak{m}$ is power conjugated with $\dot{\omega}$. In the expression of the external power, β describes possible applied body couples, so that, after the usual invariance procedure on a part $\mathfrak{b}$ of $\mathcal{B}_0$ of $\mathcal{P}_{\mathfrak{b}}^{ext}(\dot{\mathbf{x}}, \dot{\omega})$ - where now $\dot{\omega}$ is a specification of $\dot{\nu}$ -, we get the standard integral balance of forces (16) and an integral balance of couples given by

$$\int_{\mathfrak{b}} \left((\mathbf{x} - \mathbf{x}_0) \times \bar{\mathbf{b}} + \beta\right) d^3\mathbf{X} + \int_{\mathfrak{b}} \left((\mathbf{x} - \mathbf{x}_0) \times \mathbf{P}\mathbf{n} + \mathbb{M}\mathbf{n}\right) d\mathcal{H}^2. \tag{114}$$

The arbitraryness of $\mathfrak{b}$ implies

$$Div\mathbb{M} + \beta - \mathsf{e}\mathbf{P}\mathbf{F}^T = \mathbf{0} \tag{115}$$

which displays the standard results that in Cosserat materials Cauchy stress is not symmetric.

In the case of infinitesimal deformations, the linearized measure of infinitesimal strain ε_c displais clearly the influence on the gross deformation of the local independent rotation. It reads

$$\varepsilon_c = \nabla\mathbf{u} - \mathsf{e}\omega. \tag{116}$$

Cosserat's scheme has been developed not only in elastic range. Cosserat plasticity is available and has been formulated in [54] and [174] to account for plastic phenomena. Hardening has been introduced in [114].

2.5.4 Strain gradient dependent materials

Lenght scale dependent effects are recognized in material behavior by means of various types of experiments. A paradigmatic example is Hall-Petch effect [94], [152]: The strength of polycrystalline aggregates increases with decreasing grain size. Various other experimental evidences of length scale dependent effects can be found in the current scientific literature (see, e.g., [131], [145], [159]). These effects are due to non-local interactions with limited range so that they may be described by resorting to higher order gradients of deformation. However, it is not possible in principle to add simply higher order gradients of $\mathbf{F}$ to the list of state variables and to maintain a form of the dissipation inequality analogous to the one of simple materials. In fact, with reference to elastic processes, a constitutive choice for the free energy of the type $\psi = \Psi(\tilde{\mathbf{x}}(\cdot))$, with $\Psi(\tilde{\mathbf{x}}(\cdot))$ a functional of the entire deformation, is incompatible with a local dissipation inequality of the form $\dot{\psi} - \mathbf{P} \cdot \dot{\mathbf{F}} \leq 0$, unless $\psi = \tilde{\psi}(\mathbf{F})$ (see [89]). Of course, a special case of $\psi = \Psi(\tilde{\mathbf{x}}(\cdot))$ is a structure of the form $\psi = \tilde{\psi}\left(\mathbf{F}, \nabla\mathbf{F}, \nabla^2\mathbf{F}, ..., \nabla^n\mathbf{F}\right)$.

An analogous result when ψ is of the type $\psi = \tilde{\psi}\left(\mathbf{F},\nabla\mathbf{F},\nabla^2\mathbf{F},...,\nabla^n\mathbf{F},\alpha\right)$, with α some list of internal variables [161].

To assure thermodynamic compatibility to constitutive expressions of the form $\psi = \tilde{\psi}\left(\mathbf{F},\nabla\mathbf{F}\right)$, or e.g. $\psi = \tilde{\psi}\left(\mathbf{F},\nabla\mathbf{F},\nabla^2\mathbf{F}\right)$, appearing in second- and third-grade elasticity, it is necessary to modify the mechanical dissipation inequality by adding a rate of supply of mechanical energy that we denote here with $(*)$ - as shown first in [57]. The modified expression of the mechanical dissipation inequality is then given by

$$\dot{\psi} - \mathbf{P}\cdot\dot{\mathbf{F}} - (*) \leq 0. \tag{117}$$

However, the nature of $(*)$ is left unspecified in [57]. A basic result presented first in [15] shows us that the general framework of multifield theories allows us to specify completely the nature of the rate of supply of mechanical energy $(*)$. Really, we need two ingredients:

(*i*) absence of bulk interactions acting directly on the substructure, namely $\bar{\beta} = \mathbf{0}$, and

(*ii*) an internal constraint linking directly the morphological descriptor to the gross deformation, that is, for example, $\nu = \tilde{\nu}\left(\mathbf{F}\right)$.

Under these conditions, we say that the substructure is *latent*: "Though its effects are felt in the balance equations, all relevant quantities can be expressed in terms of geometric quantities pertaining to apparent placements" [15]. Of course, the concept of latence is not exclusively restricted to the assumption of an internal constraint of type $\nu = \tilde{\nu}\left(\mathbf{F}\right)$. Temperature, higher order gradients of $\mathbf{F}$ and their rates may occur in the list of entries of $\tilde{\nu}\left(\cdot\right)$. Here, the choice of $\nu = \tilde{\nu}\left(\mathbf{F}\right)$ allows us just to explain how second grade elasticity can be considered as a special case of the multifield setting.

As a consequence of (i), the local version of the local mechanical dissipation inequality (40) reduces to

$$\dot{\psi} - \mathbf{P}\cdot\dot{\mathbf{F}} - Div\left(\mathcal{S}\dot{\nu}\right) \leq 0, \tag{118}$$

so that, by comparison with (117), we get

$$(*) = Div\left(\mathcal{S}\dot{\nu}\right). \tag{119}$$

The constraint $\nu = \tilde{\nu}\left(\mathbf{F}\right)$ implies that the constitutive structure $\psi = \tilde{\psi}\left(\mathbf{F},\nu,\nabla\nu\right)$ reduces to $\psi = \tilde{\psi}\left(\mathbf{F},\nabla\mathbf{F}\right)$.

The rate of supply of mechanical energy $(*)$ necessary to justify a constitutive dependence of the energy on $\nabla\mathbf{F}$ is then a consequence of substructural events that induce a weakly non-local character in the constitutive equations.

To explain clearly the issue, we may focus the attention on the special case of *micromorphic* bodies in linear setting, the one formulated in [137] (see also relevant remarks and references in the Introduction). In this special case, one assumes that each material element is a unit cell containing "a molecule of a polymer, a crystallite of a polycrystal or a grain of a granular material" [137] and may admit deformations independently of the neighboring fellows. As a consequence, ν describes a local micro-deformation and is a second-order tensors, so that $\mathcal{M}$ coincides with $Hom\left(\mathbb{R}^3,\mathbb{R}^3\right)$. Since the manifold of substructural shapes coincides thus with a linear space in this case, the linearized theory follows naturally. If we focus the attention on it, we may define a measure of *relative* deformation γ by

$$\gamma = \nabla\mathbf{u} - \nu \tag{120}$$

($\mathbf{u}$ the displacement) and assume that along isothermal processes the state of each material element be defined by the three-plet $(\varepsilon, \gamma, grad\nu)$. It is essential to note how this point of view contains as a special case the model of Cosserat materials. To obtain it, in fact, it is sufficient to select ν as a second-order tensor such that $sym\nu = \mathbf{0}$ and $skew\nu \in SO(3)$.

Calculations developed along the general path discussed in previous sections, allow us to observe that the balance of standard and substructural interactions merge the one into the other and one gets

$$\mathbf{b}_a + div\,(\sigma - div\mathcal{S}_a) = 0 \tag{121}$$

in absence of inertial effects. Moreover, if one assumes as internal constraint that the relative deformation γ vanishes, that is $\nabla\mathbf{u} = \nu$, a special case of $\nu = \tilde{\nu}(\mathbf{F})$, than the list of constitutive entries $(\varepsilon, \gamma, grad\nu)$ reduces to $(\varepsilon, grad\mathbf{u})$ and (121) to the balance of forces in second grade linear elasticity.

More complicated is the matter in non-linear setting when one considers the internal constraint $\nu = \tilde{\nu}(\mathbf{F})$ without attributing a special meaning to ν. However, even in this case one may obtain a result and for a free energy of the type $\tilde{\psi}(\mathbf{F}, \nabla\mathbf{F})$ one finds [15] the balance of forces

$$\mathbf{b} + Div\left(\partial_{\mathbf{F}}\psi - Div\left(\partial_{\nabla\mathbf{F}}\psi\right) - Div\left(\mathbf{F}skw\left(\partial_{\nabla\mathbf{F}}\psi\mathbf{F}^{-1}\right)\right)\right) = \mathbf{0}, \tag{122}$$

in absence of inertial effects.

2.5.5 Liquid crystals

Liquid crystals are a paradigmatic example of complex bodies. They are characterized by stick molecules smeared in a ground fluid. Such molecules may arrange themselves in various manners that characterize different phases [50].

Nematic phase. In nematic phase, the stick molecules are ordered along prevailing directions but they have no orientation. In other words, there is a head-to-tail symmetry. As morphological descriptor, we may attach to each point an indicator of the prevailing direction of the stick molecules there (as proposed first in [60], [61]). In this way, $\mathcal{M}$ may be selected to be the unit sphere in $\mathbb{R}^3$ but with the constraint that diametrically opposite points are identified to account for the head-to-tail symmetry. With this constraint, $\mathcal{M}$ is isomorphic to the projective plane P^2 and the morphological descriptor is thus an element of it. The explicit constitutive structure of the self-force and the microstress can be obtained from the Oseen-Frank potential (see [17]) as derivatives with respect to ν and its gradient respectively.

Alternatively, if one would like to account more deeply for the geometrical features of the local distribution of stick molecules within each material element, one could adopt as a morphological descriptor a second order symmetric tensor $\mathbf{D}$ with unitary trace ($tr\mathbf{D} = \mathbf{1}$), or better its deviatoric part $\mathbf{D}_D$. In particular, one selects $\mathbf{D}_D$ as to be expressed by $\mathbf{D}_D = \zeta\left(\varsigma \otimes \varsigma - \frac{1}{3}\mathbf{I}\right)$, with ς a unit vector, namely $\varsigma \in S^2$, and $\zeta \in \left[-\frac{1}{2}, 1\right]$. In this way, one has two morphological descriptors: the vector ς representing the prevailing direction of stick molecules - really one selects $\varsigma \in P^2$ - and a scalar ζ indicating the *degree of orientation* (as defined in [65]). Since $\mathbf{D}$ is symmetric, the distribution it describes is an ellipsoid.

We have then a first set of substructural interactions power conjugated with the rate of ς and a second set conjugated with the rate of ζ. Each set is balanced independently.

Biaxial nematics. Optical biaxiality can emerge in nematic liquid crystals. When it occurs, the symmetry of the molecules is reduced to that of a rectangular box. In this case, one needs two other scalar morphological descriptors, namely the *degree of prolation* d_g and the *degree of triaxiality* d_t defined respectively by

$$d_g = \frac{1}{2}\left(\prod_{i=1}^{3}(3\lambda_i - 1)\right)^{\frac{1}{3}} \quad , \quad d_t = \left(6\sqrt{6}\prod_{i=1}^{3}|\lambda_i - \lambda_{i+1}|\right)^{\frac{1}{3}}, \tag{123}$$

with λ_i the $i-th$ eigenvalue of $\mathbf{D}$ (as proposed first in [20]). These degrees characterize the geometry of the ellipsoid associated with $\mathbf{D}$.

Alternatively, one may select $\mathcal{M}$ coincident with the quotient between the special unitary group $SU(2)$ and the group of quaternions (see [132]).

Smectic-A phase. In the smectic-A phase, liquid crystals are organized in layers in which the stick molecules tend to be aligned orthogonally to the layer interface. Within each layer the molecules flow freely; in the orthogonal direction they may permeate from a layer into another. In such a direction the behavior is basically the one of a one-dimensional crystal. Natural ingredients for describing the smectic-A phase are a unit vector ς that represents at each point the local orientational order, and a scalar function w parametrizing the layers. More precisely, we may write [18] $w(\mathbf{x}, t, a\lambda)$, with λ an appropriate length scale and a running in a set of integers, to account for possible unequal spacing of layers. At a coarse grained scale and with reference to the current configuration, we may imagine that $w(\mathbf{x}, t, \cdot)$ be defined in a continuum approximation on an interval of the real line so that $|gradw|^{-1}$ measures the current thickness of the layers. Then, we can select the order parameter as the pair (ς, w); however, far from the defect core, where tilt is absent, we have

$$\varsigma = \frac{gradw}{|gradw|}, \tag{124}$$

and the simplest choice for the potential ψ in the incompressible case (where incompressibility is intended at 'gross' scale) is of the form (see [58])

$$\psi(w, gradw) = \frac{1}{2}\gamma_1(|gradw| - 1)^2 + \frac{1}{2}\gamma_2(div\varsigma)^2, \tag{125}$$

with the identification (124), γ_1 and γ_2 material constants. In (125), the term $(|gradw| - 1)^2$ accounts for the compression of layers while $(div\varsigma)^2$ describes the nematic phase and is the first addendum of (three constant) Frank's potential (see [17], p. 55). Inertial effects can be considered by putting $\chi = \frac{1}{2}\rho\alpha|\dot{\varsigma}|^2$, with α a material constant. Of course, the assumption of incompressibility at a gross scale is not incompatible with the assumed compressibility of the layers that may rearrange with one another without altering the volume.

2.5.6 Bodies with polymeric linear chains

Bodies characterized by polymeric chains smeared in a melt are described variously, depending on physical circumstances (see [107]). Each material element is considered as a patch of matter containing a family of polymeric 'linear' chains. Except the case of dilute solutions, interactions may occur between neighboring material elements. They have a weakly non-local character of gradient type. Such kind of interactions in polymeric fluids may also be generated by turbulence even in dilute polymer solutions and can be the source of terms involving spatial gradients of the substructural descriptors in the evolution

equations describing the substructural changes of shape of the families of polymer chains [48].

To select an appropriate morphological descriptor, one may describe first each chain by means of an end-to-end stretchable vector $\mathbf{r}$. Moreover, at each point $\mathbf{X}$ of $\mathcal{B}_0$ we have a distribution function $f_{P(\mathbf{X})}(\mathbf{r})$ of $\mathbf{r}$ representing the population of chains within the material element placed at $\mathbf{X}$. Then, one may identify ν with a second order symmetric tensor $\mathcal{R}$ given by

$$\mathcal{R}(\mathbf{X}) = \langle \mathbf{r} \otimes \mathbf{r} \rangle_{f_{P(\mathbf{X})}(\mathbf{r})}. \tag{126}$$

This choice is suggested by the need to be indifferent to the transformation $\mathbf{r} \to -\mathbf{r}$. The parenthesis $\langle \cdot \rangle$ denotes ensemble average over the family of chains described by $f_{P(\mathbf{X})}(\mathbf{r})$.

Then, the manifold of substructural shapes $\mathcal{M}$ coincides with the (linear) space of symmetric tensors with positive determinant $Sym^{+}\left(\mathbb{R}^3, \mathbb{R}^3\right)$.

Balance equations can be derived by following the guidelines of the general format described in previous sections. In requiring the invariance of the external power with respect to the action of $SO(3)$, one needs to take into account that in this special case the relation (12) becomes now

$$\dot{\mathcal{R}}^{*} = \dot{\mathcal{R}} + \mathcal{A}\dot{\mathbf{q}}(t) \tag{127}$$

and the linear operator $\mathcal{A}$ is then a third-order tensor whose covariant components are given by $\mathcal{A}_{ijk} = \mathsf{e}_{ilj}\mathcal{R}_{lk} - \mathcal{R}_{il}\mathsf{e}_{jlk}$. To obtain the explicit expression of $\mathcal{A}$, one should take into account that under the action of $SO(3)$ over $Sym^{+}\left(\mathbb{R}^3, \mathbb{R}^3\right)$, we have $\mathcal{R}_{\mathbf{q}} = \mathbf{Q}^{T}\mathcal{R}\mathbf{Q} = \exp(\mathsf{eq})\,\mathcal{R}\exp(\mathsf{eq})$, where, as usual, e is Ricci's alternating symbol, $\mathbf{q}$ a vector and $\mathcal{R}_{\mathbf{q}}$ the value of $\mathcal{R}$ after the action of an arbitrary element $\mathbf{Q}$ of $SO(3)$. From the relation $\mathcal{A} = \frac{d\mathcal{R}_{\mathbf{q}}}{d\mathbf{q}}|_{\mathbf{q}=\mathbf{0}}$, one then get the explicit expression of $\mathcal{A}$ [122].

2.5.7 Polyelectrolyte polymers and polymer stars

Polymeric chains my undergo polarization as in the case polyelectrolyte polymers or may be arranged as stars. In the former case, we may imagine to assign at each point $\mathbf{X}$ not only the dyadic tensor $\mathcal{R}$ defined above but also a polarization vector p as in the case of ferroelectrics. By indicating by B_{p_m} a ball of $\mathbb{R}^3$ centered at zero and with radius equal to p_m, the maximum amplitude of the polarization, we have $\mathcal{M} = Sym^{+}\left(\mathbb{R}^3, \mathbb{R}^3\right) \times B_{p_m}$ and we may construct the relevant mechanical theory, once an explicit expression for the free energy ψ has been selected, adding, in presence of external electric fields, the electromagnetic energy. In the case of polymer stars, the picture becomes more articulated and we may imagine to have $\mathcal{M} = Sym^{+}\left(\mathbb{R}^3, \mathbb{R}^3\right) \times B_{p_m} \times (0, b)$, with $b > 0$. In this case, at each $\mathbf{X}$, we add an arbitrary element of the interval $(0, b)$ of the real line that describes the *radius of gyration* of the polymeric molecules [107], [115].

2.5.8 Superfluid Helium

Superfluid Helium displays complexity that can be profitably described within the setting of multifield theories.

In particular, in the case of superfluid Helium ^4He the manifold of substructural shapes can be choosen to be the unit circle in the complex plane, that is $\mathcal{M} = S^1 \subset \mathbb{C}$. Then, one should choose a free energy ψ with Ginzburg-Landau structure with complex entries [115], [17].

In the case of superfluid Helium ^3He in the dipole loched-A phase, $\mathcal{M}$ coincides simply with $SO(3)$ so that this type of superfluid Helium can be described by the Cosserat scheme [132].

3 A SPECIAL CASE DEVELOPED IN DETAIL: ELASTIC MICROCRACKED BODIES

Microcracks distributed throughout a body rouse often mechanisms of stress-strain concentration which can be source of plastic phenomena and/or macroscopic rupture and may generate loss of serviceability of structures. The effects of distributed microcracks on the whole mechanical behavior of bodies can be tangible already in the elastic regime where they alter the distribution of stresses and strains. To treat cases in which the microcracks are not dilute over the body, multifield approach is necessary [109], [124], [125], [127].

In fact, in the common modelling of microcracked materials, one tries to determine an equivalent material *without* microcracks that behaves *like* the original microcracked body at least in linear elastic regime. To this aim, different methods are proposed in literature. In a 1976 pioneer paper, Budiansky and O'Connell introduced in linear elasticity the *self-consistent method* to derive *homogenized* (also defined '*effective*') elastic moduli of bodies endowed with flat microcracks of planar elliptic shape [12].

A basic assumption is that "the statistical distribution of sizes, shapes, locations and orientations of the cracks are supposed to be sufficiently random and uncorrelated to render the body homogeneous and uncorrelated in the large" [12]. Possible effects due to the closure of the cracks are also neglected and the microcracks are considered in elastic phase, i.e. they do not evolve irreversibly.

Modifications of the self-consistent method are the *generalized self-consistent method* [96], the *differential scheme* [95] and the *Mori-Tanaka method* [140] (comparisons among them are in [154]). In these methods, the interaction between neighboring microcracks are accounted for only indirectly. For example, in the self-consistent method one evaluates at an intermediate step the displacement field around a microcrack embedded in an uncracked linear elastic material. Such a material is endowed with the unknown homogenized stiffness to take into account in the real material the interactions of the other microcracks with the one considered. In going on and determining the homogenized stiffness, one obtains also unphysical consequences: The stiffness vanishes when the microcracks density reaches a value lesser than 1. Other homogenization methods avoid this shortcoming by reducing the interactions among microcracks. In other words, such methods work well when microcracks interact weakly. However, when microcracks are dense or the matter is sufficiently soft, we need to account for microcrack-microcrack interactions. To describe them we should make use of a multifield approach as described above. The point of view described here has been formulated in [109], [127] and then developed in [124], [125], [170], [171]. Such a model is able to show effects of strain localization which do not appear in models based on a linear Cauchy's continuum but have experimental counterparts in the linear setting.

3.1 Kinematics of Microcracked Bodies

Since we consider that microcracks are not dilute over the body, we assume that the generic material element is a patch of matter endowed with a family of microcracks. Moreover, we consider each microcrack either as a sharp defects - a planar compact bounded region not penetrated by material bonds - or as an elliptic void with one dimension very small with respect to the others. If the body is free of microcracks, the current placement $\mathbf{x}$ of a material element is obtained by means of the standard deformation $\tilde{\mathbf{x}}$ defined in Section 2.

When microcracks are present throughout the body and may deform without growing further[14], after a deformation, each material point will occupy a place $\mathbf{x}'$ (different from $\mathbf{x}$ in principle) in a current configuration $\mathcal{B}'$. The discrepancy between $\mathbf{x}$ and $\mathbf{x}'$ is due to the possible 'enlargement' of the existing microcracks that induce a kinematical perturbation

[14]Phenomena like coalescence and nucleation are not considered here.

on the deformative behavior. The region $\mathcal{B}'$ is assumed to be regular and to be obtained from $\mathcal{B}_0$ by means of a one-to-one continuously differentiable mapping

$$\mathcal{B}_0 \ni \mathbf{X} \overset{\tilde{\mathbf{x}}'}{\longmapsto} \mathbf{x}' = \tilde{\mathbf{x}}'(\mathbf{X}) \in \mathcal{B}'. \tag{128}$$

Moreover, a mapping $\mathfrak{f}$ such that

$$\mathbf{x}' = (\mathfrak{f} \circ \tilde{\mathbf{x}})(\mathbf{X}) \tag{129}$$

and $\mathcal{B}' = \mathfrak{f}(\mathcal{B})$ can be defined.

The standard displacement is then $\mathbf{u} = \mathbf{x} - \mathbf{X}$ while the 'incremental' displacement (microdisplacement) due to the presence of microcracks is indicated with $\mathsf{d} = \tilde{\mathbf{x}}'(\mathbf{X}) - \tilde{\mathbf{x}}(\mathbf{X})$.

In other words, if the microcracks are absent, the relative change of placement between neighboring patches is measured through the displacement field $\mathbf{u}$. When microcracks occur and deform, they induce an additional displacement d that 'perturbs' $\mathbf{u}$. The vector d is thus a coarse grained descriptor of the influence of microcracks on the gross mechanical behavior. It takes the role of ν, so that $\mathcal{M}$ coincides with the entire translational space over $\mathcal{E}^3$ or, alternatively, with $\mathbb{R}^3$.

We remark here that d is considered to be defined over $\mathcal{B}_0$ so that we have a mapping

$$\mathcal{B}_0 \ni \mathbf{X} \overset{\tilde{\mathsf{d}}}{\longmapsto} \mathsf{d} = \tilde{\mathsf{d}}(\mathbf{X}) \in \mathbb{R}^3. \tag{130}$$

Let us indicate with $\mathbf{F}_{tot}$ the gradient of $\tilde{\mathbf{x}}'$ at $\mathbf{X}$. By chain rule we get

$$\mathbf{F}_{tot} = \nabla \tilde{\mathbf{x}}'(\mathbf{X}) = \nabla (\mathfrak{f} \circ \tilde{\mathbf{x}})(\mathbf{X}) = ((grad\mathfrak{f}) \nabla \tilde{\mathbf{x}})(\mathbf{X}) = \mathbf{F}^{(m)}\mathbf{F} \tag{131}$$

where

$$\mathbf{F}^{(m)} = grad\mathfrak{f}(\mathbf{x}) \tag{132}$$

is the gradient of deformation from $\mathcal{B}$ to $\mathcal{B}'$, i.e. $\mathbf{F}^{(m)} \in Hom(T_{\mathbf{x}}\mathcal{B}, T_{\mathbf{x}'}\mathcal{B}')$.

If we indicate with d_a the spatial counterpart of d (i.e. the specialized version of ν_a) given in terms of mapping $\tilde{\mathsf{d}}_a$ and $\tilde{\mathsf{d}}$ by $\mathsf{d}_a = \tilde{\mathsf{d}}_a(\mathbf{x}) = \left(\tilde{\mathsf{d}} \circ \tilde{\mathbf{x}}^{-1}\right)(\mathbf{x})$, we get first $\nabla \mathsf{d} = (grad\mathsf{d}_a)\,\mathbf{F}$ by chain rule, then

$$\mathbf{F}^{(m)} = grad\mathfrak{f}(\mathbf{x}) = \mathbf{I} + grad\mathsf{d}_a = \mathbf{I} + (\nabla \mathsf{d})\,\mathbf{F}^{-1} \tag{133}$$

so that we may express $\mathbf{F}_{tot}$ in terms of the additive decomposition

$$\mathbf{F}_{tot} = \mathbf{F} + \nabla \mathsf{d}. \tag{134}$$

This is one of the cases in which the measures of deformation involve the gradient of the morphological descriptor. In the present case, in fact, we may define an overall right Cauchy-Green tensor $\mathbf{C}_{tot}$ given by $\mathbf{C}_{tot} = \mathbf{F}_{tot}^T \mathbf{F}_{tot}$ so that by (134) we recognize the influence of $\nabla \mathsf{d}$ on the macroscopic deformation.

The direct description of the kinematics of microcracked bodies just sketched here can be obtained rigorously by using the procedure involving limits of bodies as described in [53].

3.2 Balance Equations and Identification of the Constitutive Structure from a Lattice Model

Balance equations can be derived by using the general procedure described in Section 2 with ν identified with d. In particular, one should take into account that in this case the linear operator $\mathcal{A}$ is given by $-\mathsf{d}\times$. To prove such a relation one should first recall that any proper orthogonal tensor $\mathbf{Q} \in SO(3)$ can be expressed by means of the exponential map as $\mathbf{Q} = \exp(\mathbf{eq})$, with e Ricci's permutation index and $\mathbf{q}$ a vector. After the action of $SO(3)$ over $\mathbb{R}^3$ each d changes in $\mathsf{d}_{\mathbf{q}} = \mathbf{Q}\mathsf{d} = \exp(\mathsf{eq})\mathsf{d}$. As a consequence, we get $\mathcal{A} = \frac{d\mathsf{d}_{\mathbf{q}}}{d\mathbf{q}}\Big|_{\mathbf{q}=\mathbf{0}} = \mathsf{ed}$ which proves our previous statement.

The balance of standard forces is still (18). There are no bulk interactions acting directly over microcracks - they are voids, roughly speaking - also, peculiar substructural inertia is absent so that (21) reduces to

$$Div\mathcal{S} - \mathbf{z} = 0. \tag{135}$$

Moreover, by taking into account the special expression of $\mathcal{A}$, (22) changes in

$$skw\left(\mathbf{S}\mathbf{F}^T + \mathbf{z} \otimes \mathsf{d} + \mathcal{S}^T(\nabla\mathsf{d})\right) = 0. \tag{136}$$

Constitutive relations for standard and substructural measures of interactions follow once the explicit expression of the elastic energy is available in terms of $\mathbf{F}$, d, $\nabla\mathsf{d}$. Experimental data may allow us to get numerical values for the coefficients. In absence of them we may try to construct a lattice model of the material element –i.e. of the microcracked body– from which we derive constitutive relations by means of an identification procedure based on the power equivalence with the continuum model[15]. Below we follow such a procedure in linear elastic setting.

Figure 4 shows the prototype model adopted in the numerical simulations. It is constituted by two lattices: The former –called *macro-lattice*– is made of rigid balls while the latter –called *micro-lattice*– is made of empty elastic ellipsoids. Links are elastic and carry only axial forces. The macro-lattice represents the molecular level while the micro-lattice describes microcrack distribution.

Let $\mathbf{A}$ and $\mathbf{B}$ be two material points of the macro-lattice (the spheres) placed at $\mathbf{a}$ and $\mathbf{b}$ respectively, and the two mass centers of the ellipsoids $\mathbf{H}$ and $\mathbf{K}$ be placed at the points $\mathbf{h}$ and $\mathbf{k}$. It is assumed that *the ellipsoids can only deform along a plane orthogonal to the major axis, along a direction e_h, prescribed for each ellipsoid*. Measures of deformation in the discrete system are (i) the relative displacement d^h between the margins of each ellipsoid along the direction h orthogonal to its major axis, (ii) the elongation $\left(\mathsf{d}^h - \mathsf{d}^k\right)$ of each link connecting neighboring ellipsoids, (iii) the elongation $\left(\mathbf{u}^a - \mathsf{d}^h\right)$ of each link between macro and micro-lattice, (iv) the elongation $\left(\mathbf{u}^a - \mathbf{u}^b\right)$ of each link in the microlattice.

The identification procedure follows two basic steps.

Step 1) The density of the internal power in the continuum is equalized to the power developed in the *RVE*, namely

$$\mathbf{P}\cdot\nabla\mathbf{u} + \mathbf{z}\cdot\mathsf{d} + \mathcal{S}\cdot\nabla\mathsf{d} = \frac{1}{V_{RVE}}\left(\sum_{i=1}^{L}\mathbf{t}_i\cdot\left(\mathbf{u}^a - \mathbf{u}^b\right) + \right.$$
$$\left. + \sum_{l=1}^{L_N}\mathbf{z}_l\cdot\left(\mathbf{u}^a - \mathsf{d}^h\right) + \sum_{h=1}^{M}\mathbf{z}_0^h\cdot\mathsf{d}^h + \sum_{j=1}^{L_M}\mathbf{z}_j\cdot\left(\mathsf{d}^h - \mathsf{d}^k\right)\right), \tag{137}$$

[15]We follow ideas of Cauchy, Born, Voigt, Stakgold and Ericksen [64], [169] and adapt them to the multifield setting adopted here.

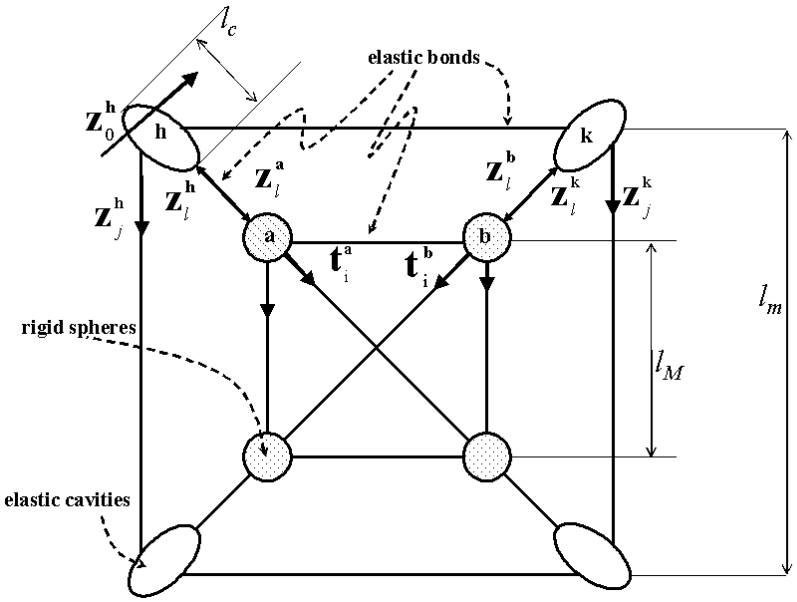

Figure 4. Representative Volume Element (RVE) of the discrete model

where L is the number of bonds in the macro-lattice, L_N the number of bonds between macro and micro-lattice, M the number of ellipsoids and L_M the number of bonds of the micro-lattice. In (137), $\mathbf{t}_i$ is the force between the two points $\mathbf{a}$ and $\mathbf{b}$ along the *i-th* direction, $\mathbf{z}_j$ the force between $\mathbf{h}$ and $\mathbf{k}$ along the *j-th* rod (connecting the two ellipsoids $\mathbf{H}$ and $\mathbf{K}$), $\mathbf{z}_0^h$ the force due to the displacement d^h, $\mathbf{z}_l$ the force between the material point $\mathbf{a}$ and the ellipsoid $\mathbf{h}$ along the *l-th* direction.

Step 2) We assume that the macrolattice undergoes a homogeneous deformation, and that each shell deforms also homogeneously but differently from the neighboring ones. In this way, we may find a point $\bar{\mathbf{x}}$ in the RVE such that

$$\mathsf{d}^h = \mathsf{d}\left(\bar{\mathbf{x}}\right) + \nabla \mathsf{d}\left(\mathbf{x}\right)\left(\mathbf{h}-\mathbf{x}\right), \quad \mathbf{u}^a - \mathbf{u}^b = \nabla \mathbf{u}\left(\bar{\mathbf{x}}\right)\left(\mathbf{a}-\mathbf{b}\right), \tag{138}$$

$$\mathsf{d}^h - \mathsf{d}^k = \nabla \mathsf{d}\left(\bar{\mathbf{x}}\right)\left(\mathbf{h}-\mathbf{k}\right), \quad \mathbf{u}^a - \mathsf{d}^h = \nabla \mathbf{u}\left(\bar{\mathbf{x}}\right)\left(\mathbf{a}-\bar{\mathbf{x}}\right) - \nabla \mathsf{d}\left(\bar{\mathbf{x}}\right)\left(\mathbf{h}-\bar{\mathbf{x}}\right). \tag{139}$$

Then, by inserting (138)-(139) in (137) and identifying common terms, one gets

$$\mathbf{P} = \frac{1}{V_{RVE}}\left(\sum_{i=1}^{L}\mathbf{t}_i \otimes \left(\mathbf{a}-\mathbf{b}\right) + \sum_{i=1}^{L_N}\mathbf{z}_l \otimes \left(\mathbf{a}-\mathbf{x}\right)\right), \tag{140}$$

$$\mathbf{z} = \frac{1}{V_{RVE}}\sum_{h=1}^{M}\mathbf{z}_0^h, \tag{141}$$

$$\mathcal{S} = \frac{1}{V_{RVE}}\left(\sum_{h=1}^{M}\mathbf{z}_0^h \otimes \left(\mathbf{h}-\mathbf{x}\right) + \sum_{j=1}^{L_M}\mathbf{z}_j \otimes \left(\mathbf{h}-\mathbf{k}\right) - \sum_{l=1}^{L_N}\mathbf{z}_l \otimes \left(\mathbf{h}-\mathbf{x}\right)\right). \tag{142}$$

Once constitutive equations are assigned to rods and shells in the lattice, the linear expressions of the constitutive equations (140)-(142) are given by

$$\left\{\begin{array}{c} \mathbf{P}=\mathbb{A}\nabla\mathbf{u}-\mathbb{A}'\nabla\mathsf{d} \\ \mathbf{z}=\mathbb{C}\mathsf{d} \\ \mathcal{S}=\mathbb{G}\nabla\mathsf{d}-\mathbb{G}'\nabla\mathbf{u} \end{array}\right. . \tag{143}$$

With reference to the special geometry adopted in Figure 4, explicit expressions of the constitutive tensors $\mathbb{A}$, $\mathbb{A}'$, $\mathbb{C}$, $\mathbb{G}'$ and $\mathbb{G}$ are indicated below:

$$\mathbb{A}=\frac{EA}{l_M}\begin{bmatrix} 2+\frac{1}{\sqrt{2}} & 0 & 0 & \frac{1}{\sqrt{2}} \\ 0 & \frac{1}{\sqrt{2}} & \frac{1}{\sqrt{2}} & 0 \\ 0 & \frac{1}{\sqrt{2}} & \frac{1}{\sqrt{2}} & 0 \\ \frac{1}{\sqrt{2}} & 0 & 0 & 2+\frac{1}{\sqrt{2}} \end{bmatrix}+\frac{\frac{1}{2}l_M^2\frac{2E^*A}{\sqrt{2}(l_m-l_M)}}{\left|l_M^2-l_m^2\right|}\begin{bmatrix} 1 & 0 & 0 & 1 \\ 0 & 1 & 1 & 0 \\ 0 & 1 & 1 & 0 \\ 1 & 0 & 0 & 1 \end{bmatrix}, \tag{144}$$

$$\mathbb{A}'=\mathbb{G}'=\frac{\frac{1}{2}l_m l_M\frac{2E^*A}{\sqrt{2}(l_m-l_M)}}{\left|l_M^2-l_m^2\right|}\begin{bmatrix} 1 & 0 & 0 & 1 \\ 0 & 1 & 1 & 0 \\ 0 & 1 & 1 & 0 \\ 1 & 0 & 0 & 1 \end{bmatrix}, \tag{145}$$

$$\mathbb{C}=\frac{2\frac{E\hat{A}}{\pi l_c}}{l_m^2}\begin{bmatrix} 1 & 0 \\ 0 & 1 \end{bmatrix}, \tag{146}$$

$$\mathbb{G}=\frac{1}{2}\frac{EA}{\pi l_c}\begin{bmatrix} 1 & 0 & 0 & 1 \\ 0 & 1 & 1 & 0 \\ 0 & 1 & 1 & 0 \\ 1 & 0 & 0 & 1 \end{bmatrix}+\frac{\frac{1}{2}l_m^2\frac{2E^*A}{\sqrt{2}(l_m-l_M)}}{\left|l_M^2-l_m^2\right|}\begin{bmatrix} 1 & 0 & 0 & 1 \\ 0 & 1 & 1 & 0 \\ 0 & 1 & 1 & 0 \\ 1 & 0 & 0 & 1 \end{bmatrix}. \tag{147}$$

They depend on the Young modulus E of the rods between neighboring spheres, the Young modulus E^* of the rods between elastic shells and rigid spheres (it is a parameter that allows us to describe the interactions between each microcrack and the surrounding matter), the area A of the cross section of the rods among rigid spheres and between rigid spheres and elastic shells, the characteristic lengths l_m and l_M, the characteristic length l_c of the shells in the lattice, the cross section area $\hat{A}$ of rods between adjacent microcracks.
Remark 7. Only the *ratio* between the material scales l_M and l_m is significant in the numerical developments.

Our procedure aims to match a discrete simulations of the material at a mesolevel with its coarse grained continuum representation. In spirit there are stringent analogies, with respect to the final target, with the quasi-continuum method, the coarse-grained molecular dynamics, and the dynamic atomistic-continuum modelling based on matching conditions. The choice of appropriate values for the material and geometrical quantities characterizing the discrete model and determining (144)-(147) is a delicate matter of modeling.

When we imagine to eliminate the mesolattice, thus the corresponding terms in (144)-(147), the final results must be the constitutive equations of the real material in a virgin state free of microcracks, so E, A, and l_M must be selected accordingly.

The length l_c is the averaged maximal dimension of the microcracks, the average being calculated over the population of microcracks. The length l_m is strictly associated with

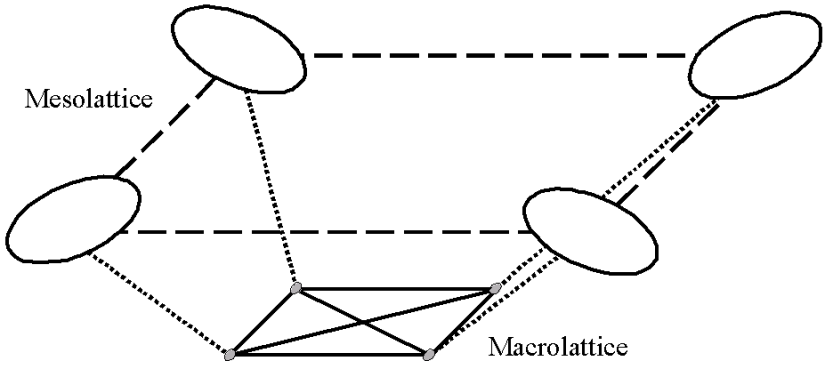

Figure 5. Three-dimensional schematic view of the basic cell of the lattice model.

the density of microcracks: For fixed symmetry properties, namely the cubic one here, the density increases as l_m decreases. In principle both l_c and l_m can be evaluated by means of X-ray techniques (see, e.g.,[103]). The remaining coefficients might be derived by mean of an appropriate inverse analysis.

Let us consider, for example, a strip of microcracked material loaded by two opposite tensile unitary forces. Calculate the total displacement $\mathbf{u}_{tot}$ between the points of application of the two forces and also the analogous displacement by imagining the strip made of uncracked material. The difference of the two values is the perturbation $\bar{\mathsf{d}}$ induced by the microcracks. At this point, once for the special material under examination E, A, l_M, l_c and l_m have been selected with the criteria described above, we should choose E^* and $\hat{A}$ in order to fit the value $\bar{\mathsf{d}}$. Of course, the solution is not unique because we may select the parameters E, A, l_M, l_c, l_m, E^* and $\hat{A}$ in different ways. When experimental analyses suggest that the microcrack distribution displays some symmetry and we organize the lattice taking into account it, the identification procedure preserves such a symmetry.

The discrete model chosen here is only a simple device useful to simulate the mechanical behavior of the material element. The selection of the values of the geometric and constitutive quantities of the lattice is guided by the possibility to fit experimental data about the displacements in the real material.

3.3 Numerical Examples

Different examples, developed in the setting of standard finite element method, are here illustrated. A set of constitutive parameters concerning the macro-lattice and the micro-lattice is chosen as in Table 1. The behavior of four different two-dimensional speciemens under tensile force is analyzed.

Numerical simulations display the occurrence of strain localization phenomena already in linear elastic setting. Such phenomena cannot be obtained in a natural way by using standard homogenized models based on Cauchy continuum in the same linear setting. It is worth noting that the possibility of obtaining localization zones in a fairly natural way depends basically on the presence of $\nabla\mathsf{d}$ in the constitutive equations (see comments and additional results in [124] and [125]).

Two constitutive parameters have a prominent influence on the shape of the localization zones. They are (i) the ratio ϖ between Young modulus E^* of inter-lattice links and Young modulus E of the links in the macro and micro-lattice and (ii) the ratio $\frac{l_m}{l_M}$ between the length scales of the micro-lattice and of the macro-lattice.

In particular, when the *coupling coefficient* ϖ increases, the amplitude of the localization

$l_m\ (mm)$	see Figure 4	75
$l_M\ (mm)$	see Figure 4	5
$E\ \left(\frac{N}{mm^2}\right)$	modulus of the macro-lattice and micro-lattice bonds	10^3
$E^*\ \left(\frac{N}{mm^2}\right)$	modulus of the inter-lattice bonds	10^3
$A\ (mm^2)$	section area of the rods in the macro-lattice	1
$\hat{A}\ (mm^2)$	area of the cross section of the strip utilized in deriving d_0	0.0314
$l_c\ (mm)$	see Figure 4	1

Table 1. Summary of the symbols used in the two dimensional examples of elastic microcracked bodies

zones increases too; if a fixed value for l_M is assumed, when l_m increases, the perturbation of the displacement field induced by microcracks diffuses progressively and reduces the intensity of the localization phenomenon.

When $\varpi = 0$ the analytical problem is uncoupled and the macro-displacement $\mathbf{u}$ corresponds to the displacement obtained in the same situation in a body free of microcracks.

Moreover, the inter-lattice modulus E^* is a measure of the influence of the microcrack distribution on the macroscopic behavior of the body. A way to measure E^* is to compare experimental results with numerical tests. In the simulation below E^* has been chosen coincident with E.

3.3.1 Rectangular slab with different discontinuities

Consider a rectangular slab of microcracked body of length $3L$ and width L. Three cases with macroscopic discontinuities are considered and the gross mechanical behavior of the slab is studied by using numerical simulations. For each case the same boundary conditions are imposed in terms of macrodisplacement (to avoid rigid body motions) and standard tractions. No prescriptions are given in term of microdisplacement. Moreover, microtraction vanishes on the whole boundary of the slab. This last condition is in agreement with the physical circumstance that no direct load can be applied on the microcracks at the boundary of the slab since these microcracks lose their identity there becoming just corrugations of the boundary itself.

Figure 6 shows the case of a double notched domain, Figure 8 the case of a central discontinuity and Figure 10 that of a central square hole. These figures are assembled as to represent, from left to right, (i) the boundary conditions, (ii) the underformed configuration and (iii) the deformed configuration amplified with an amplifying factor equal to 10. In Figure 8 the amplifying factor is 50.

Numerical results are collected respectively in Figures 7, 9 and 11 where the macro and microdisplacement along the orizonthal (x) and vertical (y) axes are shown. Strain localization zones appear in the region near the tips of the two cracks showing in both cases the same shape.

Analogously, strain localization zones occur also when the discontinuity in the rectangular domain is a central crack as in the case of Figure 9. Once again, the region interested are those near the tips of the crack.

This kind of behaviour remains almost the same even when the central crack is substituted by a central hole of square shape. Such results are presented in Figure 11.

3.3.2 Square slab with square hole

In the previous sections the behaviour of a rectangular slab with a central square hole has been considered amid other examples. Here, the length of the slab is reduced up to

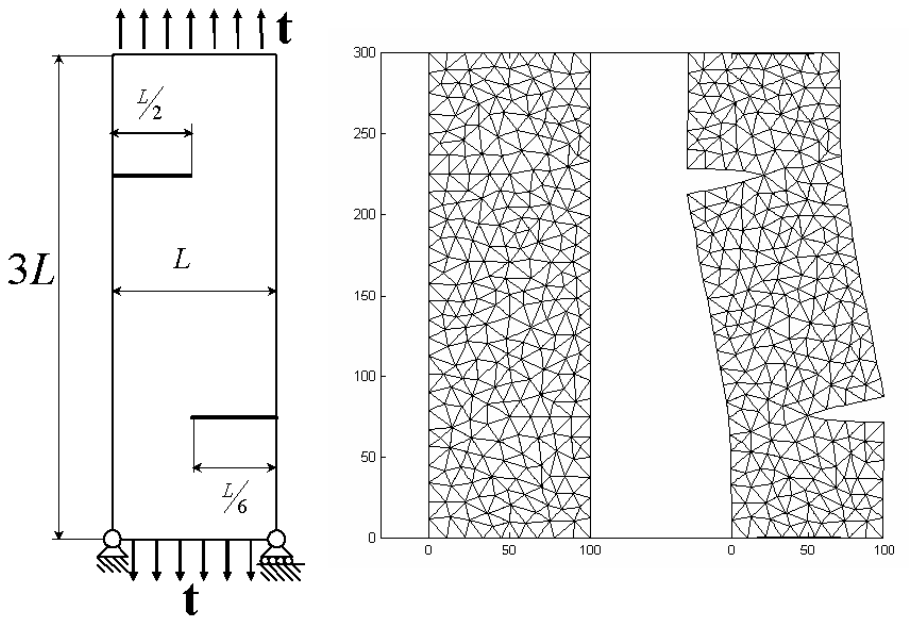

Figure 6. Double notched rectangular slab, from left to rigth: (*i*) dimensions of the domain and boundary conditions, (*ii*) undeformed mesh and (*iii*) deformed mesh a multiplying factor equals to 10

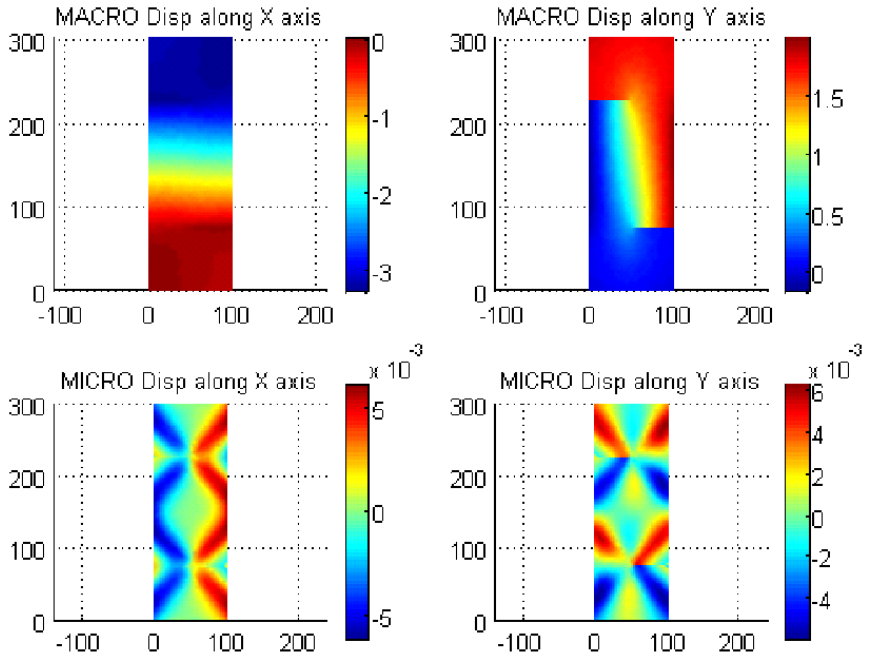

Figure 7. Numerical solution in term of macro and microdisplacement along the orizonthal (x) and vertical (y) axes for the case of Figure 6

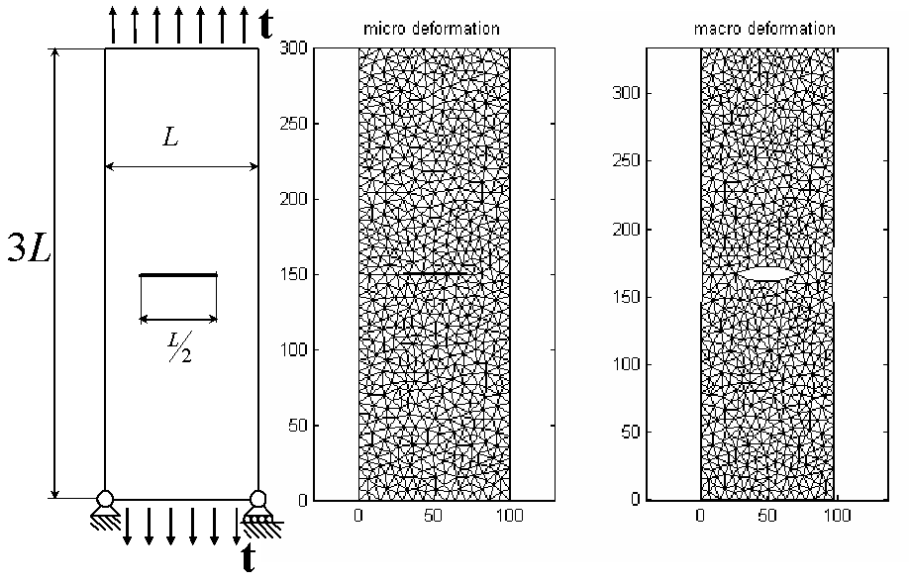

Figure 8. Rectangular slab with a central crack, from left to right: (*i*) dimension of the domain and boundary conditions, (*ii*) undeformed mesh and (*iii*) deformed mesh a multiplying factor equals to 50

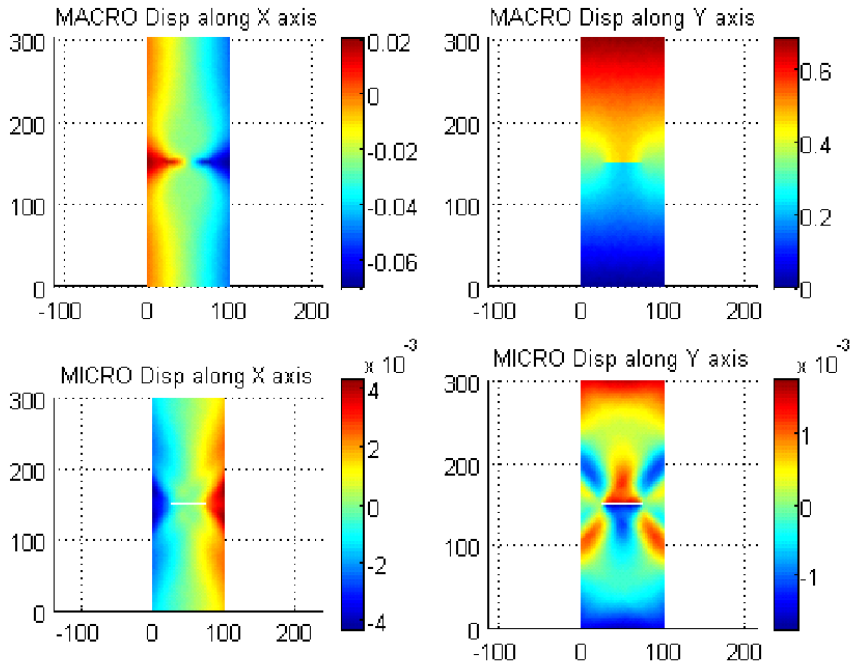

Figure 9. Numerical solution in term of macro and microdisplacement along the orizonthal (x) and vertical (y) axes for the case of Figure 8

render the slab a square. The boundary conditions are the same values as in the previous examples. In this case, strain localizations zones are less concentrated but are still placed in the regions near the corners of the central hole subject to dilatation. This fact underlines the influence of size effects on the topology of strain localization zones.

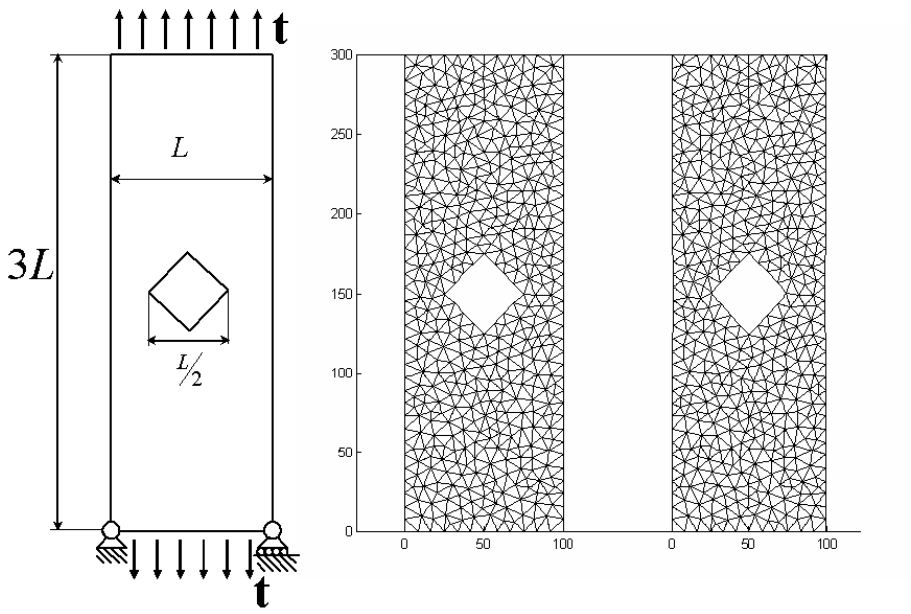

Figure 10. Rectangular slab with a central rhombic hole, from left to rigth: (*i*) dimension of the domain and boundary conditions, (*ii*) undeformed mesh and (*iii*) deformed mesh with an amplifying factor equal to 10

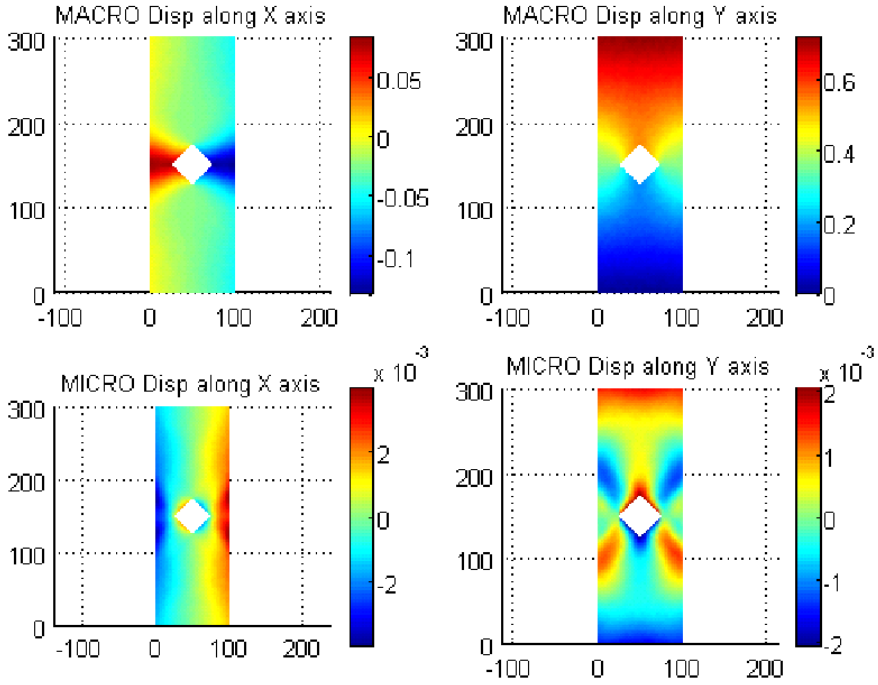

Figure 11. Numerical solution in term of macro and microdisplacement along the orizonthal (x) and vertical (y) axes for the case of Figure 10

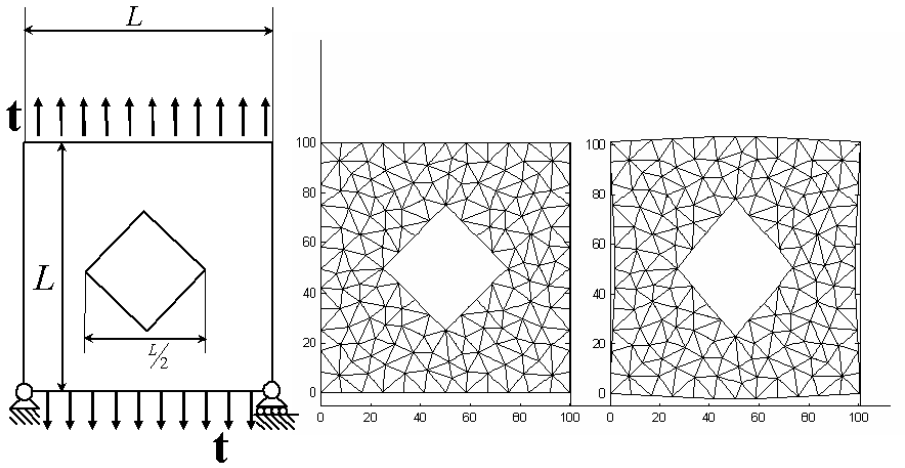

Figure 12. Square slab with a square rhombic hole, from left to rigth: (*i*) dimensions of the domain and boundary conditions, (*ii*) undeformed mesh and (*iii*) deformed mesh a multiplying factor equals to 10

3.4 Microcrack Randomness

The constitutive relations obtained in Section 3.2 contain both elastic moduli and material internal lengths. In particular, the former are functions of the elastic moduli of the links in the lattice, while the latter are the characteristic lengths of the RVE. In particular, the constitutive properties are most sensitive to the values of l_m, i.e. the distance between neighboring microcracks.

Experiments based on imaging or scattering techniques show that real distributions of microcracks vary randomly throughout the body [103]. As a consequence, the interactions between microcracks may be considered random. So, the interactions between each microcrack and the surrounding material are random too.

To describe this randomness, we may follow different strategies involving the geometry of the lattice and/or the elastic constants.

Even when we consider random the geometry of the mesoscopic texture, we find a consequent randomness of the interactions because the substructural interactions depend on the characteristic length of the mesoscopic scale. To account for microcrack randomness, we assume as deterministic all material and geometric parameters of the lattice model of the RVE except the length l_m of the mesoscale which is then considered as a random field $\mathcal{B}_0 \ni \mathbf{X} \longmapsto l_m(\mathbf{X})$ over the body.

We cannot consider l_m as a Gaussian field because such choice would imply physically impossible values of l_m like, for example, negative values. We then adopt for l_m a shifted lognormal model with a lower cut-off at l_M, following in this way [123].

The characteristic length l_m of the mesoscopic scale is then considered as a special translation field with the shifted log-normal structure

$$l_m(\mathbf{X}) = r + exp[\mu_{Y^*} + \sigma_{Y^*} Y(\mathbf{X})] \tag{148}$$

where r, μ_{Y^*} and σ_{Y^*} are parameters that need to be selected in order to obtain target values μ_{l_m} and σ_{l_m} of the mean and the variance of l_m respectively and to match the physical condition $l_m > l_M$ at each $\mathbf{X}$; moreover Y is a real valued Gaussian homogeneous field. The scalar $\delta = \frac{\sigma_{l_m}}{\mu_{l_m}} - r$ is the coefficient of variation of the shifted log-normal process.

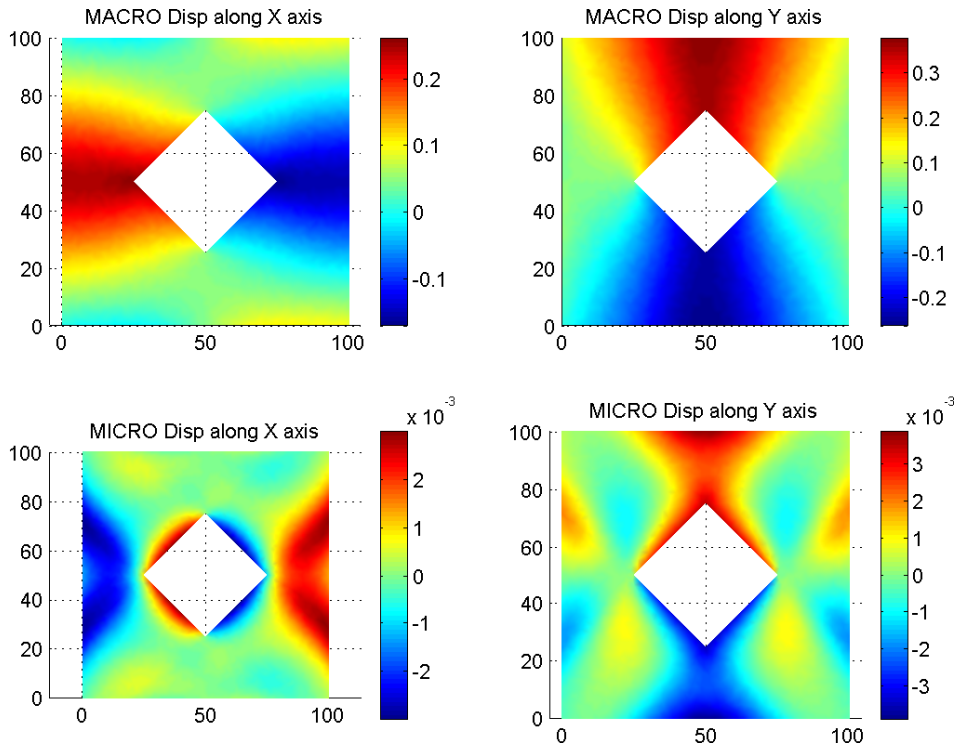

Figure 13. Numerical solution in term of macro and microdisplacement along the orizonthal (x) and vertical (y) axes for the case of Figure 13

Various cases of spatial correlation can be considered for l_m. In particular, perfect spatial correlation and absence of spatial correlation are respectively upper and lower bounds.

The assumption of perfect spatial random correlation is too strong, and physically not plausible, because one assumes that the value of l_m at a certain $\mathbf{X}$ is strictly related to all the other values of l_m over the whole body, independently of its size. Even the absence of correlation can be considered a limit case because we are treating situations in which microcracks are not dilute over the body.

The cases of perfect correlation and absence of correlation are discussed with numerical experiments in [123]. Here, we treat just an intermediate case in two-dimensional setting.

In the plane $0X_1X_2$, we embed a two-dimensional body and develop there numerical calculations. The field $\mathbf{X} \longmapsto l_m(\mathbf{X})$ is then defined over the body in $0X_1X_2$ and is assumed to be such that its spatial covariance is given by

$$C_{l_m l_m}(X_1, X_2) = \sigma_{l_m}^2 exp[-(cX_1)^2 - (cX_2)^2] \tag{149}$$

where c is a parameter proportional to the correlation distance.

Notice that the assumption of some type of random correlation implies a non-local constitutive behavior of the body, while the absence of random correlation corresponds to a completely local behavior.

3.4.1 Numerical example and comparisons

As a sample case, we analyze the square membrane in Figure 14.

On the left side, only vertical displacements are allowed, except at a fixed point.

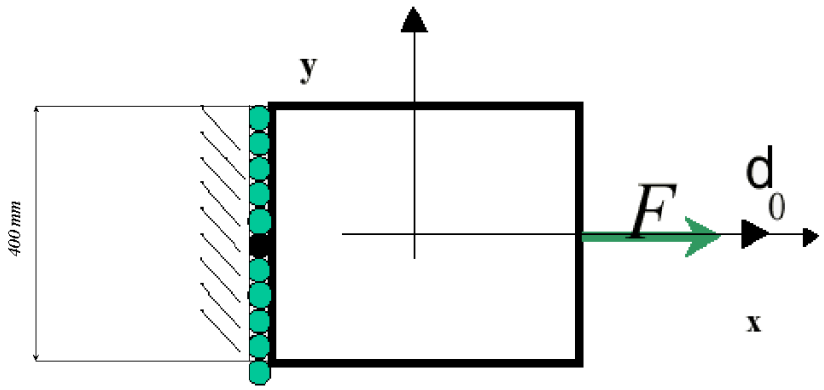

Figure 14.

A mixed boundary value problem is considered: in the middle of the right side we apply a tensile force F, assuming that it is sustained by the standard Cauchy stress, and assign in a tentative way the boundary value d_0.

Note that, as in the example of Section 2.4, we might not assign any condition on d on the right-hand-side of the membrane and we could consider a boundary condition of the type $\mathcal{S}\mathbf{n} = \mathbf{0}$, with $\mathbf{n}$ the outward unit normal at the boundary.

As mentioned previously, the possible assumption that the microtractions $\mathcal{S}\mathbf{n}$ vanish at the boundary is the only one which is physically reasonable.

The mesh is made of 1600 square finite elements and the shape functions used for the macrodisplacement and the microdisplacement are linear.

The numerical procedure goes as follows:

- Step 1. We generate sample values of l_m by using the stochastic structure of l_m represented in (148) and a Monte-Carlo technique. Three further sub-steps are necessary: (i) calibration of the marginal distribution and the covariance function to obtain the target statistical properties of l_m, (ii) generation of samples of the Gaussian field Y, (iii) generation of the translation field l_m. A total of 10,000 samples has been considered in the simulation below.

- Step 2. For each sample, we develop finite element analyses by using the same scheme of deterministic cases treated previously.

- Step 3. We calculate statistics of the results. In particular, we obtain *mean*, *coefficient of variation* (c.o.v.), *skewness* and *kurtosis* of the distribution of displacements, according with the correlation structure in (149).

Evident strain localization phenomena are due to the cooperation of microcracks. The same origin can be attributed to the patterns in the portraits of momenta of the displacement fields. Such a cooperation is ruled by the presence of self-interactions $\mathbf{z}$ and weakly non-local interactions $\mathcal{S}$.

The patterns in the portraits of the skewness and the kurtosis are indicators toward the transition from the elastic to the irreversible behavior. In the localization zones, in fact, the distributions are far from Gaussian. This circumstance suggests the presence of a net of strongly interacting microcracks 'oriented' along the strain localization paths. Such a net, in fact, could break the symmetry of the distribution and its Gaussian properties.

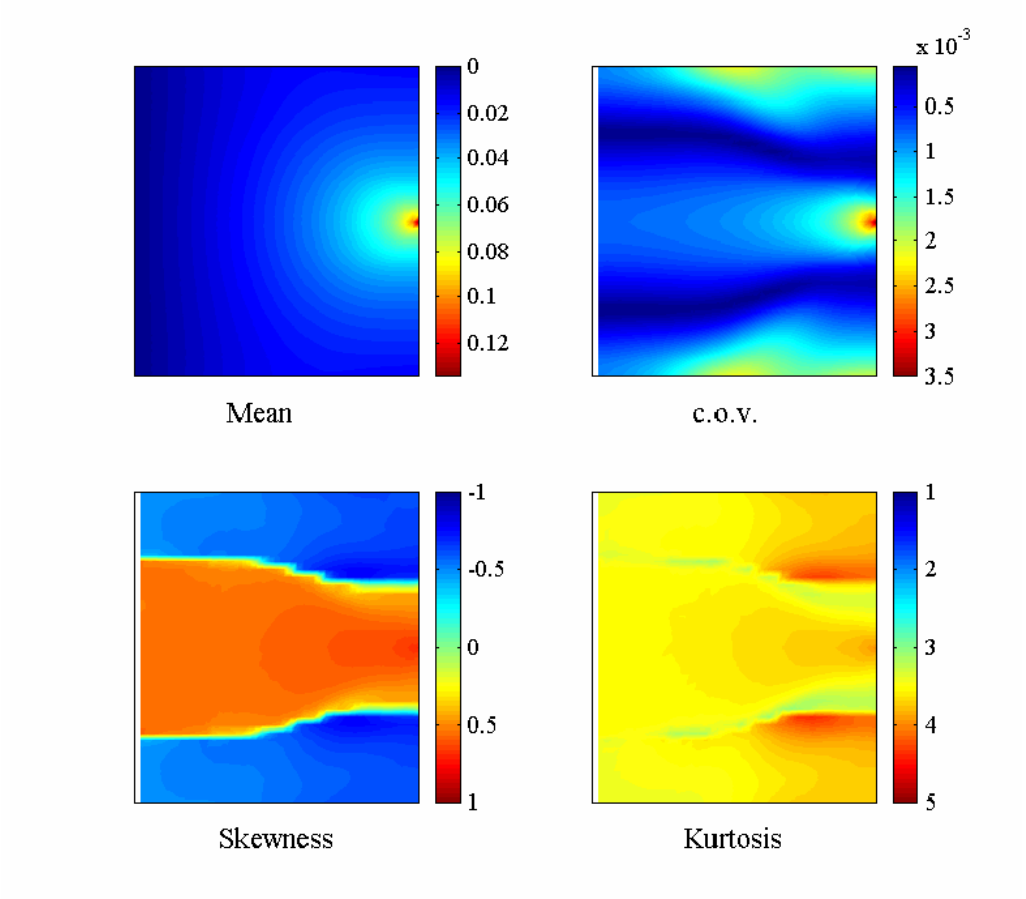

Figure 15. Macro-displacement along x axis: a) mean, b) c.o.v.; c) skewness; d) kurtosis

Finally, we could imagine that similar patterns could be common to various special cases of complex bodies in which physical circumstances suggest contemporary presence of morphological descriptors and their gradients in the list of entries of the energy.

4 INTERPOLATION OVER MANIFOLDS AND THE CONSTRUCTION OF FINITE ELEMENTS

For standard finite elements used - say - in linear elasticity, we write the displacement $\mathbf{u} = \mathbf{x} - \mathbf{X}$ at a certain point $\mathbf{X}$ in terms of shape functions and nodal values of the displacement itself as

$$\mathbf{u} = \Phi_{\mathbf{u}} \hat{\mathbf{u}}, \tag{150}$$

where $\Phi_{\mathbf{u}}$ is the matrix of shape functions at $\mathbf{X}$ and $\hat{\mathbf{u}}$ the vector of nodal values which does not depend on $\mathbf{X}$. We have also used the same approximation for the microdisplacement d in Section 3 in analyzing elastic microcracked bodies, as we shall see in detail later. In both cases we work well because, at each $\mathbf{X}$, both $\mathbf{u}$ and d belong to linear spaces, precisely to two different copies of $\mathbb{R}^3$. In fact, at each $\mathbf{X}$, any combination of nodal displacements $\hat{\mathbf{u}}$ multiplied by arbitrary shape functions is also an element of $\mathbb{R}^3$ so that it may be a candidate for a possible $\mathbf{u}$. The same reasoning holds for d.

Let us assume for a while that $\tilde{\nu}$ takes values on the unit sphere S^2. An arbitrary combination of elements of S^2 - that may be selected as nodal values - does not necessarily

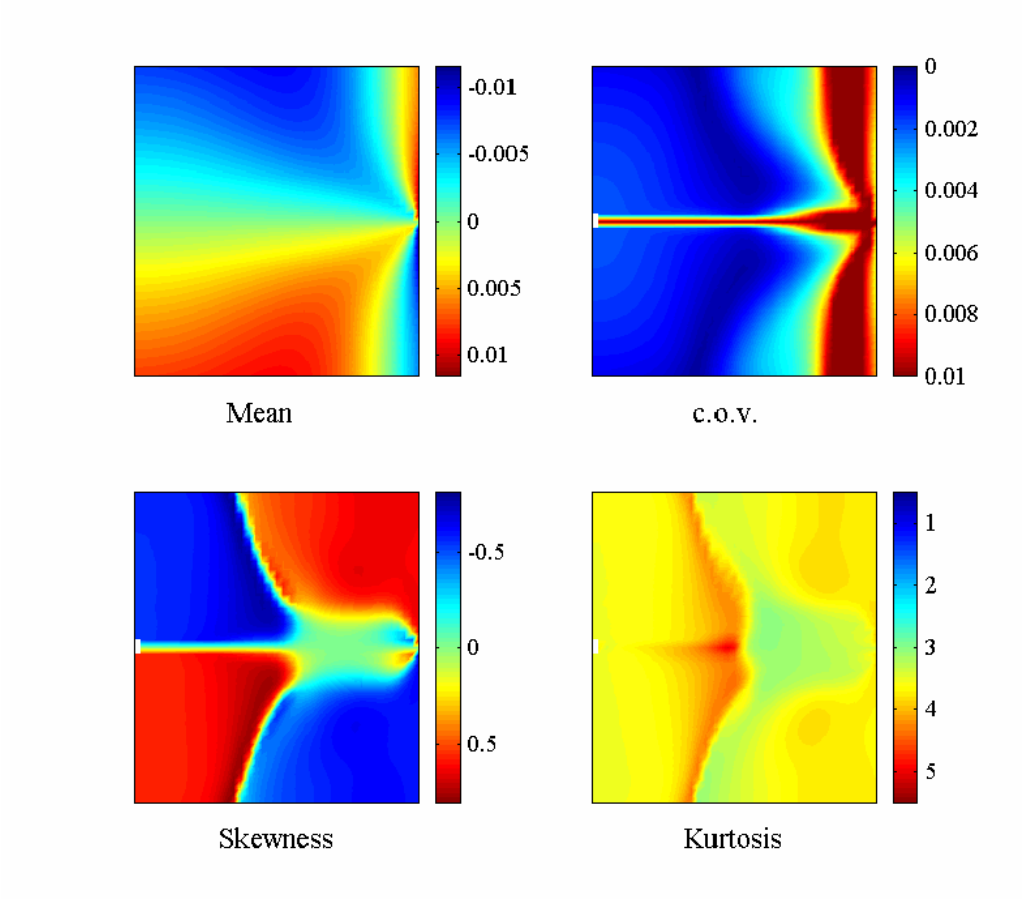

Figure 16. Macro-displacement along y axis: a) mean, b) c.o.v.; c) skewness; d) kurtosis

belong to S^2 because S^2 itself is not a linear space. The same problem occurs in the case in which one considers an abstract manifold $\mathcal{M}$ of substructural shapes that does not coincide in general with a linear space.

A way to solve the problem is *to embed $\mathcal{M}$ in a linear space* $\mathfrak{L}^{(N)}$ of appropriate dimension N.

In previous sections we have considered $\mathcal{M}$ with finite dimension: an embedding in a linear space is always available by Whitney theorem [185]. More specifically, *isometric* embeddings of $\mathcal{M}$ in a linear space are also available by Nash theorems [143], [144]. Isometric embeddings are also preferable from a physical point of view because the isometry preserves the substructural kinetic energy when it admits a quadratic form: in this case, in fact, the coefficients of this quadratic form are the coefficients of the metric over $\mathcal{M}$. However, even isometric embeddings are not unique, so that the choice of a specific embedding becomes matter of modeling.

Below, we construct first a general scheme for linearized multifield elasticity by means of the isometric emebedding of $\mathcal{M}$ in a linear space $\mathfrak{L}^{(N)}$. Then, we construct various types of finite elements for the resulting scheme. To simplify notations, we write such finite elements for the multifield model of elastic microcracked bodies discussed in Section 3. However, the path leading to them can be followed in general for any type of 'linearized multifield theory'.

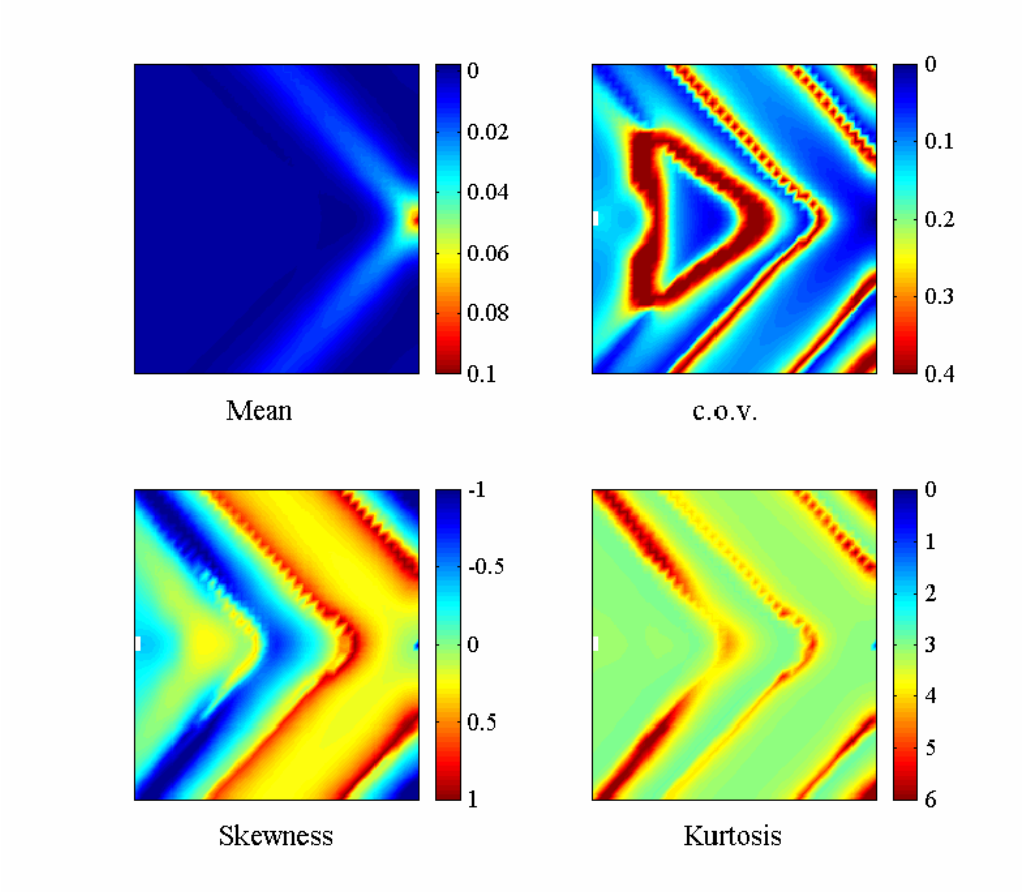

Figure 17. Micro-displacement along x axis: a) mean, b) c.o.v.; c) skewness; d) kurtosis

4.1 Linearized Multifield Elasticity

In standard elasticity of simple bodies, the linearization procedure is based on the systematic use of Fréchet derivative of maps between Banach spaces. Such a use relies upon the circumstance that the Euclidean structure of the point space in which the body is placed permits us to regard the set of maps $\tilde{\mathbf{x}}$'s (the space of placements) as an open set in a Banach space when there are no displacement boundary conditions (see [129], Chap. 4). In the general multifield setting, a basic difficulty arises. Since $\mathcal{M}$ does not coincide in general with a linear space, we may construct norms for the maps $\tilde{\nu}$'s of various nature but all based on the natural ways to define (in a certain sense) 'distances' over $\mathcal{M}$, as discussed in [49].

That plausible resulting norms, compatible with physical requirements, induce a natural Banach structure on the space of $\tilde{\nu}$'s, namely C_ν, is a rather delicate matter when $\mathcal{M}$ is not embedded. On the contrary, once we select $\mathcal{M}$ finite-dimensional and embed it in an appropriate linear space, results of H. Brézis and Y. Li [10] apply and one may consider C_ν as an appropriate Sobolev space.

Since our aim is to obtain a linearization, the embedding in $\mathfrak{L}^{(N)}$ and the Euclidean structure there (induced by the scalar product) may allow us to circumvent the general problem and consider, in the special case of the embedding, the space $\mathcal{C}$ of pairs of maps $(\tilde{\mathbf{x}}, \tilde{\nu})$ as a manifold modeled[16] over a Banach space which is sufficient for the use of Fréchet

[16]The manifolds treated in Section 2.1 are modeled over the Euclidean space because local charts take values in the Euclidean space.

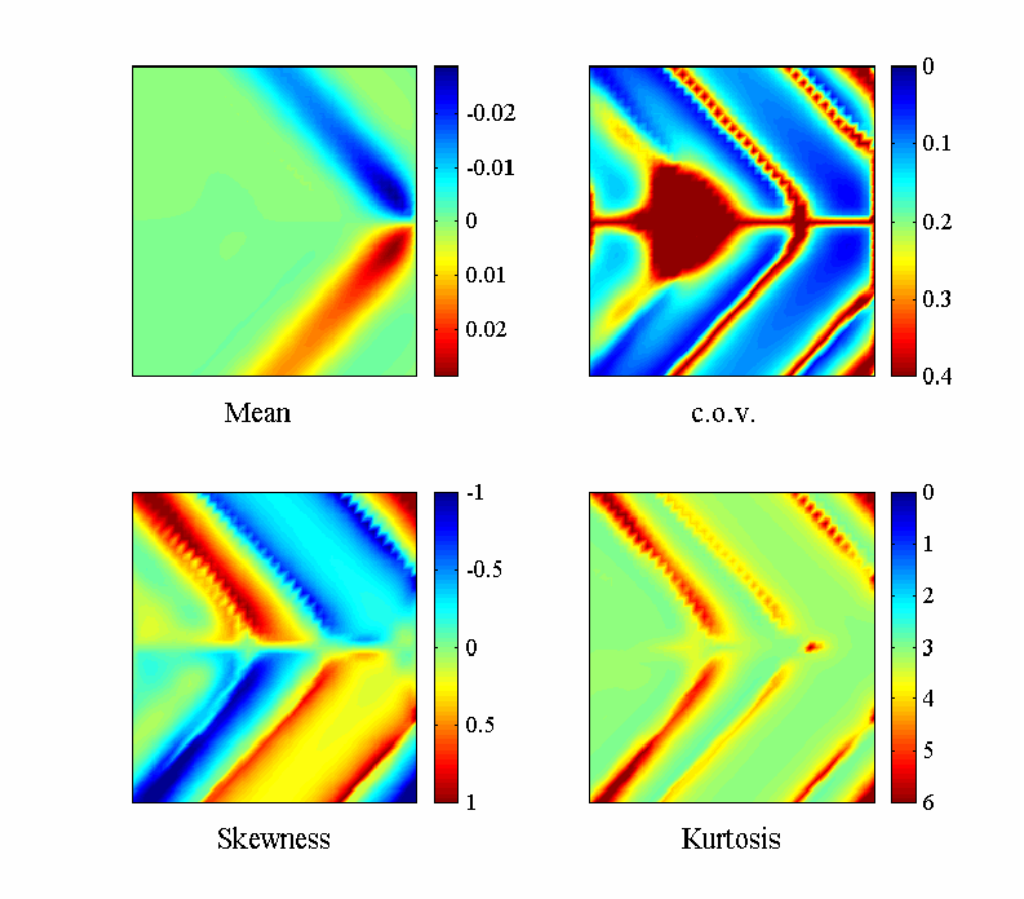

Figure 18. Micro-displacement along y axis: a) mean, b) c.o.v.; c) skewness; d) kurtosis

derivative that we make here. We remark once more that the choice of the appropriate isometric embedding (in particular the regularity of it [143], [144]) is a stringent matter of mechanical modeling.

Two basic assumptions apply:

H1. We act in the regime of infinitesimal deformations, i.e., $\left|(\nabla \mathbf{u})^i_J\right| << 1$ and presume that we may 'confuse' $\mathcal{B}_0$ with $\mathcal{B}$, in the sense that if $\mathbf{v}$ indicates a vector field tangent to $\mathbf{x}$, then $\mathbf{v} \approx \mathbf{u}$ at any $\mathbf{X}$ in $\mathcal{B}_0$. Moreover, we confuse ν with ν_a for consequent obvious reasons.

H2. We embed isometrically $\mathcal{M}$ in a linear space $\mathfrak{L}^{(N)}$, i.e. $\mathcal{M} \overset{N}{\hookrightarrow} \mathfrak{L}^{(N)}$, and assume the existence of a (physically significant) parallelism there.

We consider fields

$$\mathcal{B} = \tilde{\mathbf{x}}\left(\mathcal{B}_0\right) \ni \mathbf{x} \overset{\tilde{\mathbf{v}}}{\longmapsto} \mathbf{v} = \tilde{\mathbf{v}}\left(\mathbf{x}\right) \in T_{\mathbf{x}}\mathcal{E}^3, \tag{151}$$

$$\mathcal{B} = \tilde{\mathbf{x}}\left(\mathcal{B}_0\right) \ni \mathbf{x} \overset{\tilde{\upsilon}}{\longmapsto} \upsilon = \tilde{\upsilon}\left(\tilde{\nu}\left(\mathbf{x}\right)\right) \in T_{\nu}\mathcal{M}, \tag{152}$$

such that $\mathbf{v}$ and υ vanish where boundary conditions are imposed in terms of displacement and morphological descriptor. We make a slight abuse of notation (i) by writing ν and $\mathcal{M}$

as before the embedding and (ii) by indicating the fields defined just above the same letters of the actual rates $\mathbf{v}$ and υ.

The notation $L(A)(\bar{\mathbf{x}},\mathbf{v})(\bar{\nu},\upsilon)$ is used here to indicate the linearization of A 'about' the pair of maps $(\bar{\mathbf{x}},\bar{\nu})$.

In what follows we superpose a bar over 'objects' calculated at $(\bar{\mathbf{x}},\bar{\nu})$ and consider $\mathbf{v}$ and υ relative to $(\bar{\mathbf{x}},\bar{\nu})$.

Let $[0,\bar{t}]\ni t\longmapsto(\tilde{\mathbf{x}},\tilde{\nu})(t)$ be a smooth curve over $\mathcal{C}$ emanating from $(\bar{\mathbf{x}},\bar{\nu})$, i.e. such that $(\tilde{\mathbf{x}},\tilde{\nu})(0)=(\bar{\mathbf{x}},\bar{\nu})$. Since $\tilde{\mathbf{v}}(t)$ and $\tilde{\upsilon}(t)$ are associated with $\bar{\mathbf{x}}$ and $\bar{\nu}$ respectively, we say that $\tilde{\mathbf{v}}$ and $\tilde{\upsilon}$ *cover* $\bar{\mathbf{x}}$ and $\bar{\nu}$.

At each $\mathbf{X}$, the linearizations of the maps $\mathbf{x}\longmapsto\mathbf{F}$ and $\nu\longmapsto\nabla\nu$ 'about' $(\bar{\mathbf{x}},\bar{\nu})$ are then given by

$$L(\mathbf{F})(\bar{\mathbf{x}},\mathbf{v})=\bar{\mathbf{F}}+\nabla\mathbf{v}, \tag{153}$$

$$L(\nabla\nu)(\bar{\nu},\upsilon)=\overline{\nabla\nu}+\nabla\upsilon, \tag{154}$$

where $\nabla\mathbf{v}$ and $\nabla\upsilon$ are covariant derivatives of $\mathbf{v}$ and υ respectively. Previous formulas make sense because we have a parallel transport on $\tilde{\mathbf{x}}$ obtained by pointwise parallel transport of $\mathbf{F}$ over curves on $\mathcal{E}^3$, as well as we may use the parallelism assumed over $\mathcal{M}$ by H2 to transport $\nabla\nu$ along curves there. Moreover, since $\mathcal{M}$ is embedded and $\mathcal{L}^{(N)}$ is complete, we may also use geodetics to transport $\nabla\nu$.

The subsequent step is to consider the maps

$$\varsigma\longmapsto\tilde{\mathbf{P}}\circ\varsigma, \tag{155}$$

$$\varsigma\longmapsto\tilde{\mathbf{z}}\circ\varsigma, \tag{156}$$

$$\varsigma\longmapsto\tilde{\mathcal{S}}\circ\varsigma, \tag{157}$$

where $\varsigma=(\mathbf{F},\nu,\nabla\nu)$, and to linearize them 'about' $(\bar{\mathbf{x}},\bar{\nu})$. Under the assumption that they are sufficiently smooth to allow localization, we get at each $\mathbf{X}$

$$\begin{aligned} L\left(\tilde{\mathbf{P}}\right)(\bar{\mathbf{x}},\mathbf{v})(\bar{\nu},\upsilon) &= \bar{\mathbf{P}}+\overline{\partial_{\mathbf{F}}\mathbf{P}}\nabla\mathbf{v}+\overline{\partial_{\nu}\mathbf{P}}\upsilon+\overline{\partial_{\nabla\nu}\mathbf{P}}\nabla\upsilon= \\ &= \bar{\mathbf{P}}+\mathsf{A}_1^{(P)}\nabla\mathbf{v}+\mathsf{A}_2^{(P)}\upsilon+\mathsf{A}_3^{(P)}\nabla\upsilon= \\ &= \bar{\mathbf{P}}+\mathbf{L}^{(P)}(\nabla\mathbf{v},\upsilon,\nabla\upsilon), \end{aligned} \tag{158}$$

$$\begin{aligned} L(\tilde{\mathbf{z}})(\bar{\mathbf{x}},\mathbf{v})(\bar{\nu},\upsilon) &= \bar{\mathbf{z}}+\overline{\partial_{\mathbf{F}}\mathbf{z}}\nabla\mathbf{v}+\overline{\partial_{\nu}\mathbf{z}}\upsilon+\overline{\partial_{\nabla\nu}\mathbf{z}}\nabla\upsilon= \\ &= \bar{\mathbf{z}}+\mathsf{A}_1^{(z)}\nabla\mathbf{v}+\mathsf{A}_2^{(z)}\upsilon+\mathsf{A}_3^{(z)}\nabla\upsilon= \\ &= \bar{\mathbf{z}}+\mathbf{L}^{(z)}(\nabla\mathbf{v},\upsilon,\nabla\upsilon), \end{aligned} \tag{159}$$

$$\begin{aligned} L\left(\tilde{\mathcal{S}}\right)(\bar{\mathbf{x}},\mathbf{v})(\bar{\nu},\upsilon) &= \bar{\mathcal{S}}+\overline{\partial_{\mathbf{F}}\mathcal{S}}\nabla\mathbf{v}+\overline{\partial_{\nu}\mathcal{S}}\upsilon+\overline{\partial_{\nabla\nu}\mathcal{S}}\nabla\upsilon= \\ &= \bar{\mathcal{S}}+\mathsf{A}_1^{(\mathcal{S})}\nabla\mathbf{v}+\mathsf{A}_2^{(\mathcal{S})}\upsilon+\mathsf{A}_3^{(\mathcal{S})}\nabla\upsilon= \\ &= \bar{\mathcal{S}}+\mathbf{L}^{(\mathcal{S})}(\nabla\mathbf{v},\upsilon,\nabla\upsilon), \end{aligned} \tag{160}$$

where the $\mathsf{A}_i^{(\cdot)}$'s are tensors indicating formally the partial derivatives of the measures of interaction. For different circumstances, some of the $\mathsf{A}_i^{(\cdot)}$'s may vanish, so that we use the more general notation $\mathbf{L}^{(y)}\left(\nabla\mathbf{v}, \upsilon, \nabla\upsilon\right)$ to indicate that the measure of interaction y is expressed by a linear operator depending in general on $\nabla\mathbf{v}, \upsilon, \nabla\upsilon$.

We may reduce our treatment to the case in which $\bar{\mathbf{P}} = \mathbf{0}$, $\bar{\mathbf{z}} = \mathbf{0}$, and $\bar{\mathcal{S}} = \mathbf{0}$. Moreover, thanks to H1, we may substitute $\mathbf{v}$ with the displacement $\mathbf{u}$, so that we obtain linear constitutive equations of the form

$$\mathbf{P} = \mathbf{L}^{(P)}\left(\nabla\mathbf{u}, \upsilon, \nabla\upsilon\right), \tag{161}$$

$$\mathbf{z} = \mathbf{L}^{(z)}\left(\nabla\mathbf{u}, \upsilon, \nabla\upsilon\right), \tag{162}$$

$$\mathcal{S} = \mathbf{L}^{(\mathcal{S})}\left(\nabla\mathbf{u}, \upsilon, \nabla\upsilon\right). \tag{163}$$

In this case, the elastic energy is expressed by a quadratic form

$$\tilde{w}\left(\nabla\mathbf{u}, \upsilon, \nabla\upsilon\right) = Quad\left(\nabla\mathbf{u}, \upsilon, \nabla\upsilon\right) \tag{164}$$

such that its partial derivatives with respect to its entries furnish relevant measures of interaction.

With the linearization procedure explained roughly here we follow the linearization path discussed deeply in [129] and adapt it to the multifield setting. With respect to standard non-linear elasticity, a crucial point envisaged here is the hypothesis H2 concerning the isometric embedding of $\mathcal{M}$ in a linear space.

By construction, the linearization procedure above may be used also to describe the effects of superimposed infinitesimal deformations and 'infinitesimal' changes in substructural shapes over a given state where $\bar{\mathbf{P}}$, $\bar{\mathbf{z}}$, and $\bar{\mathcal{S}}$ do not vanish.

In this sense, the fields $\tilde{\mathbf{v}}$ and $\tilde{\upsilon}$ used just above play the role of *virtual* variations of a given morphology of the body.

4.2 Finite Element Models in the Linear Setting

In the linearized setting described above, various types of finite elements can be built up. Here, for the sake of simplicity, we construct some of them with reference to the model of elastic microcracked bodies discussed in Section 3 so that ν coincides with the microdisplacement d. We write everything with respect to $\mathcal{B}$ without making distinction with $\mathcal{B}_0$ because we are in infinitesimal deformation regime. In this way we reduce also the weight of the notation.

Just for reader's convenience, before going on, we recall the linearized constitutive equations introduced in Section 3, namely

$$\mathbf{P} = \mathbb{A}\nabla\mathbf{u} + \mathbb{A}'\nabla\mathsf{d}, \tag{165}$$

$$\mathbf{z} = \mathbb{C}\mathsf{d}, \tag{166}$$

$$\mathcal{S} = \mathbb{G}'\nabla\mathbf{u} + \mathbb{G}\nabla\mathsf{d}, \tag{167}$$

that are special cases of (161)-(163).

Let us denote by

- $\partial\mathcal{B}_u$ the part of the boundary of $\mathcal{B}$ on which the displacement $\mathbf{u}$ is prescribed;
- $\partial\mathcal{B}_{\mathsf{d}}$ the part on which d is prescribed;

- $\partial\mathcal{B}_{\mathbf{t}}$ the part on which the traction $\mathbf{Pn}$ is prescribed ($\partial\mathcal{B}_{\mathbf{t}}$ does not intersect $\partial\mathcal{B}_{\mathbf{u}}$, i.e. $\partial\mathcal{B}_{\mathbf{u}} \cup \partial\mathcal{B}_{\mathbf{t}} = \partial\mathcal{B}$ and $\partial\mathcal{B}_{\mathbf{u}} \cap \partial\mathcal{B}_{\mathbf{t}} = \varnothing$);
- $\partial\mathcal{B}_{\tau}$ the part on which $\mathcal{S}\mathbf{n}$ is prescribed ($\partial\mathcal{B}_{\mathsf{d}} \cap \partial\mathcal{B}_{\tau} = 0$; and $\partial\mathcal{B}_{\mathsf{d}} \cup \partial\mathcal{B}_{\tau} = \partial\mathcal{B}$).

We shall assume that $\partial\mathcal{B}_{\mathbf{u}} \equiv \partial\mathcal{B}_{\mathsf{d}}$ and $\partial\mathcal{B}_{\mathbf{t}} \equiv \partial\mathcal{B}_{\tau}$ although in principle they could be different. For this reason we continue to write them with their own specific subscript.

To construct finite elements on $\mathcal{B}$ we must first define a *tessellation* $\{\mathcal{B}_e\}$ of $\mathcal{B}$ made of M regular parts of $\mathcal{B}$. The following notations apply in the sequel of this section:

- $\partial\mathcal{B}_{e\mathbf{u}} = \partial\mathcal{B}_e \cap \partial\mathcal{B}_{\mathbf{u}}$,
- $\partial\mathcal{B}_{e\mathsf{d}} = \partial\mathcal{B}_e \cap \partial\mathcal{B}_{\mathsf{d}}$,
- $\partial\mathcal{B}_{e\mathbf{t}} = \partial\mathcal{B}_e \cap \partial\mathcal{B}_{\mathbf{t}}$,
- $\partial\mathcal{B}_{e\tau} = \partial\mathcal{B}_e \cap \partial\mathcal{B}_{\tau}$,
- $\partial\mathcal{B}_{ij} = \partial\mathcal{B}_i \cap \partial\mathcal{B}_j$, with i and j indicating different elements of the tessellation $\{\mathcal{B}_e\}$.

As usual in finite element methods (FEM), some points (finite in number) in each $\mathcal{B}_e$ play the role of *nodes* in calculations. Here, the *degrees of freedom* of each node are listed in an array containing both the *nodal displacement* $\hat{\mathbf{u}}_e$ and the *nodal micro displacement* $\hat{\mathsf{d}}_e$. The subscript e indicates that $\hat{\mathbf{u}}_e$ and $\hat{\mathsf{d}}_e$ pertain to the generic finite element $\mathcal{B}_e$.

Each node may have *two* (one-dimensional case, 1D), *four* (2D) or *six* (3D) degrees of freedom in terms of displacements.

Matrices of *shape functions* $\Phi^e_{\mathbf{u}}$ and Φ^e_{d} need to be introduced to obtain *element displacements* $\mathbf{u}_e$ and d_e along each element $\mathcal{B}_e$ in the standard way, namely

$$\mathbf{u}_e = \Phi^e_{\mathbf{u}}\hat{\mathbf{u}}_e \quad , \quad \mathsf{d}_e = \Phi^e_{\mathsf{d}}\hat{\mathsf{d}}_e. \tag{168}$$

With reference to each $\mathcal{B}_e$, we write *weak* integral versions of the balance equations of standard and substructural interactions (roughly speaking, the equality between external and internal *virtual* power of all interactions over $\mathcal{B}$ is possibly modified by the addition of different conditions as we shall see later). To this aim we introduce vector-valued *test functions*[17] $\widetilde{\mathbf{u}}_e$ and $\widetilde{\mathsf{d}}_e$ with the physical meaning of displacements, multiply local balances time the variations $\delta\widetilde{\mathbf{u}}_e$ and $\delta\widetilde{\mathsf{d}}_e$ and integrate on each $\mathcal{B}_e$. In developing calculations we meet integral terms of the type

$$\int_{\mathcal{B}_e} \left(\delta\,(\text{test. funct.}) \cdot (\text{Differential operator})\,(\mathbf{u}_e, \mathsf{d}_e)\right) d^3\mathbf{x}, \tag{169}$$

so we need to assume tacitly that $\widetilde{\mathbf{u}}_e$ and $\widetilde{\mathsf{d}}_e$ satisfy standard regularity properties assuring that the above mentioned integrals make sense.

Test functions $\mathbf{t}_e$ and τ_e analogous to $\widetilde{\mathbf{u}}_e$ and $\widetilde{\mathsf{d}}_e$ need to be introduced to obtain mixed finite elements written both in terms of displacements and tractions. Test functions $\mathbf{t}_e$ and

[17] We do not discuss here the analytical properties of the solutions. In any case we are in a situation in which basic analytical properties of finite elements can be applied (see [37]). Note, in fact, that the choice of a positive definite potential energy and the boundedness of the constitutive tensors in (165)-(167), written explicitly in Section 3, assure the uniqueness of the solution thanks to Lax-Milgram theorem. Consequently, *a-priori* estimates of the errors can be obtained by standard procedures for elliptic systems (see [175] and [37]).

τ_e have in this context the physical meaning of tractions. In principle $\widetilde{\mathbf{u}}_e$, $\widetilde{\mathsf{d}}_e$, $\mathbf{t}_e$ and τ_e are arbitrary (provided that they satisfy standard regularity conditions) and do not correspond with true displacements and tractions. Of course it is possible to identify $\widetilde{\mathbf{u}}_e$ with $\mathbf{u}_e$, $\widetilde{\mathsf{d}}_e$ with d_e throughout each finite element $\mathcal{B}_e$ as well as $\mathbf{t}_e$ with $\mathbf{P}\mathbf{n}_e$ and τ_e with $\mathcal{S}\mathbf{n}_e$ at the boundary of each element without loss of generality; i.e. it is possible to identify each test function with the corresponding real field. Of course, $\mathbf{n}_e$ is the outward unit normal at the boundary of $\mathcal{B}_e$.

We denote by $\widetilde{\mathbf{u}}_e^{(i)}$ and $\widetilde{\mathsf{d}}_e^{(i)}$ the *test displacements* of the i-th element and by $\mathbf{t}_e^{(i)}$ and $\tau_e^{(i)}$ standard and generalized *test tractions* at the boundary of the i-th element: $\mathbf{t}_e$ and τ_e are conjugated with $\widetilde{\mathbf{u}}_e$ and $\widetilde{\mathsf{d}}_e$ respectively. At the common interface $\partial\mathcal{B}_{ij}$ *continuity conditions* need be satisfied for any i and j.

Continuity conditions:

$$\widetilde{\mathbf{u}}_e^{(i)} - \widetilde{\mathbf{u}}_e^{(j)} = 0 \quad \text{on } \partial\mathcal{B}_{ij}, \tag{170}$$

$$\widetilde{\mathsf{d}}_e^{(i)} - \widetilde{\mathsf{d}}_e^{(j)} = 0 \quad \text{on } \partial\mathcal{B}_{ij}, \tag{171}$$

$$\mathbf{t}_e^{(i)} - \mathbf{t}_e^{(j)} = 0 \quad \text{on } \partial\mathcal{B}_{ij}, \tag{172}$$

$$\tau_e^{(i)} - \tau_e^{(j)} = 0 \quad \text{on } \partial\mathcal{B}_{ij}, \tag{173}$$

$$\widetilde{\mathbf{u}}_e = \overline{\mathbf{u}}_e \quad \text{on } \partial\mathcal{B}_{e\mathbf{u}}, \tag{174}$$

$$\widetilde{\mathsf{d}}_e = \overline{\mathsf{d}}_e \quad \text{on } \partial\mathcal{B}_{e\mathsf{d}}, \tag{175}$$

$$\mathbf{t}_e = \overline{\mathbf{t}}_e \quad \text{on } \partial\mathcal{B}_{e\mathbf{t}}, \tag{176}$$

$$\tau_e = \overline{\tau}_e \quad \text{on } \partial\mathcal{B}_{e\tau}, \tag{177}$$

where $\overline{\mathbf{u}}_e$, $\overline{\mathsf{d}}_e$, $\overline{\mathbf{t}}_e$ and $\overline{\tau}_e$ are prescribed data.

As common in FEM, we need to relax (170)-(173) and consider at each interface between adjacent elements continuity conditions involving integrals like

$$\int_{\partial\mathcal{B}_{ij}} \delta\lambda_{\mathbf{u}}^T \left(\widetilde{\mathbf{u}}_e^{(i)} - \widetilde{\mathbf{u}}_e^{(j)}\right) d\mathcal{H}^2 + \int_{\partial\mathcal{B}_{ij}} \delta\lambda_{\mathsf{d}}^T \left(\widetilde{\mathsf{d}}_e^{(i)} - \widetilde{\mathsf{d}}_e^{(j)}\right) d\mathcal{H}^2 +$$

$$+ \int_{\partial\mathcal{B}_{ij}} \delta\mu_{\mathbf{t}}^T \left(\mathbf{t}_e^{(i)} + \mathbf{t}_e^{(j)}\right) d\mathcal{H}^2 + \int_{\partial\mathcal{B}_{ij}} \delta\mu_{\tau}^T \left(\tau_e^{(i)} + \tau_e^{(j)}\right) d\mathcal{H}^2 \tag{178}$$

Here, $\delta\lambda$ and $\delta\mu$ are multipliers defined only on the interfaces $\partial\mathcal{B}_{ij}$ and such that

$$\delta\lambda_{\mathbf{u}}^{(i)} = -\delta\lambda_{\mathbf{u}}^{(j)} = \delta\lambda_{\mathbf{u}}, \quad \delta\lambda_{\mathsf{d}}^{(i)} = -\delta\lambda_{\mathsf{d}}^{(j)} = \delta\lambda_{\mathsf{d}}, \tag{179}$$

$$\delta\mu_{\mathbf{t}}^{(i)} = \delta\mu_{\mathbf{t}}^{(j)} = \delta\mu_{\mathbf{t}}, \quad \delta\mu_{\tau}^{(i)} = \delta\mu_{\tau}^{(j)} = \delta\mu_{\tau}. \tag{180}$$

With these premises, different FEM can be built up. Some of them are described in what follows. In constructing FEM we adapt the way typically used in standard linear elasticity to the multifield case treated here.

4.3 Additional Remarks

Before describing in detail some finite elements that can be constructed in the situation summarized above, we add other remarks about the embedding of $\mathcal{M}$ and the nature of boundary conditions.

Remark 1

For some special models, the manifold of substructural shapes $\mathcal{M}$ is naturally a *submanifold* of some linear space. In this case, to construct numerical algorithms, we may (i) assume that *a priori* the morphological descriptor map $\tilde{\nu}$ may take values over the whole pertinent linear space, then (ii) we may *add* an *internal constraint* forcing $\tilde{\nu}$ to go in $\mathcal{M}$.

Roughly speaking, we may think of reaching values of ν moving freely within the pertinent linear space *even outside* $\mathcal{M}$ and to come back in $\mathcal{M}$ itself by means of some internal constraint. Such a point of view renders more easy in some circumstances the selection of appropriate numerical algorithms (see in some special cases [32] and [6]).

A paradigmatic example of this kind of reasoning is the one of ferroelectrics described in Section 2. The local polarization vector p belongs to the ball B_{p_m}. In the spirit of the framework described in Section 2 we should consider now B_{p_m} as a manifold per se, living outside everything. In this way we can develop the relevant mechanics as in previous sections. However, B_{p_m} is also naturally a submanifold of $\mathbb{R}^3$ so that one may think of the morphological descriptor p as an element of $\mathbb{R}^3$, develop the relevant mechanics and add the side condition $|\mathsf{p}| \leq p_m$.

The same scheme applies also to materials undergoing spontaneous magnetization due to different sources like the application of external electromagnetic fields or deformation. The natural morphological descriptor of the local magnetization state is a vector belonging to the unitary ball in $\mathbb{R}^3$. Here, a special subcase deserves particular attention. In fact, in saturation conditions the local magnetization is constant and just its orientation may vary from place to place so that it is described by a unit vector ς and $\mathcal{M}$ coincides with the unit sphere S^2. Even in this case we may consider S^2 as an abstract manifold or as a submanifold of $\mathbb{R}^3$ defined by the side condition $|\varsigma| = 1$. Moreover, another constraint applies: Since ς is constrained to have unitary length, its possible inertia must be only of rotational nature. Before going on, we recall that we have obtained an explicit expression of the inertial component $\beta^{(in)}$ of substructural bulk actions by requiring that its power $\beta^{(in)} \cdot \dot{\nu}$ equals the negative rate of the substructural kinetic energy, if existing (see Section 2). However, in adopting such a procedure, the identification of $\beta^{(in)}$ is obtained unless a powerless term. In coming back to the case of micromagnetics in saturation conditions, we then realize that such a possible powerless therm plays a role. Rotational inertia occurring in micromagnetics is, in fact, of this type and is not derived from a kinetic energy. We may select, in fact, $\beta^{(in)} = -\varsigma \times \dot{\varsigma}$ which vanishes when multiplied by $\dot{\varsigma}$ (i.e. $(\varsigma \times \dot{\varsigma}) \cdot \dot{\varsigma} = 0$ trivially). Moreover, if we leave also out the standard deformation and select a free energy of the type

$$\psi = \tilde{\psi}(\varsigma, \nabla\varsigma) = \frac{1}{2} \|\nabla\varsigma\|^2, \tag{181}$$

with normalized material constants, the balance of substructural interactions reduces to

$$\dot{\varsigma} = -\varsigma \times \Delta\varsigma, \tag{182}$$

which coincides with Landau-Lifshitz-Gilbert equation in the case in which only gyromagnetic effects are accounted for.

Remark 2

In the finite element models developed below in linearized setting, there are various boundary conditions involving boundary values of the morphological descriptor ν and of the micro-traction $\mathcal{S}\mathbf{n}$. They generate Cauchy or Neumann boundary value problems or combinations of them. From a mathematical point of view the assignment of ν and $\mathcal{S}\mathbf{n}$ on some portions of the boundary is natural. However, there is doubt about the possibility to have at disposal loading devices allowing us to furnish physical concreteness to these kind of boundary conditions in all cases. We can tell a few words in general. The question must be tacked case by case. For example, in the case of liquid crystals we can assign the orientation of the stick molecules at the boundary by making use of appropriate (chemical and/or mechanical) treatments of the walls of the container of the liquid crystal itself. In the case of microcracked bodies, the condition $\mathcal{S}\mathbf{n} = \mathbf{0}$ seems to be the sole boundary condition in terms of microtractions with physical meaning. The reason is that at the boundary microcracks loose their identity since they are determined just by the *surrounding* matter so that at the boundary they become just corrugations of the boundary itself, as mentioned previously.

In general we could act in two different manners:

(*a*) We may think of a sort of limit layer theory and consider the external boundary as a sort of membrane 'packing up' the body. In this way, we may assume the existence of two surface densities $\bar{U}(\mathbf{x})$ and $U(\nu)$ such that

$$\mathbf{P}\mathbf{n} = \mathbf{t} = \rho_0 \partial_{\mathbf{x}} \bar{U} \quad , \quad \mathcal{S}\mathbf{n} = \tau = \rho_0 \partial_\nu U, \tag{183}$$

where $\bar{U}$ and U plays here the rôle of surface potentials as suggested in [21]. A concrete example of this idea can be found in [9] with reference to nematic liquid crystals.

(*b*) In the case in which the substructure becomes 'latent' in Capriz's sense and an internal length scale can be easily recognized. Series expansions with respect to the internal length may allow us to transform the boundary value (multifield) problem that we handle in a hierarchy of (multiscale, in some sense) problems that require just prescriptions of data in terms of standard tractions or displacements. This kind of point of view has been proposed in [88] with reference to Cosserat elastic bodies but it has been not yet developed in general.

4.4 Compatible Models

Two models of finite elements written only in terms of displacements are presented here. Both models *require a-priori the validity of the constitutive relations* above. They *differ* in terms of boundary conditions of both prescribed data and type of continuity required at the interfaces between neighboring finite element.

4.4.1 Model 1

We *assume* that at the boundary $\partial\mathcal{B}_e$ of the generic element $\mathcal{B}_e$ the following conditions are satisfied *a-priori*:

$$\mathbf{u}_e = \widetilde{\mathbf{u}}_e \quad , \quad \mathsf{d}_e = \widetilde{\mathsf{d}}_e, \tag{184}$$

$$\mathbf{P}\mathbf{n}_e = \mathbf{t}_e \quad , \quad \mathcal{S}\mathbf{n}_e = \tau_e, \tag{185}$$

In other words, *we prescribe that at the boundary of each element the test functions coincide with the related true fields.*

We assume also the validity *a-priori* of the following conditions

$$\widetilde{\mathbf{u}}_e^{(i)} - \widetilde{\mathbf{u}}_e^{(j)} = 0 \quad \text{on } \partial\mathcal{B}_{ij}, \tag{186}$$

$$\widetilde{\mathsf{d}}_e^{(i)} - \widetilde{\mathsf{d}}_e^{(j)} = 0 \quad \text{on } \partial\mathcal{B}_{ij}, \tag{187}$$

$$\widetilde{\mathbf{u}}_e^{(i)} - \widetilde{\mathbf{u}}_e^{(j)} = 0 \quad \text{on } \partial\mathcal{B}_{ij}, \tag{188}$$

$$\widetilde{\mathsf{d}}_e^{(i)} - \widetilde{\mathsf{d}}_e^{(j)} = 0 \quad \text{on } \partial\mathcal{B}_{ij}. \tag{189}$$

We *impose* balance equations, the equilibrium conditions at each interface and the boundary conditions over $\partial\mathcal{B}_{e\mathbf{t}}$ and $\partial\mathcal{B}_{e\tau}$.

The integral version of the equilibrium problem, pertaining to the generic element $\mathcal{B}_e$, is given by[18]

$$\begin{aligned}
&\int_{\mathcal{B}_e} \delta\mathbf{u} \cdot \left(div\left(\mathbb{A}\nabla\mathbf{u}+\mathbb{A}'\nabla\mathsf{d}\right) - \mathbf{b}\right) d^3\mathbf{x} + \int_{\mathcal{B}_e} \delta\mathsf{d} \cdot \left(div\left(\mathbb{A}'\nabla\mathbf{u}+\mathbb{G}\nabla\mathsf{d}\right) - \mathbb{C}\mathsf{d}\right) d^3\mathbf{x} + \\
&+ \int_{\partial\mathcal{B}_{e\mathbf{t}}} \delta\mathbf{u} \cdot \left(\left(\mathbb{A}\nabla\mathbf{u}+\mathbb{A}'\nabla\mathsf{d}\right)\mathbf{n} - \overline{\mathbf{t}}\right) d\mathcal{H}^2 + \int_{\partial\mathcal{B}_{e\tau}} \delta\mathsf{d} \cdot \left(\left(\mathbb{A}'\nabla\mathbf{u}+\mathbb{G}\nabla\mathsf{d}\right)\mathbf{n} - \overline{\tau}\right) d\mathcal{H}^2 + \\
&+ \int_{\partial\mathcal{B}_e^*} \delta\mathbf{u} \cdot \left(\mathbb{A}\nabla\mathbf{u}+\mathbb{A}'\nabla\mathsf{d}\right)\mathbf{n} d\mathcal{H}^2 + \int_{\partial\mathcal{B}_e^*} \delta\mathsf{d} \cdot \left(\mathbb{A}'\nabla\mathbf{u}+\mathbb{G}\nabla\mathsf{d}\right)\mathbf{n} d\mathcal{H}^2 = 0,
\end{aligned} \tag{190}$$

where $\delta\mathbf{u}$ and $\delta\mathsf{d}$ are standard variations vanishing at the boundary where the displacements are prescribed and $\partial\mathcal{B}_e^*$ is the part of the boundary of $\mathcal{B}_e^*$ *internal* to $\mathcal{B}$.

In obtaining the previous integral balance, we make use of (178) identifying $\delta\mu_{\mathbf{t}}$ with $\delta\mathbf{u}$ and $\delta\mu_\tau$ with $\delta\mathsf{d}$. Such an assumption is peculiar of "Model 1".

By integrating (190) by parts we get

$$\begin{aligned}
&\int_{\mathcal{B}_e} \left(\delta\left(\nabla\mathbf{u}\right) \cdot \left(\mathbb{A}\nabla\mathbf{u}+\mathbb{A}'\nabla\mathsf{d}\right) + \delta\mathsf{d} \cdot \mathbb{C}\mathsf{d} + \delta\left(\nabla\mathsf{d}\right) \cdot \left(\mathbb{G}\nabla\mathsf{d} + \mathbb{A}'\nabla\mathbf{u}\right)\right) d^3\mathbf{x} = \\
&= \int_{\mathcal{B}_e} \delta\mathbf{u} \cdot \mathbf{b} d^3\mathbf{x} + \int_{\partial\mathcal{B}_{e\mathbf{t}}} \delta\mathbf{u} \cdot \overline{\mathbf{t}} d\mathcal{H}^2 + \int_{\partial\mathcal{B}_{e\mathbf{t}}} \delta\mathsf{d} \cdot \overline{\tau} d\mathcal{H}^2,
\end{aligned} \tag{191}$$

then, with the use of (168), it follows that

$$\begin{aligned}
&\delta\hat{\mathbf{u}}_e \cdot \left(\int_{\mathcal{B}_e} \left(\left(\nabla\Phi_{\mathbf{u}}^e\right)^T \mathbb{A}\nabla\Phi_{\mathbf{u}}^e\hat{\mathbf{u}}_e + \nabla\Phi_{\mathbf{u}}^e\mathbb{A}'\nabla\Phi_{\mathsf{d}}^e\hat{\mathsf{d}}_e\right) d^3\mathbf{x}\right) + \\
&+\delta\hat{\mathsf{d}}_e \cdot \left(\int_{\mathcal{B}_e} \left(\Phi_{\mathsf{d}}^{eT}\mathbb{C}\Phi_{\mathsf{d}}^e\hat{\mathsf{d}}_e + \left(\nabla\Phi_{\mathsf{d}}^e\right)^T \mathbb{G}\nabla\Phi_{\mathsf{d}}^e\hat{\mathsf{d}}_e + \Phi_{\mathsf{d}}^{eT}\mathbb{A}'\nabla\Phi_{\mathbf{u}}^e\hat{\mathbf{u}}_e\right) d^3\mathbf{x}\right) = \\
&= \delta\hat{\mathbf{u}}_e \cdot \left(\int_{\mathcal{B}_e} \Phi_{\mathbf{u}}^{eT}\mathbf{b} d^3\mathbf{x} + \int_{\partial\mathcal{B}_e} \Phi_{\mathbf{u}}^{eT}\overline{\mathbf{t}} d\mathcal{H}^2\right) + \delta\hat{\mathsf{d}}_e \cdot \left(\int_{\partial\mathcal{B}_{e\tau}} \Phi_{\mathsf{d}}^{eT}\overline{\tau} d\mathcal{H}^2\right),
\end{aligned} \tag{192}$$

which holds for *any* choice of the variations $\delta\hat{\mathbf{u}}_e$ and $\delta\hat{\mathsf{d}}_e$. As a consequence, we reduce our equilibrium problem to the study of the algebraic system

$$\mathbf{K}\left\{\begin{array}{c} \hat{\mathbf{u}}_e \\ \hat{\mathsf{d}}_e \end{array}\right\} = \left\{\begin{array}{c} \mathbf{r}_{\mathbf{u}}^e \\ \mathbf{r}_{\mathsf{d}}^e \end{array}\right\}, \tag{193}$$

[18] From now on the index "e" is often suppressed when a given field is under some integral on $\mathcal{B}_e$ or part of its boundary when the symbology can be simplified.

where the stiffness matrix $\mathbf{K}$ is given by

$$\mathbf{K} = \begin{bmatrix} \int_{\mathcal{B}_e} \left((\nabla \Phi^e_{\mathbf{u}})^T \, \mathbb{A} \nabla \Phi^e_{\mathbf{u}} \right) d^3\mathbf{x} & \int_{\mathcal{B}_e} \Phi^{eT}_{\mathsf{d}} \mathbb{A}' \nabla \Phi^e_{\mathbf{u}} d^3\mathbf{x} \\ \int_{\mathcal{B}_e} \Phi^{eT}_{\mathsf{d}} \mathbb{A}' \nabla \Phi^e_{\mathbf{u}} d^3\mathbf{x} & \int_{\mathcal{B}_e} \left(\Phi^{eT}_{\mathsf{d}} \mathbb{C} \Phi^e_{\mathsf{d}} + (\nabla \Phi^e_{\mathsf{d}})^T \, \mathbb{G} \nabla \Phi^e_{\mathsf{d}} \right) d^3\mathbf{x} \end{bmatrix} \tag{194}$$

and

$$\left\{ \begin{array}{c} \mathbf{r}^e_{\mathbf{u}} \\ \\ \mathbf{r}^e_{\mathsf{d}} \end{array} \right\} = \left\{ \begin{array}{c} \int_{\mathcal{B}_e} \Phi^{eT}_{\mathbf{u}} \mathbf{b} d^3\mathbf{x} + \int_{\partial \mathcal{B}_{e\mathbf{t}}} \Phi^{eT}_{\mathbf{u}} \overline{\mathbf{t}} d\mathcal{H}^2 \\ \\ \int_{\mathcal{B}_e} \Phi^{eT}_{\mathsf{d}} \overline{\tau} d^3\mathbf{x} \end{array} \right\}. \tag{195}$$

This finite element scheme has been used to obtain the numerical results collected in Section 3.

4.4.2 Model 2

We *assume* that the following conditions are satisfied *a-priori* at the boundary $\partial \mathcal{B}_e$ of the generic element $\mathcal{B}_e$

$$\mathbf{u}_e = \widetilde{\mathbf{u}}^{(i)}_e \qquad \text{on } \partial \mathcal{B}_e, \tag{196}$$

$$\mathsf{d}_e = \widetilde{\mathsf{d}}^{(i)}_e \qquad \text{on } \partial \mathcal{B}_e, \tag{197}$$

$$\mathbf{t}^{(i)}_e + \mathbf{t}^{(j)}_e = 0 \qquad \text{on } \partial \mathcal{B}_{ij}, \tag{198}$$

$$\tau^{(i)}_e + \tau^{(j)}_e = 0 \qquad \text{on } \partial \mathcal{B}_{ij}. \tag{199}$$

Then we *impose* the balances of standard and substructural interactions together with the following boundary conditions:

$$\left(\mathbb{A} \nabla \mathbf{u} + \mathbb{A}' \nabla \mathsf{d} \right) \mathbf{n}_e - \mathbf{t} = \mathbf{0} \quad \text{on } \partial \mathcal{B}_e, \tag{200}$$

$$\left(\mathbb{A}' \nabla \mathbf{u} + \mathbb{G} \nabla \mathsf{d} \right) \mathbf{n}_e - \tau = \mathbf{0} \quad \text{on } \partial \mathcal{B}_e, \tag{201}$$

$$\mathbf{u}^{(i)}_e - \mathbf{u}^{(j)}_e = 0 \quad \text{on } \partial \mathcal{B}_{ij}, \tag{202}$$

$$\mathsf{d}^{(i)}_e - \mathsf{d}^{(j)}_e = 0 \quad \text{on } \partial \mathcal{B}_{ij}, \tag{203}$$

$$\mathbf{u}_e = \overline{\mathbf{u}}_e \quad \text{on } \partial \mathcal{B}_{e\mathbf{u}}, \tag{204}$$

$$\mathsf{d}_e = \overline{\mathsf{d}}_e \quad \text{on } \partial \mathcal{B}_{e\mathsf{d}}, \tag{205}$$

$$\mathbf{t} = \overline{\mathbf{t}} \quad \text{on } \partial \mathcal{B}_{e\mathbf{t}}, \tag{206}$$

$$\tau = \overline{\tau} \quad \text{on } \partial \mathcal{B}_{e\tau}. \tag{207}$$

With reference to a generic element $\mathcal{B}_e$, we then write the weak version of the balance equations with previous boundary conditions as

$$\int_{\mathcal{B}_e} \delta\mathbf{u}\cdot\left(div\left(\mathbb{A}\nabla\mathbf{u}+\mathbb{A}'\nabla\mathsf{d}\right)-\mathbf{b}\right)d^3\mathbf{x}+\int_{\mathcal{B}_e}\delta\mathsf{d}\cdot\left(div\left(\mathbb{A}'\nabla\mathbf{u}+\mathbb{G}\nabla\mathsf{d}\right)-\mathbb{C}\mathsf{d}\right)d^3\mathbf{x}+$$
$$+\int_{\partial\mathcal{B}_e}\delta\mathbf{u}\cdot\left(\left(\mathbb{A}\nabla\mathbf{u}+\mathbb{A}'\nabla\mathsf{d}\right)\mathbf{n}-\mathbf{t}\right)d\mathcal{H}^2+\int_{\partial\mathcal{B}_{e\tau}}\delta\mathsf{d}\cdot\left(\left(\mathbb{A}'\nabla\mathbf{u}+\mathbb{G}\nabla\mathsf{d}\right)\mathbf{n}-\tau\right)d\mathcal{H}^2+$$
$$+\int_{\partial\mathcal{B}_e^*}\delta\mathbf{t}\cdot\mathbf{u}d\mathcal{H}^2-\int_{\partial\mathcal{B}_e^*}\delta\tau\cdot\mathsf{d}d\mathcal{H}^2-\int_{\partial\mathcal{B}_{e\mathbf{u}}}\delta\mathbf{t}\cdot\left(\mathbf{u}-\overline{\mathbf{u}}\right)d\mathcal{H}^2-\int_{\partial\mathcal{B}_{e\mathsf{d}}}\delta\tau\cdot\left(\mathsf{d}-\overline{\mathsf{d}}\right)d\mathcal{H}^2+$$
$$+\int_{\partial\mathcal{B}_{e\mathbf{t}}}\delta\mathbf{u}\cdot\left(\mathbf{t}-\overline{\mathbf{t}}\right)d\mathcal{H}^2+\int_{\partial\mathcal{B}_{e\tau}}\delta\mathsf{d}\cdot\left(\tau-\overline{\tau}\right)d\mathcal{H}^2=0. \quad (208)$$

In obtaining the last relation, we use some integrals like the ones in (178) and identify $\delta\lambda_{\mathbf{u}}$ with $\delta\mathbf{t}$ and $\delta\lambda_{\mathsf{d}}$ with $\delta\tau$. This type of identification is an assumption peculiar of Model 2.

Variations of test functions vanish on the portion of the boundary where the relevant fields are prescribed, i.e. $\delta\mathbf{u}=0$ on $\partial\mathcal{B}_{e\mathbf{u}}$. Consequently, by integrating by parts, we obtain

$$\int_{\mathcal{B}_e}\left(\delta\left(\nabla\mathbf{u}\right)\cdot\left(\mathbb{A}\nabla\mathbf{u}+\mathbb{A}'\nabla\mathsf{d}\right)+\delta\mathsf{d}\cdot\mathbb{C}\mathsf{d}+\delta\left(\nabla\mathsf{d}\right)\cdot\left(\mathbb{G}\nabla\mathsf{d}+\mathbb{A}'\nabla\mathbf{u}\right)\right)d^3\mathbf{x}=$$
$$=\int_{\mathcal{B}_e}\delta\mathbf{u}\cdot\mathbf{b}d^3\mathbf{x}+\int_{\partial\mathcal{B}_e}\delta\mathbf{u}\cdot\mathbf{t}d\mathcal{H}^2+\int_{\partial\mathcal{B}_e}\delta\mathsf{d}\cdot\tau d\mathcal{H}^2+\int_{\partial\mathcal{B}_e^*}\delta\mathbf{t}\cdot\mathbf{u}d\mathcal{H}^2+$$
$$+\int_{\partial\mathcal{B}_e^*}\delta\tau\cdot\mathsf{d}d\mathcal{H}^2+\int_{\partial\mathcal{B}_{e\mathbf{u}}}\delta\mathbf{t}\cdot\left(\mathbf{u}-\overline{\mathbf{u}}\right)d\mathcal{H}^2+\int_{\partial\mathcal{B}_{e\mathsf{d}}}\delta\tau\cdot\left(\mathsf{d}-\overline{\mathsf{d}}\right)d\mathcal{H}^2-$$
$$-\int_{\partial\mathcal{B}_{e\mathbf{t}}}\delta\mathbf{u}\cdot\left(\mathbf{t}-\overline{\mathbf{t}}\right)d\mathcal{H}^2-\int_{\partial\mathcal{B}_{e\tau}}\delta\mathsf{d}\cdot\left(\tau-\overline{\tau}\right)d\mathcal{H}^2. \quad (209)$$

We assume also

$$\mathbf{u}_e=\overline{\mathbf{u}}_e \quad \text{on } \partial\mathcal{B}_{e\mathbf{u}}, \quad (210)$$

$$\mathsf{d}_e=\overline{\mathsf{d}}_e \quad \text{on } \partial\mathcal{B}_{e\mathsf{d}}, \quad (211)$$

$$\delta\mathbf{u}=\mathbf{0} \quad \text{on } \partial\mathcal{B}_{e\mathbf{u}}, \quad (212)$$

$$\delta\mathsf{d}=0 \quad \text{on } \partial\mathcal{B}_{e\mathsf{d}}. \quad (213)$$

By using (168), after some algebra we obtain

$$\delta\hat{\mathbf{u}}_e\cdot\left(\int_{\mathcal{B}_e}\left(\left(\nabla\Phi^e_{\mathbf{u}}\right)^T\mathbb{A}\nabla\Phi^e_{\mathbf{u}}\hat{\mathbf{u}}_e+\nabla\Phi^e_{\mathbf{u}}\mathbb{A}'\nabla\Phi^e_{\mathsf{d}}\hat{\mathsf{d}}_e\right)d^3\mathbf{x}\right)+$$
$$+\delta\hat{\mathsf{d}}_e\cdot\left(\int_{\mathcal{B}_e}\left(\Phi^{eT}_{\mathsf{d}}\mathbb{C}\Phi^e_{\mathsf{d}}\hat{\mathsf{d}}_e+\left(\nabla\Phi^e_{\mathsf{d}}\right)^T\mathbb{G}\nabla\Phi^e_{\mathsf{d}}\hat{\mathsf{d}}_e+\Phi^{eT}_{\mathsf{d}}\mathbb{A}'\nabla\Phi^e_{\mathbf{u}}\hat{\mathbf{u}}_e\right)d^3\mathbf{x}\right)=$$
$$=\delta\hat{\mathbf{u}}_e\cdot\left(\int_{\mathcal{B}_e}\Phi^{eT}_{\mathbf{u}}\mathbf{b}d^3\mathbf{x}+\int_{\partial\mathcal{B}_{e\mathbf{t}}}\Phi^{eT}_{\mathbf{u}}\overline{\mathbf{t}}d\mathcal{H}^2\right)+\delta\hat{\mathsf{d}}_e\cdot\int_{\partial\mathcal{B}_{e\tau}}\Phi^{eT}_{\mathsf{d}}\overline{\tau}d\mathcal{H}^2+\delta\hat{\mathbf{u}}_e\cdot\int_{\partial\mathcal{B}_e^*}\Phi^{eT}_{\mathbf{u}}\mathbf{t}d\mathcal{H}^2+$$
$$+\delta\hat{\mathsf{d}}_e\cdot\int_{\partial\mathcal{B}_e^*}\Phi^{eT}_{\mathsf{d}}\tau d\mathcal{H}^2+\int_{\partial\mathcal{B}_e^*}\delta\mathbf{t}\cdot\Phi^e_{\mathbf{u}}\hat{\mathbf{u}}_e d\mathcal{H}^2+\int_{\partial\mathcal{B}_e^*}\delta\tau\cdot\Phi^e_{\mathsf{d}}\hat{\mathsf{d}}_e d\mathcal{H}^2. \quad (214)$$

The previous relation suggests the introduction of *new matrices of shape functions* for $\mathbf{t}$ and τ, namely $\Phi^e_{\mathbf{t}}$ and Φ^e_τ respectively, such that

$$\mathbf{t}_e = \Phi^e_{\mathbf{t}}\hat{\mathbf{t}}_e \quad , \quad \tau_e = \Phi^e_\tau \hat{\tau}_e \quad \text{on } \partial\mathcal{B}_e, \tag{215}$$

where $\hat{\mathbf{t}}_e$ and $\hat{\tau}_e$ are nodal tractions on $\partial\mathcal{B}_e$.

Since (214) holds for *any* variation $\delta\hat{\mathbf{u}}_e$, $\delta\hat{\mathsf{d}}_e$, $\delta\hat{\mathbf{t}}_e$, $\delta\hat{\tau}_e$, we reduce the equilibrium problem to the analysis of the algebraic system

$$\mathbf{K}_1 \left\{ \begin{array}{c} \hat{\mathbf{u}}_e \\ \hat{\mathsf{d}}_e \\ \hat{\mathbf{t}}_e \\ \hat{\tau}_e \end{array} \right\} = \left\{ \begin{array}{c} \mathbf{r}^e_{\mathbf{u}} \\ \mathbf{r}^e_{\mathsf{d}} \\ 0 \\ 0 \end{array} \right\}. \tag{216}$$

The stiffness matrix $\mathbf{K}_1$ is given by

$$\mathbf{K}_1 = \left[\begin{array}{cccc} (\mathbf{K}_1)_{11} & (\mathbf{K}_1)_{12} & (\mathbf{K}_1)_{13} & 0 \\ (\mathbf{K}_1)_{21} & (\mathbf{K}_1)_{22} & 0 & (\mathbf{K}_1)_{24} \\ (\mathbf{K}_1)_{31} & 0 & 0 & 0 \\ 0 & (\mathbf{K}_1)_{42} & 0 & 0 \end{array} \right], \tag{217}$$

where

$$(\mathbf{K}_1)_{11} = \int_{\mathcal{B}_e} \left((\nabla\Phi^e_{\mathbf{u}})^T \, \mathbb{A} \nabla\Phi^e_{\mathbf{u}} \right) d^3\mathbf{x}, \tag{218}$$

$$(\mathbf{K}_1)_{12} = \int_{\mathcal{B}_e} \Phi^{eT}_{\mathsf{d}} \mathbb{A}' \nabla\Phi^e_{\mathbf{u}} d^3\mathbf{x}, \tag{219}$$

$$(\mathbf{K}_1)_{13} = -\int_{\partial\mathcal{B}^*_e} \Phi^{eT}_{\mathbf{u}} \Phi^e_{\mathbf{t}} d\mathcal{H}^2, \tag{220}$$

$$(\mathbf{K}_1)_{21} = \int_{\mathcal{B}_e} \Phi^{eT}_{\mathsf{d}} \mathbb{A}' \nabla\Phi^e_{\mathbf{u}} d^3\mathbf{x}, \tag{221}$$

$$(\mathbf{K}_1)_{22} = \int_{\mathcal{B}_e} \left(\Phi^{eT}_{\mathsf{d}} \mathbb{C} \Phi^e_{\mathsf{d}} + (\nabla\Phi^e_{\mathsf{d}})^T \, \mathbb{G} \nabla\Phi^e_{\mathsf{d}} \right) d^3\mathbf{x}, \tag{222}$$

$$(\mathbf{K}_1)_{24} = -\int_{\partial\mathcal{B}^*_e} \Phi^{eT}_{\mathsf{d}} \Phi^e_\tau d\mathcal{H}^2, \tag{223}$$

$$(\mathbf{K}_1)_{31} = -\int_{\partial\mathcal{B}^*_e} \Phi^{eT}_{\mathbf{t}} \Phi^e_{\mathbf{u}} d\mathcal{H}^2, \tag{224}$$

$$(\mathbf{K}_1)_{42} = -\int_{\partial\mathcal{B}^*_e} \Phi^{eT}_\tau \Phi^e_{\mathsf{d}} d\mathcal{H}^2, \tag{225}$$

while $\mathbf{r}^e_{\mathbf{u}}$ and $\mathbf{r}^e_{\mathsf{d}}$ are the same vectors obtained in Model 1 above.

4.5 Mixed Finite Elements Models

By the locution 'mixed finite element models' we indicate models that involve both the displacements $\mathbf{u}$ and d and the tractions $\mathbf{t}$ and τ in the array of unknown. In standard linear elasticity they are based on Hellinger-Reissner principle and basically require only the validity *a-priori* of the constitutive equations. To formulate them here, we need a version of Hellinger-Reissner principle extended to cover the linearized multifield setting adopted[19].

As in the case of compatible models we present below two different schemes: The validity of constitutive equations is assumed in both cases; they differ in terms of boundary conditions assumed to be valid *a-priori*.

4.5.1 Model 3

A mixed model may be obtained from Model 2 by removing the conditions $\mathbf{u} = \overline{\mathbf{u}} \Rightarrow \delta\mathbf{u} = 0$ on $\partial\mathcal{B}_{\mathbf{u}}$ and $\mathsf{d} = \overline{\mathsf{d}} \Rightarrow \delta\mathsf{d} = 0$ on $\partial\mathcal{B}_{e\mathsf{d}}$. In this way the weak form of equilibrium conditions read

$$\begin{aligned}
&\delta\hat{\mathbf{u}}_e \cdot \left(\int_{\mathcal{B}_e} \left((\nabla\Phi^e_{\mathbf{u}})^T \, \mathbb{A} \nabla\Phi^e_{\mathbf{u}} \hat{\mathbf{u}}_e + \nabla\Phi^e_{\mathbf{u}} \mathbb{A}' \nabla\Phi^e_{\mathsf{d}} \hat{\mathsf{d}}_e \right) d^3\mathbf{x} \right) + \\
&+\delta\hat{\mathsf{d}}_e \cdot \left(\int_{\mathcal{B}_e} \left(\Phi^{eT}_{\mathsf{d}} \mathbb{C} \Phi^e_{\mathsf{d}} \hat{\mathsf{d}}_e + (\nabla\Phi^e_{\mathsf{d}})^T \, \mathbb{G} \nabla\Phi^e_{\mathsf{d}} \hat{\mathsf{d}}_e + \Phi^{eT}_{\mathsf{d}} \mathbb{A}' \nabla\Phi^e_{\mathbf{u}} \hat{\mathbf{u}}_e \right) d^3\mathbf{x} \right) = \\
&= \delta\hat{\mathbf{u}}_e \cdot \left(\int_{\mathcal{B}_e} \Phi^{eT}_{\mathbf{u}} \mathbf{b} d^3\mathbf{x} + \int_{\partial\mathcal{B}_{e\mathbf{t}}} \Phi^{eT}_{\mathbf{u}} \overline{\mathbf{t}} d\mathcal{H}^2 \right) + \delta\hat{\mathsf{d}}_e \cdot \int_{\partial\mathcal{B}_{e\tau}} \Phi^{eT}_{\mathsf{d}} \overline{\tau} d\mathcal{H}^2 + \\
&+\delta\hat{\mathbf{u}}_e \cdot \int_{\partial\mathcal{B}^*_e \cup \partial\mathcal{B}_{e\mathbf{u}}} \Phi^{eT}_{\mathbf{u}} \Phi^e_{\mathbf{t}} \hat{\mathbf{t}}_e d\mathcal{H}^2 + \delta\hat{\mathsf{d}}_e \cdot \int_{\partial\mathcal{B}^*_e \cup \partial\mathcal{B}_{e\mathsf{d}}} \Phi^{eT}_{\mathsf{d}} \Phi^e_{\tau} \hat{\tau}_e d\mathcal{H}^2 + \\
&+\delta\hat{\mathbf{t}}_e \cdot \int_{\partial\mathcal{B}^*_e \cup \partial\mathcal{B}_{e\mathbf{u}}} \Phi^{eT}_{\mathbf{t}} \Phi^e_{\mathbf{u}} \hat{\mathbf{u}}_e d\mathcal{H}^2 - \delta\hat{\mathbf{t}}_e \cdot \int_{\partial\mathcal{B}_{e\mathbf{u}}} \Phi^{eT}_{\mathbf{t}} \overline{\mathbf{u}} d\mathcal{H}^2 + \\
&+\delta\hat{\tau}_e \cdot \int_{\partial\mathcal{B}^*_e \cup \partial\mathcal{B}_{e\mathsf{d}}} \Phi^{eT}_{\tau} \Phi^e_{\mathsf{d}} \hat{\mathsf{d}}_e d\mathcal{H}^2 - \delta\hat{\tau}_e \cdot \int_{\partial\mathcal{B}_{e\mathsf{d}}} \Phi^{eT}_{\tau} \bar{\mathsf{d}} d\mathcal{H}^2. \qquad (226)
\end{aligned}$$

The arbitrariness of $\delta\hat{\mathbf{u}}_e$, $\delta\hat{\mathsf{d}}_e$, $\delta\hat{\mathbf{t}}$, $\delta\hat{\tau}_e$ implies the algebraic problem

$$\mathbf{K}_1 \left\{ \begin{array}{c} \hat{\mathbf{u}}_e \\ \hat{\mathsf{d}}_e \\ \hat{\mathbf{t}}_e \\ \hat{\tau}_e \end{array} \right\} = \left\{ \begin{array}{c} \mathbf{r}^e_{\mathbf{u}} \\ \mathbf{r}^e_{\mathsf{d}} \\ \zeta^e_{\mathbf{t}} \\ \zeta^e_{\tau} \end{array} \right\}, \qquad (227)$$

where $\mathbf{K}_1$ is given by (217) and

$$\zeta^e_{\mathbf{t}} = -\int_{\partial\mathcal{B}_{e\mathbf{u}}} \Phi^{eT}_{\mathbf{t}} \overline{\mathbf{u}} d\mathcal{H}^2, \qquad (228)$$

$$\zeta^e_{\tau} = -\int_{\partial\mathcal{B}_{e\mathsf{d}}} \Phi^{eT}_{\tau} \bar{\mathsf{d}} d\mathcal{H}^2. \qquad (229)$$

[19] See also [141] for a discussion of mixed variational principles for linear elastic microcracked bodies in linearized setting.

4.5.2 Model 4

To build up the second mixed model, we *assume*

$$\widetilde{\mathbf{u}}_e^{(i)} - \widetilde{\mathbf{u}}_e^{(j)} = 0 \quad \text{on } \partial\mathcal{B}_{ij}, \tag{230}$$

$$\widetilde{\mathsf{d}}_e^{(i)} - \widetilde{\mathsf{d}}_e^{(j)} = 0 \quad \text{on } \partial\mathcal{B}_{ij}. \tag{231}$$

Moreover, we *impose* the balances of standard and substructural interactions together with the following boundary conditions:

$$\mathbf{u}_e = \widetilde{\mathbf{u}}_e \quad \text{on } \partial\mathcal{B}_{e\mathbf{u}}, \tag{232}$$

$$\mathsf{d}_e = \widetilde{\mathsf{d}}_e \quad \text{on } \partial\mathcal{B}_{e\mathsf{d}}, \tag{233}$$

$$\left(\mathbb{A}\nabla\mathbf{u}+\mathbb{A}'\nabla\mathsf{d}\right)\mathbf{n}_e - \mathbf{t} = \mathbf{0} \quad \text{on } \partial\mathcal{B}_e, \tag{234}$$

$$\left(\mathbb{A}'\nabla\mathbf{u}+\mathbb{G}\nabla\mathsf{d}\right)\mathbf{n}_e - \tau = \mathbf{0} \quad \text{on } \partial\mathcal{B}_e, \tag{235}$$

$$\mathbf{t}_e^{(i)} - \mathbf{t}_e^{(j)} = 0 \quad \text{on } \partial\mathcal{B}_{ij}, \tag{236}$$

$$\tau_e^{(i)} - \tau_e^{(j)} = 0 \quad \text{on } \partial\mathcal{B}_{ij}, \tag{237}$$

$$\widetilde{\mathbf{u}}_e = \overline{\mathbf{u}}_e \quad \text{on } \partial\mathcal{B}_{e\mathbf{u}}, \tag{238}$$

$$\widetilde{\mathsf{d}}_e = \overline{\mathsf{d}}_e \quad \text{on } \partial\mathcal{B}_{e\mathsf{d}}, \tag{239}$$

$$\mathbf{t}_e = \overline{\mathbf{t}}_e \quad \text{on } \partial\mathcal{B}_{e\mathbf{t}}, \tag{240}$$

$$\tau_e = \overline{\tau}_e \quad \text{on } \partial\mathcal{B}_{e\tau}. \tag{241}$$

The weak for of the equilibrium conditions reads

$$\begin{aligned}
&\int_{\mathcal{B}_e} \delta\mathbf{u}\cdot\left(div\left(\mathbb{A}\nabla\mathbf{u}+\mathbb{A}'\nabla\mathsf{d}\right)-\mathbf{b}\right)d^3\mathbf{x} + \int_{\mathcal{B}_e}\delta\mathsf{d}\cdot\left(div\left(\mathbb{A}'\nabla\mathbf{u}+\mathbb{G}\nabla\mathsf{d}\right)-\mathbb{C}\mathsf{d}\right)d^3\mathbf{x} + \\
&+\int_{\partial\mathcal{B}_e}\delta\mathbf{u}\cdot\left(\left(\mathbb{A}\nabla\mathbf{u}+\mathbb{A}'\nabla\mathsf{d}\right)\mathbf{n}-\mathbf{t}\right)d\mathcal{H}^2 + \int_{\partial\mathcal{B}_{e\tau}}\delta\mathsf{d}\cdot\left(\left(\mathbb{A}'\nabla\mathbf{u}+\mathbb{G}\nabla\mathsf{d}\right)\mathbf{n}-\tau\right)d\mathcal{H}^2 - \\
&-\int_{\partial\mathcal{B}_e}\delta\mathbf{t}\cdot(\mathbf{u}-\widetilde{\mathbf{u}})\,d\mathcal{H}^2 - \int_{\partial\mathcal{B}_e}\delta\tau\cdot\left(\mathsf{d}-\widetilde{\mathsf{d}}\right)d\mathcal{H}^2 + \\
&+\int_{\partial\mathcal{B}_e^*}\delta\widetilde{\mathbf{u}}\cdot\mathbf{t}\,d\mathcal{H}^2 + \int_{\partial\mathcal{B}_e^*}\delta\widetilde{\mathsf{d}}\cdot\tau\,d\mathcal{H}^2 - \\
&-\int_{\partial\mathcal{B}_{e\mathbf{u}}}\delta\mathbf{t}\cdot(\widetilde{\mathbf{u}}-\overline{\mathbf{u}})\,d\mathcal{H}^2 - \int_{\partial\mathcal{B}_{e\mathsf{d}}}\delta\tau\cdot\left(\widetilde{\mathsf{d}}-\overline{\mathsf{d}}\right)d\mathcal{H}^2 + \\
&+\int_{\partial\mathcal{B}_{e\mathbf{t}}}\delta\widetilde{\mathbf{u}}\cdot\left(\mathbf{t}-\overline{\mathbf{t}}\right)d\mathcal{H}^2 + \int_{\partial\mathcal{B}_{e\tau}}\delta\widetilde{\mathsf{d}}\cdot(\tau-\overline{\tau})\,d\mathcal{H}^2 = 0
\end{aligned} \tag{242}$$

To derive (242) we use integrals like the ones in (178) and identify $\delta\mu_{\mathbf{t}}$ with $\delta\widetilde{\mathbf{u}}$ and $\delta\mu_{\tau}$ with $\delta\widetilde{\mathsf{d}}$. This last assumption is peculiar of Model 4.

By integrating by parts and taking into account the boundary conditions, we obtain

$$\begin{aligned}
\int_{\mathcal{B}_e}\left(\delta\left(\nabla\mathbf{u}\right)\cdot\left(\mathbb{A}\nabla\mathbf{u}+\mathbb{A}'\nabla\mathsf{d}\right)+\delta\mathsf{d}\cdot\mathbb{C}\mathsf{d}+\delta\left(\nabla\mathsf{d}\right)\cdot\left(\mathbb{G}\nabla\mathsf{d}+\mathbb{A}'\nabla\mathbf{u}\right)\right)d^3\mathbf{x}=\\
=\int_{\mathcal{B}_e}\delta\mathbf{u}\cdot\mathbf{b}d^3\mathbf{x}+\int_{\partial\mathcal{B}_e}\delta\mathbf{u}\cdot\mathbf{t}d^2\mathcal{H}+\int_{\partial\mathcal{B}_e}\delta\mathsf{d}\cdot\tau d^2\mathcal{H}+\\
+\int_{\partial\mathcal{B}_e}\delta\mathbf{t}\cdot\mathbf{u}d\mathcal{H}^2+\int_{\partial\mathcal{B}_e}\delta\tau\cdot\mathsf{d}d\mathcal{H}^2-\\
-\int_{\partial\mathcal{B}_e}\delta\mathbf{t}\cdot\widetilde{\mathbf{u}}d\mathcal{H}^2-\int_{\partial\mathcal{B}_e}\delta\tau\cdot\widetilde{\mathsf{d}}d\mathcal{H}^2+\int_{\partial\mathcal{B}_e}\delta\widetilde{\mathbf{u}}\cdot\mathbf{t}d\mathcal{H}^2+\int_{\partial\mathcal{B}_e}\delta\widetilde{\mathsf{d}}\cdot\tau d\mathcal{H}^2+\\
+\int_{\partial\mathcal{B}_{e\mathbf{u}}}\delta\mathbf{t}\cdot\widetilde{\mathbf{u}}d\mathcal{H}^2+\int_{\partial\mathcal{B}_{e\mathsf{d}}}\delta\tau\cdot\widetilde{\mathsf{d}}d\mathcal{H}^2+\\
+\int_{\partial\mathcal{B}_{e\mathbf{u}}}\delta\widetilde{\mathbf{u}}\cdot\mathbf{t}d\mathcal{H}^2+\int_{\partial\mathcal{B}_{e\mathsf{d}}}\delta\widetilde{\mathsf{d}}\cdot\tau d\mathcal{H}^2-\int_{\partial\mathcal{B}_{e\mathbf{u}}}\delta\mathbf{t}\cdot\overline{\mathbf{u}}d\mathcal{H}^2+\\
-\int_{\partial\mathcal{B}_{e\mathsf{d}}}\delta\tau\cdot\overline{\mathsf{d}}d^2\mathcal{H}+\int_{\partial\mathcal{B}_{e\mathbf{t}}}\delta\widetilde{\mathbf{u}}\cdot\overline{\mathbf{t}}d^2\mathcal{H}+\int_{\partial\mathcal{B}_{e\tau}}\delta\widetilde{\mathsf{d}}\cdot\overline{\tau}d^2\mathcal{H}.
\end{aligned}\tag{243}$$

It appears evident the necessity of introducing other shape functions such that

$$\widetilde{\mathbf{u}}_e=\Phi^e_{\widetilde{\mathbf{u}}}\widetilde{\mathbf{u}}^{\mathbf{n}}_e\quad,\quad\widetilde{\mathsf{d}}_e=\Phi^e_{\widetilde{\mathsf{d}}}\widetilde{\mathsf{d}}^{\mathbf{n}}_e\quad\text{on }\partial\mathcal{B}_e,\tag{244}$$

where $\widetilde{\mathbf{u}}^{\mathbf{n}}_e$ and $\widetilde{\mathsf{d}}^{\mathbf{n}}_e$ are the nodal displacements for nodes on $\partial\mathcal{B}_e$.

By using (244) together with (168) and (215) we obtain

$$\begin{aligned}
\delta\hat{\mathbf{u}}_e\cdot\left(\int_{\mathcal{B}_e}\left(\left(\nabla\Phi^e_{\mathbf{u}}\right)^T\mathbb{A}\nabla\Phi^e_{\mathbf{u}}\hat{\mathbf{u}}_e+\nabla\Phi^{eT}_{\mathbf{u}}\mathbb{A}'\nabla\Phi^e_{\mathsf{d}}\hat{\mathsf{d}}_e\right)d^3\mathbf{x}\right)+\\
+\delta\hat{\mathsf{d}}_e\cdot\left(\int_{\mathcal{B}_e}\left(\Phi^{eT}_{\mathsf{d}}\mathbb{C}\Phi^e_{\mathsf{d}}\hat{\mathsf{d}}_e+\left(\nabla\Phi^e_{\mathsf{d}}\right)^T\mathbb{G}\nabla\Phi^e_{\mathsf{d}}\hat{\mathsf{d}}_e+\Phi^{eT}_{\mathsf{d}}\mathbb{A}'\nabla\Phi^e_{\mathbf{u}}\hat{\mathbf{u}}_e\right)d^3\mathbf{x}\right)=\\
=\delta\hat{\mathbf{u}}_e\cdot\int_{\mathcal{B}_e}\Phi^{eT}_{\mathbf{u}}\mathbf{b}d^3\mathbf{x}+\delta\hat{\mathbf{u}}_e\cdot\int_{\partial\mathcal{B}_e}\Phi^{eT}_{\mathbf{u}}\Phi^e_{\mathbf{t}}\hat{\mathbf{t}}_ed\mathcal{H}^2+\\
+\delta\hat{\mathsf{d}}_e\cdot\int_{\partial\mathcal{B}_e}\Phi^{eT}_{\mathsf{d}}\Phi^e_{\tau}\hat{\tau}_ed\mathcal{H}^2+\delta\hat{\mathbf{t}}_e\cdot\int_{\partial\mathcal{B}_e}\Phi^{eT}_{\mathbf{t}}\Phi^e_{\mathbf{u}}\hat{\mathbf{u}}_ed\mathcal{H}^2+\\
+\delta\hat{\tau}_e\cdot\int_{\partial\mathcal{B}_e}\Phi^{eT}_{\tau}\Phi^e_{\mathsf{d}}\hat{\mathsf{d}}_ed\mathcal{H}^2-\delta\widetilde{\mathbf{u}}^{\mathbf{n}}_e\cdot\int_{\partial\mathcal{B}^*_e\cup\partial\mathcal{B}_{e\mathbf{t}}}\Phi^{eT}_{\widetilde{\mathbf{u}}}\Phi^e_{\mathbf{t}}\hat{\mathbf{t}}_ed\mathcal{H}^2+\\
-\delta\widetilde{\mathsf{d}}^{\mathbf{n}}_e\cdot\int_{\partial\mathcal{B}^*_e\cup\partial\mathcal{B}_{e\tau}}\Phi^{eT}_{\widetilde{\mathsf{d}}}\Phi^e_{\tau}\hat{\tau}_ed^2\mathcal{H}-\delta\hat{\mathbf{t}}_e\cdot\int_{\partial\mathcal{B}^*_e\cup\partial\mathcal{B}_{e\mathbf{t}}}\Phi^{eT}_{\mathbf{t}}\Phi^e_{\widetilde{\mathbf{u}}}\widetilde{\mathbf{u}}^{\mathbf{n}}_ed\mathcal{H}^2+\\
-\delta\hat{\tau}_e\cdot\int_{\partial\mathcal{B}^*_e\cup\partial\mathcal{B}_{e\tau}}\Phi^{eT}_{\tau}\Phi^e_{\widetilde{\mathsf{d}}}\widetilde{\mathsf{d}}_ed\mathcal{H}^2-\delta\hat{\mathbf{t}}_e\cdot\int_{\partial\mathcal{B}_{e\mathbf{u}}}\Phi^{eT}_{\mathbf{t}}\overline{\mathbf{u}}d\mathcal{H}^2-\delta\hat{\tau}_e\cdot\int_{\partial\mathcal{B}_{e\mathsf{d}}}\Phi^{eT}_{\tau}\overline{\mathsf{d}}d\mathcal{H}^2+\\
+\delta\widetilde{\mathbf{u}}^{\mathbf{n}}_e\cdot\int_{\partial\mathcal{B}_{e\mathbf{t}}}\Phi^{eT}_{\widetilde{\mathbf{u}}}\overline{\mathbf{t}}d\mathcal{H}^2+\delta\widetilde{\mathsf{d}}^{\mathbf{n}}_e\cdot\int_{\partial\mathcal{B}_{e\tau}}\Phi^{eT}_{\widetilde{\mathsf{d}}}\overline{\tau}d\mathcal{H}^2.
\end{aligned}\tag{245}$$

The arbitrariness of $\delta\hat{\mathbf{u}}_e$, $\delta\widehat{\mathsf{d}}_e$, $\delta\widetilde{\mathbf{u}}^{\mathbf{n}}_e$, $\delta\widetilde{\mathsf{d}}^{\mathbf{n}}_e$, $\delta\hat{\tau}_e$, $\delta\hat{\mathbf{t}}_e$ implies the following algebraic problem:

$$\mathbf{K}_2 \left\{ \begin{array}{c} \hat{\mathbf{u}}_e \\ \widehat{\mathsf{d}}_e \\ \widetilde{\mathbf{u}}^{\mathbf{n}}_e \\ \widetilde{\mathsf{d}}^{\mathbf{n}}_e \\ \hat{\tau}_e \\ \hat{\mathbf{t}}_e \end{array} \right\} = \left\{ \begin{array}{c} \mathbf{r}^e_{\mathbf{u}} \\ \mathbf{r}^e_{\mathsf{d}} \\ \overline{\mathbf{r}}^e_{\mathbf{u}} \\ \overline{\mathbf{r}}^e_{\mathsf{d}} \\ \zeta^e_{\mathbf{t}} \\ \zeta^e_{\tau} \end{array} \right\}. \tag{246}$$

The matrix $\mathbf{K}_2$ is given by

$$\mathbf{K}_2 = \left[\begin{array}{cccccc} (\mathbf{K}_2)_{11} & (\mathbf{K}_2)_{12} & 0 & 0 & (\mathbf{K}_2)_{15} & 0 \\ (\mathbf{K}_2)_{21} & (\mathbf{K}_2)_{22} & 0 & 0 & 0 & (\mathbf{K}_2)_{26} \\ 0 & 0 & 0 & 0 & (\mathbf{K}_2)_{35} & 0 \\ 0 & 0 & 0 & 0 & 0 & (\mathbf{K}_2)_{46} \\ (\mathbf{K}_2)_{51} & 0 & (\mathbf{K}_2)_{53} & 0 & 0 & 0 \\ 0 & (\mathbf{K}_2)_{62} & 0 & (\mathbf{K}_2)_{64} & 0 & 0 \end{array} \right], \tag{247}$$

where

$$(\mathbf{K}_2)_{11} = \int_{\mathcal{B}_e} \left((\nabla\Phi^e_{\mathbf{u}})^T \, \mathbb{A} \nabla\Phi^e_{\mathbf{u}} \right) d^3\mathbf{x}, \tag{248}$$

$$(\mathbf{K}_2)_{12} = \int_{\mathcal{B}_e} \Phi^{eT}_{\mathsf{d}} \mathbb{A}' \nabla\Phi^e_{\mathbf{u}} d^3\mathbf{x}, \tag{249}$$

$$(\mathbf{K}_2)_{15} = -\int_{\partial\mathcal{B}_e} \Phi^{eT}_{\mathbf{u}} \Phi^e_{\mathbf{t}} d\mathcal{H}^2, \tag{250}$$

$$(\mathbf{K}_2)_{21} = \int_{\mathcal{B}_e} \Phi^{eT}_{\mathsf{d}} \mathbb{A}' \nabla\Phi^e_{\mathbf{u}} d^3\mathbf{x}, \tag{251}$$

$$(\mathbf{K}_2)_{22} = \int_{\mathcal{B}_e} \left(\Phi^{eT}_{\mathsf{d}} \mathbb{C} \Phi^e_{\mathsf{d}} + (\nabla\Phi^e_{\mathsf{d}})^T \, \mathbb{G} \nabla\Phi^e_{\mathsf{d}} \right) d^3\mathbf{x}, \tag{252}$$

$$(\mathbf{K}_2)_{26} = -\int_{\partial\mathcal{B}_e} \Phi^{eT}_{\mathsf{d}} \Phi^e_{\tau} d\mathcal{H}^2, \tag{253}$$

$$(\mathbf{K}_2)_{35} = \int_{\partial\mathcal{B}^*_e \cup \partial\mathcal{B}_{e\mathbf{t}}} \Phi^{eT}_{\widetilde{\mathbf{u}}} \Phi^e_{\mathbf{t}} d\mathcal{H}^2, \tag{254}$$

$$(\mathbf{K}_2)_{46} = \int_{\partial\mathcal{B}^*_e \cup \partial\mathcal{B}_{e\tau}} \Phi^{eT}_{\widetilde{\mathsf{d}}} \Phi^e_{\tau} d^2\mathcal{H}, \tag{255}$$

$$(\mathbf{K}_2)_{51} = -\int_{\partial\mathcal{B}^*_e \cup \partial\mathcal{B}_{e\mathbf{t}}} \Phi^{eT}_{\mathbf{t}} \Phi^e_{\mathbf{u}} d\mathcal{H}^2, \tag{256}$$

$$(\mathbf{K}_2)_{53} = \int_{\partial\mathcal{B}^*_e \cup \partial\mathcal{B}_{e\mathbf{t}}} \Phi^{eT}_{\mathbf{t}} \Phi^e_{\widetilde{\mathbf{u}}} d\mathcal{H}^2, \tag{257}$$

$$(\mathbf{K}_2)_{62} = -\int_{\partial\mathcal{B}_e} \Phi^{eT}_{\tau} \Phi^e_{\mathsf{d}} d\mathcal{H}^2, \tag{258}$$

$$(\mathbf{K}_2)_{64} = \int_{\partial\mathcal{B}^*_e \cup \partial\mathcal{B}_{e\tau}} \Phi^{eT}_{\tau} \Phi^e_{\widetilde{\mathsf{d}}} d\mathcal{H}^2. \tag{259}$$

Moreover, $\mathbf{r}^e_{\mathbf{u}}$ and $\mathbf{r}^e_{\mathsf{d}}$ are given by (195), $\xi^e_{\mathbf{t}}$ and ξ^e_{τ} by (228) and (229), while

$$\overline{\mathbf{r}}^e_{\mathbf{u}} = \int_{\partial\mathcal{B}_{e\mathbf{t}}} \Phi^{eT}_{\widetilde{\mathbf{u}}} \overline{\mathbf{t}} d\mathcal{H}^2, \tag{260}$$

$$\overline{\mathbf{r}}^e_{\mathsf{d}} = \int_{\partial\mathcal{B}_{e\tau}} \Phi^{eT}_{\widetilde{\mathsf{d}}} \overline{\tau} d\mathcal{H}^2. \tag{261}$$

The four finite element models presented above are only some possible schemes. Other finite elements can be constructed depending on which boundary conditions are imposed in the weak form of equilibrium conditions.

5 INFLUENCE OF SUBSTRUCTURES ON SHARP MACROSCOPIC DISCONTINUITIES

As mentioned in Section 2, the presence of $\nabla\nu$ in the constitutive list of variables permits us to describe weakly non local interactions due to branching of substructures between domain walls and/or homophase gradient effects. In the former case, $\nabla\nu$ allows us to account for widespread minute interfaces 'smearing' them over the body. *Additional* macroscopic sharp surfaces of discontinuity may also occur as a consequence of the presence of shock or acceleration waves, or defects of various nature such as cracks. Their possible evolution is influenced by the presence of diffused interfaces due to substructural rearrangements. For example, one may consider a shock wave in a polarized ferroelectric: The shock front encounters walls of polarized domains and interacts with them. In addition, such domain walls influence the propagation of surface defects like cracks, as experiments point out.

We may face in general two circumstances: (i) macroscopic sharp discontinuity surfaces are endowed with own *surface energy* - in this case they are referred to as *structured* - or (ii) they are free of such energy so that they are *unstructured*. In the former case, surface stresses accrue: they are of standard and substructural nature; moreover one finds also the existence of a surface self-force.

Below, we summarize briefly the description of the influence of the material substructure on the evolution of sharp discontinuity surfaces. The results apply to a wide class of physical problems. We list some of them as examples:

- equilibrium and/or evolution of sharp interfaces between paraelectric and ferroelectric phases,
- equilibrium and/or evolution of damage fronts,
- equilibrium and/or evolution of sharp interfaces between isotropic and oriented phases –for example sharp interfaces between isotropic and nematic phases in liquid crystals– or between ferroelectric and paraelectric phases,
- solidification of complex fluids,
- growing defects in biological tissues.

We mention a part the analysis of the influence of the material substructure on the growth of macroscopic cracks because it is treated briefly in Section 5.2 since it presents specific problems which have interest per se from both theoretical and computational points of view.

5.1 Macroscopic Discontinuity Surfaces

We consider within $\mathcal{B}_0$ a single macroscopic sharp discontinuity surface Σ defined by

$$\Sigma \equiv \{\mathbf{X} \in cl\mathcal{B}_0, \;\; f(\mathbf{X}) = 0\}, \tag{262}$$

with f a smooth function with non-singular gradient. It is oriented by the normal vector field $\Sigma \ni \mathbf{X} \overset{\tilde{\mathbf{m}}}{\longmapsto} \mathbf{m} = \tilde{\mathbf{m}}(\mathbf{X}) = \nabla f(\mathbf{X}) / |\nabla f(\mathbf{X})|$ and we use the notation Π for the second order tensor $\mathbf{I} - \mathbf{m} \otimes \mathbf{m}$, i.e. the projection operator over Σ. The opposite of the surface gradient of $\mathbf{m}$, namely $-\nabla_\Sigma \mathbf{m}$, is indicated by L and is the curvature tensor.

Let $\mathbf{X} \longmapsto a = \tilde{a}(\mathbf{X})$ be a generic field taking values in a linear space and suffering bounded discontinuities across Σ. For $\varepsilon > 0$ we indicate by $a^{\pm}$ the limits $\lim_{\varepsilon \to 0} a(\mathbf{X} \pm \varepsilon \mathbf{m})$ which are the outer (a^+) and inner (a^-) traces of a at Σ. Then $[a] = a^+ - a^-$ denotes the jump of a across Σ and $2\langle a \rangle = a^+ + a^-$ its average.

Σ is *coherent* when the two pieces of the body separated by the surface do not suffer relative shear - in this case the jump of the gradient of deformation $\mathbf{F}$ satisfies the relation $[\mathbf{F}]\Pi = 0$ - otherwise the surface is called *incoherent*.

When Σ moves relatively to $\mathcal{B}_0$ even in 'virtual' way, we describe such a motion by means of a vector field $\Sigma \ni \mathbf{X} \overset{\tilde{\mathsf{u}}}{\longmapsto} \mathsf{u} = \tilde{\mathsf{u}}(\mathbf{X}) \in \mathbb{R}^3$ with normal component $U = \mathsf{u} \cdot \mathbf{m}$. Moreover, when the velocity $\dot{\mathbf{x}}$ suffers bounded jumps across Σ, as we assume here, we get the condition $[\dot{\mathbf{x}}] = -U[\mathbf{F}]\mathbf{m}$.

We assume also that the morphological descriptor map $\tilde{\nu}$ is *continuous* across Σ. On the contrary the jump of ν would not be defined unless $\mathcal{M}$ would not coincide with a linear space. However, across Σ, the gradient of the morphological descriptor may suffer jumps at each $\mathbf{X} \in \Sigma$, i.e. at each ν there. Under the assumption that both $\mathbf{F}$ and $\nabla\nu$ suffer bounded jumps across Σ, we define the *surface deformation gradient* $\mathbb{F}$ and the *surface gradient of the morphological descriptor* $\mathbb{N}$ at $\mathbf{X} \in \Sigma$ by

$$\mathbb{F} = \langle \mathbf{F} \rangle \Pi, \qquad \mathbb{N} = \langle \nabla\nu \rangle \Pi. \tag{263}$$

It is then evident that at each $\mathbf{X} \in \Sigma$, we have $\mathbb{F} \in Hom(T_{\mathbf{X}}\Sigma, T_{\mathbf{x}}\mathcal{B})$ and $\mathbb{N} \in Hom(T_{\mathbf{X}}\Sigma, T_\nu\mathcal{M})$.

We pay attention to the case in which the discontinuity surface is structured and may sustain surface tensions of standard and substructural nature. We describe these tensions by means of a *surface stress* $\mathbb{T}$ and a *surface microstress* $\mathbb{S}$. They are *surface tensors* in the sense that at each $\mathbf{X} \in \Sigma$, we have $\mathbb{T} \in Hom(T^*_{\mathbf{X}}\Sigma, T^*_{\mathbf{x}}\mathcal{B})$ and $\mathbb{S} \in Hom(T^*_{\mathbf{X}}\Sigma, T^*_\nu\mathcal{M})$ and assume that the related maps $\tilde{\mathbb{T}}$ and $\tilde{\mathbb{S}}$ associating $\mathbb{T}$ and $\mathbb{S}$ to each $\mathbf{X}$ are continuous and continuously differentiable over Σ.

To determine appropriate balance equations across Σ that involve surface stresses, we may follow the procedure discussed in Section 2 which requires the invariance of the external power with respect to changes in observers ruled by $SO(3)$. To this aim we consider an arbitrary part $\mathfrak{b}_\Sigma$ crossing Σ so that $\partial\mathfrak{b}_\Sigma \cap \Sigma$ is a piecewise smooth curve. Except a finite number of points, at each $\mathbf{X} \in \partial\mathfrak{b}_\Sigma \cap \Sigma$ we find a normal n in the tangent space $T_{\mathbf{X}}\Sigma$. In writing the external power of all actions over $\mathfrak{b}_\Sigma$, we must add to the expression used in Section 2 the contributions in terms of power of surface stresses. Really, we could account for the contribution of external body interactions appearing as surface counterparts of $\bar{\mathbf{b}}$ and $\bar{\beta}$, but we neglect here them for the sake of simplicity (see [22] for a treatment including them). After the use of the machinery of the $SO(3)$ invariance, we finally get the integral balances of forces and moments given respectively by

$$\int_{\mathfrak{b}_\Sigma} \bar{\mathbf{b}} d^3\mathbf{X} + \int_{\partial\mathfrak{b}_\Sigma} \mathbf{P}\mathsf{n} d\mathcal{H}^2 + \int_{\partial\mathfrak{b}_\Sigma \cap \Sigma} \mathbb{T}\mathsf{n} d\mathcal{H}^1 = \mathbf{0}, \tag{264}$$

$$\int_{\mathfrak{b}_\Sigma} \left((\mathbf{x}-\mathbf{x}_0)\times\bar{\mathbf{b}}+\mathcal{A}^*\bar{\beta}\right) d^3\mathbf{X} + \int_{\partial\mathfrak{b}_\Sigma} ((\mathbf{x}-\mathbf{x}_0)\times\mathbf{P}\mathbf{n}+\mathcal{A}^*\mathcal{S}\mathbf{n})\, d\mathcal{H}^2 + \\ + \int_{\partial\mathfrak{b}_\Sigma\cap\Sigma} ((\mathbf{x}-\mathbf{x}_0)\times\mathbb{T}\mathsf{n}+\mathcal{A}^*\mathbb{S}\mathsf{n})\, d\mathcal{H}^1 = \mathbf{0}. \tag{265}$$

Here, we consider the non-inertial bulk actions $\mathbf{b}$ and β continuous everywhere over the bulk while $\mathbf{P}$ and $\mathcal{S}$ are also continuous except at Σ where they suffer bounded discontinuities as well as the inertial components of $\bar{\mathbf{b}}$ and $\bar{\beta}$. With these assumptions, by shrinking $\mathfrak{b}_\Sigma$ to $\partial\mathfrak{b}_\Sigma\cap\Sigma$ uniformly in time, from (264) we get

$$[\mathbf{P}]\,\mathbf{m} + Div_\Sigma\mathbb{T} = -\rho_0\,[\dot{\mathbf{x}}]\,U, \tag{266}$$

while from (265), with the use of (266), we find the existence of a *surface self-force* $\mathfrak{z}\in T^*_\nu\mathcal{M}$ such that

$$\mathcal{A}^*\mathfrak{z} = \mathsf{e}\mathbb{T}\mathbb{F}^T - (\nabla_\Sigma\mathcal{A}^*)\,\mathbb{S}, \tag{267}$$

$$[\mathcal{S}]\,\mathbf{m} + Div_\Sigma\mathbb{S} - \mathfrak{z} = -\,[\partial_{\dot\nu}\mathcal{X}]\,U \tag{268}$$

(see [113] for details).

In this way we account for the circumstance that, often, we encounter in real bodies discontinuity thin layers rather than pure surfaces. So, we consider Σ endowed with a *surface free energy density* ϕ associated with the surface tensions of standard and substructural nature. The surface energy density is defined by a sufficiently smooth map $\tilde\phi$ acting as

$$(\mathbf{m},\mathbb{F},\nu,\mathbb{N}) \overset{\tilde\phi}{\longmapsto} \phi = \tilde\phi\,(\mathbf{m},\mathbb{F},\nu,\mathbb{N})\,. \tag{269}$$

The presence of the normal $\mathbf{m}$ in the list of entries of $\tilde\phi$ account for possible *anisotropy* of the surface.

When we use the mechanical dissipation inequality to find constitutive restrictions, we need to add not only the power of surface substructural interactions but also the surface free energy. Standard developments allow us to get (see [113])

$$\mathbb{T} = -\partial_{\mathbb{F}}\phi, \quad \mathfrak{z} = \partial_\nu\phi, \quad \mathbb{S} = -\partial_{\mathbb{N}}\phi. \tag{270}$$

When Σ evolves irreversibly in $\mathcal{B}_0$, its evolution is ruled by the balance

$$\mathbf{m}\cdot\,[\mathbb{P}]\,\mathbf{m} + \mathbb{C}_{\tan}\cdot\mathsf{L} + Div_\Sigma\mathfrak{c} = U\,[(\nabla\nu)^*\,\partial_{\dot\nu}\mathcal{X}]\cdot\mathbf{m} + [\mathcal{X}\,(\nu,\dot\nu)] - \frac{1}{2}\rho_0U^2\left[|\mathbf{F}\mathbf{m}|^2\right], \tag{271}$$

where

$$\mathbb{P} = \psi\mathbf{I} - \mathbf{F}^T\mathbf{P} - (\nabla\nu)^*\,\mathcal{S}, \tag{272}$$

$$\mathbb{C}_{\tan} = \phi\Pi - \mathbb{F}^T\mathbb{T} - \mathbb{N}^*\mathbb{S} \tag{273}$$

are generalized versions of the bulk and surface Eshelby stresses respectively and

$$\mathfrak{c} = -\partial_{\mathbf{m}}\phi - \mathbb{T}^T\,\langle\mathbf{F}\rangle\,\mathbf{m} - \mathbb{S}^*\,\langle\nabla\nu\rangle\,\mathbf{m} \tag{274}$$

is a surface shear. We obtain (271) by adapting to multifield theories the framework of configurational forces developed in [90].

The surface balance of forces (266) has been derived in [93] while equations (267), (268) and (271) in [113], [110], where the surface substructural interactions have been introduced. The surface balances (266), (268) and (271) satisfy not only $SO(3)$ invariance. In the Lagrangian-Hamiltonian setting it is possible to prove that they are also *covariant* in the sense that they arise also from requirements of invariance with respect to the action of the group of automorphisms of the ambient space (namely (266)), the action of an arbitrary Lie group over $\mathcal{M}$ (namely (268)) and the action of a special group of diffeomorphisms permuting possible defects in $\mathcal{B}_0$ and Σ. The relevant theorem has been proven in [49].

5.2 Cracks at a Macro-Scale

The interfacial balance equations above can be used in various situations of physical interest. Amid them there is the growth of macroscopic cracks in complex bodies. However, in this case one must pay attention to the phenomena occurring at the tip and should develop appropriate tools to describe them.

Consider first $\mathcal{B}_0$ free of cracks. When a crack occurs in the current place $\mathcal{B}$, the mapping $\tilde{\mathbf{x}}$ is pointwise one-to-one except a surface Σ which does not cross completely $\mathcal{B}_0$. The *image* in $\mathcal{B}_0$ of the real *tip* of the crack is thus the margin $\mathcal{J}$ of Σ within the interior of $\mathcal{B}_0$. We assume that $\mathcal{J}$ is a simple regular curve parametrized by arc length $\mathfrak{s} \in [0, \bar{\mathfrak{s}}]$ and represented by a point-valued mapping $\tilde{\mathbf{Z}} : [0, \bar{\mathfrak{s}}] \to \mathcal{B}_0$ so that the derivative $\mathbf{Z}_{,\mathfrak{s}}$ of $\tilde{\mathbf{Z}}(\mathfrak{s})$ with respect to $\mathfrak{s}$ is the *tangent* vector $\mathfrak{t}(\mathfrak{s})$ at $\mathbf{Z}$, while $\mathfrak{h} = -\mathbf{Z}_{,\mathfrak{s}\mathfrak{s}}$ is the curvature vector at $\mathbf{Z}$. A normal vector field $\mathfrak{n}$ is chosen along $\mathcal{J}$ to be at each $\mathbf{Z}$ an element of the tangent plane of Σ at $\mathbf{Z}$ outward Σ.

When the crack grows in the current configuration in a certain time interval $[0, \bar{t}]$, in $\mathcal{B}_0$ the surface Σ evolves in time and is $\Sigma(t)$ so that $\mathcal{J}$ has an *intrinsic relative motion* with respect to the rest of the body, while any piece of $\Sigma(t)$ far from $\mathcal{J}$ remains at rest. Of course, the motion of $\mathcal{J}$ is 'fictitious' in the sense that it is non-material because $\mathcal{B}_0$ is free of cracks and Σ is just a geometrical picture of the real crack in $\mathcal{B}$. Moreover, $\Sigma(\cdot)$ increases monotonically in time: $\Sigma(t_1) \subseteq \Sigma(t_2)$, for any $t_1 \leq t_2$. We assume also that, during the time interval $[0, \bar{t}]$, the crack does not cut completely the body.

In $\mathcal{B}_0$ the *velocity* along $\mathcal{J}$ is

$$\mathbf{v}_{tip} = \frac{\partial \tilde{\mathbf{Z}}(\mathfrak{s}, t)}{\partial t}, \tag{275}$$

where we indicate still by $\tilde{\mathbf{Z}}$ the mapping $\tilde{\mathbf{Z}} : [0, \bar{\mathfrak{s}}] \times [0, \bar{t}] \to \mathcal{B}_0$ displaying the current shape of the tip at the instant t. Only the normal component $V = \mathbf{v}_{tip} \cdot \mathfrak{n}$ of $\mathbf{v}_{tip}$ is independent of the parametrization $\mathfrak{s}$, and we shall consider just $\mathbf{v}_{tip} = V\mathfrak{n}$.

There are just constant standard surface tensions and surface microstresses along Σ. No surface self-force occurs. Also, normal motion along Σ is absent: just the tip moves. As a consequence the surface balances of standard and substructural interactions become respectively

$$[\mathbf{P}]\,\mathbf{m} = \mathbf{0}, \qquad [\mathcal{S}]\,\mathbf{m} = \mathbf{0}. \tag{276}$$

Moreover, if both the standard momentum $\rho_0 \dot{\mathbf{x}}$ and $\partial_{\dot{\nu}} \mathcal{X}$ are assumed to be bounded up to the tip, at each point $\mathbf{Z}$ of the tip itself we get

$$\int_{tip} \mathbf{P}\mathbf{n} = \mathbf{0}, \quad \int_{tip} \mathcal{S}\mathbf{n} = \mathbf{0}, \tag{277}$$

where $\int_{tip}$ indicates a special limit process which consists in evaluating an integral on the boundary of a disc centered at the tip in a plane orthogonal to the tangent $\mathfrak{t}(\mathfrak{s})$ to the tip at a given point and in shrinking the disc up to the tip uniformly in time.

We consider the margins of the crack endowed with a constant (in space) surface energy ϕ and indicate by ϕ_{tip} its tip value. We also attribute a line (constant) energy λ_{tip} along the tip: it accounts for material bonds in an infinitesimal neighborhood of the tip itself.

Let $\mathfrak{n}(\mathfrak{s})$ be the *direction of propagation of the crack* at the point $\tilde{\mathbf{Z}}(\mathfrak{s})$ of the tip. At each $\mathbf{Z}$, the evolution of the tip is ruled by the evolution equation

$$-\mathfrak{g}_{tip}V = -\phi_{tip} - \lambda_{tip}\mathfrak{K} + \mathfrak{n}\cdot\mathbf{j}, \tag{278}$$

where $\mathfrak{g}_{tip}$ is a negative 'diffusion' coefficient that must be assigned constitutively and $\mathbf{j}$ indicates the vector defined by

$$\mathbf{j} = \int_{tip}\left(\left(\frac{1}{2}\rho_0\left\|\dot{\mathbf{x}}\right\|^2 + \mathcal{K}\left(\nu,\dot{\nu}\right)\right)\mathbf{I} - \mathbb{P}\right)\mathbf{n}, \tag{279}$$

with $\mathbb{P}$ given by (272).

By indicating by J the product $\mathfrak{n}\cdot\mathbf{j}$, we interpret the difference

$$\mathfrak{f} = \mathsf{J} - \phi_{tip} - \lambda_{tip}\mathfrak{K} \tag{280}$$

as the *force driving the tip of the crack*; it accounts directly for the influence of the material substructure. J is an extended version for complex materials of the so-called J-integral. When the crack grows, so that $V > 0$, the driving force must be non-negative, namely $\mathfrak{f} \geq 0$.

The *energy release rate at the tip* is given by the power $\mathfrak{f}V$ developed by the driving force along the normal motion of the crack tip. In terms of the power of standard and substructural interactions and of kinetic and free energies, the product $\mathfrak{f}V$ is given by

$$\mathfrak{f}V = -\phi_{tip}V - \lambda_{tip}\mathfrak{K}V + \int_{tip}\left(\left(\psi + \frac{1}{2}\rho_0\left\|\dot{\mathbf{x}}\right\|^2 + \mathcal{K}\left(\nu,\dot{\nu}\right)\right)V + \mathbf{P}\mathbf{n}\cdot\dot{\mathbf{x}} + \mathcal{S}\mathbf{n}\cdot\dot{\nu}\right), \tag{281}$$

which represents *the balance of energy at the tip.*

When inertial effects are negligible, the evolution of the crack is 'quasi static'. The J-integral reduces to its quasi static counterpart J_{qs}:

$$\mathsf{J}_{qs} = \mathfrak{n}\cdot\int_{tip}\mathbb{P}\mathbf{n} \equiv \mathfrak{n}\cdot\int_{tip}\left(\psi\mathbf{I} - \mathbf{F}^T\mathbf{P} - \left(\nabla\nu\right)^*\mathcal{S}\right)\mathbf{n}. \tag{282}$$

The following proposition can be easily proven: If the material is homogeneous, Σ is planar, the crack has the margins free of standard and substructural tractions (in the sense that $\mathbf{P}^{\pm}\mathbf{m} = \mathbf{0}$ and $\mathcal{S}^{\pm}\mathbf{m} = \mathbf{0}$), J_{qs} is path-independent. Moreover, J_{qs} reduces to the standard J-integral given by $\mathfrak{n}\cdot\int_{tip}\left(\psi\mathbf{I} - \mathbf{F}^T\mathbf{P}\right)\mathbf{n}$ when the substructure is absent or its gross effects are negligible.

The relations above describe the influence of the material substructure on the evolution of a crack. Such an influence is recognized experimentally in various cases (see e.g. [76] for data in the case of ferroelectrics and [184] for materials that fail by de-cohesion or cleavage at the atomic scale).

The results collected here about crack growth in complex bodies have been obtained in [116].

5.3 Computational Strategy

For mechanical problems involving the presence of submanifolds of $\mathcal{B}_0$ (say a surface) where some fields involved suffer jumps, a reliable computational strategy seems to be the one of extended finite element method (XFEM). It is based on the partition of unity method [5] and has been developed by T. Belytschko and co-workers (see, e.g. [7], [33], [55], [83], [138], [173], [176], [177] and [188]).

Basically, one consider the submanifold where discontinuities are concentrated as the level set of some function and includes it in the list of quantities to be discretized. Moreover, with respect to nodes far from the submanifold itself, the interpolation space at nodes around it is enlarged. In this sense, the discretization of the relevant fields at these nodes is *enriched*. In the case of cracks we have two types of enrichments: (i) the former at nodes along the margins of the crack, (ii) the latter at the nodes around the tip. The fact that the nodes enriched are very few does not increase the computational cost which is reduced, on the other hand, by the absence of the need to choose an articulated mesh.

In adapting XFEM to the multifield setting, we need to discretize also the morphological descriptor field so that remarks of Section 4 apply. Both the displacement and the morphological descriptor fields need to be enriched at the relevant nodes. In principle we could choose different enrichments; however, for particular choices of the morphological descriptor the enrichment could be the same.

Below, we present an example of the possible extension of XFEM to multifield theories. It deals with the description of the interaction between a macroscopic cracks and a population of microcracks.

5.3.1 An example of the possible extention of XFEM to the multifield setting: macrocrack-microcrack interaction

When a macroscopic crack is present in a microcracked body, microcracks may interact with it influencing the propagation. The multifield setting adopted here allows us to describe such interactions. For the sake of simplicity we restrict the analysis to a two-dimensional setting.

$\mathcal{B}_0$ is reference place of a two-dimensional body. A macroscopic crack inside it is described by a smooth simple curve Γ with two ends points: one on the boundary of $\mathcal{B}_0$, the other in the interior. Except the point on the boundary, Γ is inside $\mathcal{B}_0$ and is represented by a smooth point-valued function $\mathbf{r}(s)$ with arc-length $s \in [0, \bar{s}]$. $\mathbf{r}(0)$ belongs to $\partial\mathcal{B}_0$ and $\mathbf{r}(\bar{s})$ is the crack tip denoted with $\mathbf{Z}$. $\mathbf{m}$ is the unit normal to Γ and $\mathsf{t} = \partial_s \mathbf{r}$ the tangent. Defining $\mathsf{t}_{\mathbf{Z}} = \lim_{s\to\bar{s}} \mathsf{t}\,(s)$ one wants to have $\mathsf{t}_{\mathbf{Z}} \cdot \lim_{s\to\bar{s}} \mathbf{m}\,(s) = 0$.

When the crack faces remain closed during the deformation, we have $[\mathbf{x}] \cdot \mathbf{m} = 0$, $[\mathsf{d}] \cdot \mathbf{m} = 0$.

Balance equations along the margins of the crack and at the tip can be easily obtained by specializing general interfacial and tip balances recalled previously.

The vector

$$\mathbf{j}_{q-st} = \int_{tip} \left(\psi\mathbf{I} - \mathbf{F}^T\mathbf{S} - \nabla\mathsf{d}^T\mathcal{S}\right)\mathbf{n} \tag{283}$$

represents the traction at the crack tip under quasi-static growth. The component of $\mathbf{j}_{q-st}$ along the direction of propagation of the crack, namely $\mathsf{J}_{q-st} = \mathsf{t}_Z \cdot \mathbf{j}_{q-st}$, is the J-*integral* for crack-microcrakcs interactions.

The way we describe here to extend XFEM to multifield theories follows strictly [125]. Although the treatment is restricted to the case of elastic microcracked bodies in linear setting, the path can be naturally followed in other cases once $\mathcal{M}$ is embedded (isometrically) in a linear space and the consequent linearization developed.

Below, $\partial\mathcal{B}_{\mathbf{u}}$, $\partial\mathcal{B}_{\mathsf{d}}$, $\partial\mathcal{B}_{\mathbf{t}}$ and $\partial\mathcal{B}_{\tau}$ are subsets of $\partial\mathcal{B}$ where $\mathbf{u}$, d, $\bar{\mathbf{t}}=\mathbf{P}\mathbf{n}$ and $\bar{\tau}=\mathcal{S}\mathbf{n}$ are prescribed respectively. It is also assumed that $\partial\mathcal{B}_{\mathbf{u}}\cap\partial\mathcal{B}_{\mathbf{t}}=0$, $\partial\mathcal{B}_{\mathbf{u}}\cup\partial\mathcal{B}_{\mathbf{t}}=\partial\mathcal{B}$, $\partial\mathcal{B}_{\mathsf{d}}\cap\partial\mathcal{B}_{\tau}=0$ and $\partial\mathcal{B}_{\mathsf{d}}\cup\partial\mathcal{B}_{\mathbf{u}}=\partial\mathcal{B}_0$.

Let $\mathcal{C}_t$ be a space of *continuous and piecewise differentiable* vector valued fields over $\mathcal{B}_0$. The space of *trial* functions $\mathcal{U}$ is defined by

$$\mathcal{U}=\{\tilde{\mathbf{u}},\tilde{\mathsf{d}}\in\mathcal{C}_t\mid\begin{array}{l}\mathbf{u}=\bar{\mathbf{u}}\ \text{ on }\partial\mathcal{B}_{\mathbf{u}}\\ \mathsf{d}=\bar{\mathsf{d}}\ \text{ on }\partial\mathcal{B}_{\mathsf{d}}\end{array}\}. \tag{284}$$

The trial functions satisfy the continuity conditions required for compatibility and the displacement boundary conditions. The space of *test* functions $\mathcal{U}_0$ is then defined by

$$\mathcal{U}_0=\{\delta\tilde{\mathbf{v}},\delta\tilde{\mathbf{v}}_{\mathsf{d}}\in\mathcal{C}_t\mid\begin{array}{l}\delta\mathbf{v}=0\ \text{ on }\partial\mathcal{B}_{\mathbf{u}}\\ \delta\mathbf{v}_{\mathsf{d}}=0\ \text{ on }\partial\mathcal{B}_{\mathsf{d}}\end{array}\}. \tag{285}$$

Test functions $\delta\tilde{\mathbf{v}}$ have the meaning of *virtual displacements* and vanish where trial functions satisfy the displacement boundary conditions.

By making use of the results in Section 3, we recall the *weak form* of the boundary value problem: *Given* $\mathbf{b}:\mathcal{B}\rightarrow\mathbb{R}^3$, $\bar{\mathbf{t}}:\partial\mathcal{B}_{\mathbf{t}}\rightarrow\mathbb{R}^3$, $\bar{\mathbf{u}}:\partial\mathcal{B}_{\mathbf{u}}\rightarrow\mathbb{R}^3$, $\bar{\tau}:\partial\mathcal{B}_{\mathsf{p}}\rightarrow\mathbb{R}^3$ *and* $\bar{\mathsf{d}}:\partial\mathcal{B}_{\mathsf{d}}\rightarrow\mathbb{R}^3$, *find* $\mathbf{u},\mathsf{d}\in\mathcal{U}$ *such that for all* $\delta\mathbf{v},\delta\mathbf{v}_{\mathsf{d}}\in\mathcal{U}_0$

$$(W)\left\{\begin{array}{c}\int_{\mathcal{B}_0}\nabla(\delta\mathbf{v})\cdot\mathbf{P}d^3\mathbf{X}+\int_{\mathcal{B}}\nabla(\delta\mathbf{v}_{\mathsf{d}})\cdot\mathcal{S}d^3\mathbf{X}+\\ +\int_{\mathcal{B}_0}\delta\mathbf{v}_{\mathsf{d}}\cdot\mathbf{z}d^3\mathbf{X}-\int_{\mathcal{B}_0}\delta\mathbf{v}\cdot\mathbf{b}d^3\mathbf{X}-\int_{\partial\mathcal{B}_{\tau}}\delta\mathbf{v}_{\mathsf{d}}\cdot\bar{\tau}d\mathcal{H}^2-\int_{\partial\mathcal{B}_{\mathbf{t}}}\delta\mathbf{v}\cdot\bar{\mathbf{t}}d\mathcal{H}^2=0.\end{array}\right. \tag{286}$$

In infinitesimal deformation regime and linear constitutive behavior, we then get –as in Section 4–

$$\begin{array}{c}\int_{\mathcal{B}_0}\nabla(\delta\mathbf{v})\cdot\left(\mathbb{A}\nabla\mathbf{u}-\mathbb{A}'\nabla\mathsf{d}\right)d^3\mathbf{X}+\int_{\mathcal{B}_0}\nabla(\delta\mathbf{v}_{\mathsf{d}})\cdot\left(\mathbb{G}\nabla\mathsf{d}-\mathbb{G}'\nabla\mathbf{u}\right)d^3\mathbf{X}+\\ +\int_{\mathcal{B}_0}\delta\mathbf{v}_{\mathsf{d}}\cdot\mathbb{C}\mathsf{d}d^3\mathbf{X}=\int_{\mathcal{B}_0}\delta\mathbf{v}\cdot\mathbf{b}d^3\mathbf{X}+\int_{\partial\mathcal{B}_{\tau}}\delta\mathbf{v}_{\mathsf{d}}\cdot\bar{\tau}d\mathcal{H}^2+\int_{\partial\mathcal{B}_{\mathbf{t}}}\delta\mathbf{v}\cdot\bar{\mathbf{t}}d\mathcal{H}^2,\end{array} \tag{287}$$

for any choice of $\delta\mathbf{v},\delta\mathbf{v}_{\mathsf{d}}\in\mathcal{U}_0$.

As mentioned above, XFEM does not require that the mesh be adapted to the crack which is described by means of the Level Set Method (LSM) so that it is the zero level set of a function (*signed distance function*) $f(\cdot)$ defined in a narrow band $\mathcal{B}_f$ around the crack by

$$f(\mathbf{X})=sign\left[\mathbf{m}\cdot\left(\mathbf{X}-\bar{\mathbf{X}}\right)\right]\min_{\bar{\mathbf{X}}\in\Gamma}\left|\mathbf{X}-\bar{\mathbf{X}}\right| \tag{288}$$

where $\bar{\mathbf{X}}$ is the closest point projection of $\mathbf{X}$ on Γ.

The signed distance function is approximated by

$$f^h(\mathbf{X})=\sum_{I=1}^{n_{el}}N_I(\xi)f_I \tag{289}$$

where N_I denotes the *I-th* shape function in terms of parent coordinates, f_I is the *I-th* nodal value of the $f(\mathbf{x})$ and n_{el} is the number of nodes in each element. When linear shape functions are implemented, triangular elements have $n_{el}=3$, while $n_{el}=6$ when quadratic shape functions are used, as in [173] and [172].

Below, $\mathcal{N}$ is the number of all nodes of the discretization, $\mathcal{N}^{Tip}$ the number of nodes belonging to elements containing th tip of the crack and $\mathcal{N}^{cr}$ the number of nodes belonging to elements completely cut by the crack.

Then, the XFEM approximation for the displacement field $\mathbf{u}$ is given by

$$\mathbf{u}^h(\mathbf{X}) = \sum_{I=1}^{\mathcal{N}} N_I(\mathbf{X})\,\mathbf{u}_I + \sum_{J=1}^{\mathcal{N}^{Cr}} \tilde{N}_J(\mathbf{X})\left(H(f^h(\mathbf{X})) - H(f_J)\right)\mathbf{a}_J^{\mathbf{u}} + \\ + \sum_{K=1}^{\mathcal{N}^{Tip}} \tilde{N}_K(\mathbf{X}) \sum_{\alpha=1}^{4}\left(F^{(\alpha)}(r,\theta) - F^{(\alpha)}(\mathbf{X}_K)\right)\mathbf{b}_K^{\mathbf{u}\alpha} = \mathbb{N}\left[\mathbf{u}_I, \mathbf{a}_J^{\mathbf{u}}, \mathbf{b}_K^{\mathbf{u}\alpha}\right] \tag{290}$$

while the approximation for d is given by

$$\mathsf{d}^h(\mathbf{X}) = \sum_{I=1}^{\mathcal{N}} N_I(\mathbf{X})\,\mathsf{d}_I + \sum_{J=1}^{\mathcal{N}^{Cr}} \tilde{N}_J(\mathbf{X})\left(H(f^h(\mathbf{X})) - H(f_J)\right)\mathbf{a}_J^{\mathsf{d}} + \\ + \sum_{K=1}^{\mathcal{N}^{Tip}} \tilde{N}_K(\mathbf{X}) \sum_{\alpha=1}^{4}\left(F^{(\alpha)}(r,\theta) - F^{(\alpha)}(\mathbf{X}_K)\right)\mathbf{b}_K^{\mathsf{d}\alpha} = \mathbb{N}\left[\mathsf{d}_I, \mathbf{a}_J^{\mathsf{d}}, \mathbf{b}_K^{\mathsf{d}\alpha}\right], \tag{291}$$

where $H(f(\mathbf{X}))$ is Heaviside step function modified to be symmetric across the crack and $F^{(\alpha)}(r,\theta)$ (with $\alpha = 1,2,3,4$) forms the basis for the Westergaard field near crack tip, defined as in [71] by

$$F^{\alpha}(r,\theta) = \left(\sqrt{r}\sin\frac{\theta}{2}, \sqrt{r}\cos\frac{\theta}{2}, \sqrt{r}\sin\frac{\theta}{2}\sin\theta, \sqrt{r}\cos\frac{\theta}{2}\sin\theta\right) \tag{292}$$

with r, θ polar coordinates around the tip.

It is worth noting that F^1 is discontinuous across the crack faces, while the other three functions are continuous.

In previous expressions, $\mathbf{u}_I$ is the nodal value of $\mathbf{u}$, d_I the nodal value of d, while $\mathbf{a}_J^{\mathbf{u}}$ and $\mathbf{b}_K^{\mathbf{u}}$ and $\mathbf{a}_J^{\mathsf{d}}$ and $\mathbf{b}_K^{\mathsf{d}}$ are additional degrees of freedom associated with the nodal enrichment of $\mathbf{u}$ and d around the crack respectively.

It is worth noting that both $\mathbf{u}$ and d are enriched with the same enrichment functions because either $\mathbf{u}$ and d represent displacements. Two kinds of shape functions can be used: $N_I(\mathbf{X})$ for standard finite element code and $\tilde{N}_J(\mathbf{X})$ for the enrichment functions.

Numerical examples below have been obtained by using triangular elements with linear shape functions.

We put $\mathbf{u}_I = \left\{ \begin{array}{c} u_{Ix} \\ u_{Iy} \end{array} \right\}$, $\mathbf{a}_I^{\mathbf{u}} = \left\{ \begin{array}{c} a_{Ix}^u \\ a_{Iy}^u \end{array} \right\}$, $\mathbf{b}_I^{\mathbf{u}\alpha} = \left\{ \begin{array}{c} b_{Ix}^{u\alpha} \\ b_{Iy}^{u\alpha} \end{array} \right\}$ and use similar expressions for d_I, $\mathbf{a}_J^{\mathsf{d}}$ and $\mathbf{b}_K^{\mathsf{d}\alpha}$. We then have

$$\nabla\mathbf{u} = \bar{\mathbb{B}}\tilde{\mathbf{u}} = \left[\begin{array}{ccc} \mathbb{B}_I^{\mathbf{u}} & \mathbb{B}_J^{\mathbf{a}} & \mathbb{B}_K^{\mathbf{b}\alpha} \end{array}\right] \left[\begin{array}{c} \mathbf{u}_I \\ \mathbf{a}_J^{\mathbf{u}} \\ \mathbf{b}_K^{\mathbf{u}\alpha} \end{array}\right], \text{ with } \begin{array}{c} I = 1...\mathcal{N} \\ J = 1...\mathcal{N}^{cr} \\ K = 1...\mathcal{N}^{TIP} \\ \alpha = 1,2,3,4 \end{array}, \tag{293}$$

$$\nabla\mathsf{d} = \bar{\mathbb{B}}\tilde{\mathsf{d}} = \left[\begin{array}{ccc} \mathbb{B}_I^{\mathbf{u}} & \mathbb{B}_J^{\mathbf{a}} & \mathbb{B}_K^{\mathbf{b}\alpha} \end{array}\right] \left[\begin{array}{c} \mathsf{d}_I \\ \mathbf{a}_J^{\mathsf{d}} \\ \mathbf{b}_K^{\mathsf{d}\alpha} \end{array}\right], \text{ with } \begin{array}{c} I = 1...\mathcal{N} \\ J = 1...\mathcal{N}^{cr} \\ K = 1...\mathcal{N}^{TIP} \\ \alpha = 1,2,3,4 \end{array}, \tag{294}$$

where

$$\mathbb{B}_I^{\mathbf{u}} = \begin{bmatrix} N_{I,x} & 0 \\ 0 & N_{I,y} \\ N_{I,y} & 0 \\ 0 & N_{I,x} \end{bmatrix}, \tag{295}$$

$$\mathbb{B}_J^{\mathbf{a}} = \begin{bmatrix} (\tilde{N}_J\,(H - H(\mathbf{X}_J)))_{,x} & 0 \\ 0 & (\tilde{N}_J\,(H - H(\mathbf{X}_J)))_{,y} \\ (\tilde{N}_J\,(H - H(\mathbf{X}_J)))_{,y} & 0 \\ 0 & (\tilde{N}_J\,(H - H(\mathbf{X}_J)))_{,x} \end{bmatrix},$$

$$\mathbb{B}_K^{\mathbf{b}\alpha}\Big|_{\alpha=1,2,3,4} = \begin{bmatrix} (\tilde{N}_K\,(F_K^\alpha - F_K^\alpha(\mathbf{X}_K)))_{,x} & 0 \\ 0 & (\tilde{N}_K\,(F_K^\alpha - F_K^\alpha(\mathbf{X}_K)))_{,y} \\ (\tilde{N}_K\,(F_K^\alpha - F_K^\alpha(\mathbf{X}_K)))_{,y} & 0 \\ 0 & (\tilde{N}_K\,(K_K^\alpha - F_K^\alpha(\mathbf{X}_K)))_{,x} \end{bmatrix}. \tag{296}$$

As a consequence, the equilibrium condition reduces to the algebraic equation

$$\hat{\mathbb{K}}\tilde{\mathbf{q}} = \tilde{\mathbf{f}}^{ext}, \tag{297}$$

where

$$\tilde{\mathbf{q}} = \begin{Bmatrix} \tilde{\mathbf{u}} \\ \tilde{\mathsf{d}} \end{Bmatrix}, \tag{298}$$

$$\hat{\mathbb{K}} = \begin{bmatrix} \int_{\mathcal{B}} \bar{\mathbb{B}}^T \mathbb{A} \bar{\mathbb{B}} d^3\mathbf{x} & -\int_{\mathcal{B}} \bar{\mathbb{B}}^T \mathbb{G}' \bar{\mathbb{B}} d^3\mathbf{x} \\ -\int_{\mathcal{B}} \bar{\mathbb{B}}^T \mathbb{G}' \bar{\mathbb{B}} d^3\mathbf{x} & \int_{\mathcal{B}} \left(\mathbb{N}^T \mathbb{C} \mathbb{N} + \bar{\mathbb{B}}^T \mathbb{G} \bar{\mathbb{B}}\right) d^3\mathbf{x} \end{bmatrix}, \tag{299}$$

$$\tilde{\mathbf{f}}^{ext} = \begin{Bmatrix} \tilde{\mathbf{r}}_{\mathbf{u}} \\ \tilde{\mathbf{r}}_{\mathsf{d}} \end{Bmatrix} = \begin{Bmatrix} \mathbf{r}_I^u ; \mathbf{r}_J^{a^u} ; \mathbf{r}_K^{b^u \alpha} \\ \mathbf{r}_I^{\mathsf{d}} ; \mathbf{r}_J^{a^{\mathsf{d}}} ; \mathbf{r}_K^{b^{\mathsf{d}} \alpha} \end{Bmatrix}, \quad \text{with} \quad \begin{matrix} I = 1...\mathcal{N} \\ J = 1...\mathcal{N}^{cr} \\ K = 1...\mathcal{N}^{TIP} \\ \alpha = 1,2,3,4 \end{matrix} \tag{300}$$

and

$$\mathbf{r}_I^u = \int_{\partial\mathcal{B}_t} N_I \bar{\mathbf{t}} d\mathcal{H}^2 + \int_{\mathcal{B}} N_I \mathbf{b} d^3\mathbf{X}, \tag{301}$$

$$\mathbf{r}_J^{a^u} = \int_{\partial\mathcal{B}_t} \tilde{N}_J (H - H(\mathbf{X}_J)) \bar{\mathbf{t}} d\mathcal{H}^2 + \int_{\mathcal{B}} \tilde{N}_J (H - H(\mathbf{X}_J)) \mathbf{b} d^3\mathbf{X}, \tag{302}$$

$$\mathbf{r}_K^{b^u\alpha}\Big|_{\alpha=1,2,3,4} = \int_{\partial\mathcal{B}_t} \tilde{N}_K (F^\alpha - F^\alpha(\mathbf{X}_K)) \bar{\mathbf{t}} d\mathcal{H}^2 + \int_{\mathcal{B}} \tilde{N}_K (F^\alpha - F^\alpha(\mathbf{X}_K)) \mathbf{b} d^3\mathbf{X}, \tag{303}$$

$$\mathbf{r}_I^{\mathsf{d}} = \int_{\partial\mathcal{B}_{\mathsf{p}}} N_I \bar{\tau} d\mathcal{H}^2, \quad \mathbf{r}_J^{a^{\mathsf{d}}} = \int_{\partial\mathcal{B}_{\mathsf{p}}} \tilde{N}_J (H - H(\mathbf{X}_J)) \bar{\tau} d\mathcal{H}^2, \tag{304}$$

$$\mathbf{r}_K^{b^{\mathsf{d}}\alpha}\Big|_{\alpha=1,2,3,4} = \int_{\partial\mathcal{B}_{\mathsf{p}}} \tilde{N}_K (F^\alpha - F^\alpha(\mathbf{X}_K)) \bar{\tau} d\mathcal{H}^2. \tag{305}$$

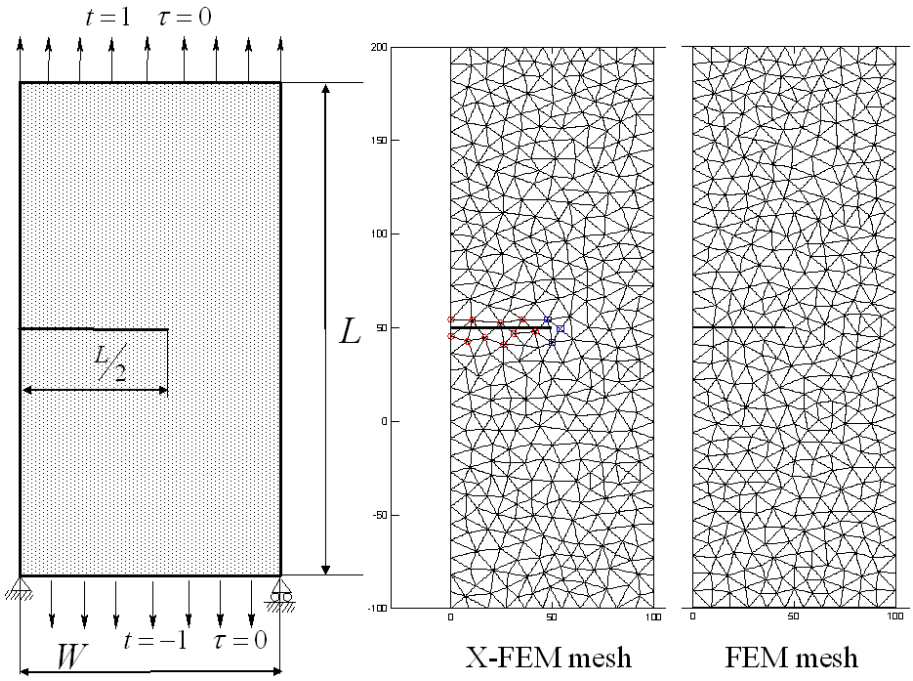

Figure 19. Strip of microcracked material cut by a straight macro-crack. In the XFEM mesh, nodes labelled with a square are enriched with branch functions while circled nodes with the step function.

Numerical simulations are developed by considering the notched strip of microcracked material shown in Figure 19. Unitary uniform traction along the vertical axis is prescribed at the top and at the bottom of the strip. Rigid body motions are avoided by means of a roll and a hinge. Both the roll and the hinge prescribe essential boundary conditions only on the standard displacement field $\mathbf{u}$. No prescriptions are imposed on the field d, since they seem to be unnecessary due to the nature of the stiffness matrix of the finite element approximation. In fact, the total stiffness matrix has *only three null eigenvalues*, which are associated with the three standard rigid body degrees of freedom of the strip in the plane. Moreover, the microstress $\bar{\mathsf{p}}$ is assumed to vanish identically all around the boundary of the strip.

Linear triangular XFEM elements have been used. Values of the material constants are the ones collected in Table 2.

Strip 100×300 mm	**154 nodes**		**318 nodes**		**423 nodes**	
	J_{q-st}	e	J_{q-st}	e	J_{q-st}	e
l_m**= 15**	2.1275	56.7461	2.3270	58.0926	2.3516	58.3520
l_m**= 25**	2.1480	57.1617	2.3575	58.5300	2.3795	58.7921
l_m**= 50**	2.1517	57.2345	2.3629	58.6067	2.3845	58.8695
l_m**= 75**	2.1521	57.2405	2.3634	58.6131	2.3850	58.8760
virgin material	2.1854	57.2578	2.3634	58.6374	2.3860	58.8787

Table 2. Values of the J- Integral, varying on the number of nodes and the distance between neighboring microcracks

Numerical results in terms of $\mathbf{u}$ and d are post-processed to compute the total (quadratic) internal energy e and the quasi-static J-integral J_{q-st}. The latter has been computed by adapting the procedure illustrated in [139].

When $\mathsf{d} = 0$, or $l_m \to \infty$, the multifield model falls naturally in a standard Cauchy continuum with cubic symmetry coinciding with the one of the lattice chosen to derive constitutive equations, as mentioned in Section 3.

Table 2 shows values of internal energy e and J-integral J_{q-st} for different values of l_m and for different numbers of nodes for a strip with dimension 100×300 mm. Once the material and the geometric parameters are fixed, for growing values of l_m, the multifield model furnishes numerical results closer and closer to those of the uncracked material.

The numerical solution in terms of $\mathbf{u}$ and d are shown in Figure 20 where strain localization effects around the crack tip are evidenced and are strictly due to the presence of the microcracks. They are indicators toward the crack growth: Their geometry suggests an increment of (standard and substructural) tractions in a manner that would push the crack to grow horizontally once some critical value of the traction at the tip is reached; this is also the suggestion of experiments and physical intuition.

It is worth noting that the simulation with $l_m = 15$ mm gives a microcracked body *softer* than that represented when $l_m = 75$ mm. This is due to the fact that a higher value of l_m implies a more dilute microcracks distribution.

Moreover, the numerical results obtained with an XFEM technique may be compared with of a standard FEM procedure, as shown in Table 3.

FEM			**XFEM**		
nodes	e	J_{q-st}	**nodes**	e	J_{q-st}
434	55.2814	2.06	**154**	57.2405	2.1521
699	57.4337	2.2518	**423**	58.8760	2.3850
932	58.0432	2.3342	**705**	59.8892	2.5964
1338	58.7763	2.3735	**1310**	61.0273	2.6136
3575	60,3773	2,5052	**2089**	61.3354	2.5997

Table 3. Comparison between FEM and XFEM in term of J integral and total energy

The difference between the XFEM and the standard FEM consists in the number of nodes (which influence the computational cost) used to develop the numerical simulations: The XFEM needs *a lesser number of nodes* with respect to the FEM to obtain the same numerical results. Moreover, when the evolution discontinuities is considered, in the XFEM the *remeshing* is unnecessary.

6 CONCLUDING REMARKS

With this section we conclude the paper but do not bring to an end the story. In fact, the computational aspects of the mechanics of complex bodies constitute fruitful and rather unexplored sources of challenging problems. The unitary point of view presented here about the structure of a wide class of models of condesed matter with exotic properties suggests in some sense a research program in the field. Many topics deserve to be investigasted and have been not touched here. We list below some of them that would deserve to be developed.

1. General alghoritms for non linear problems should be constructed in general (some of them are available in the special case of micromagnetics).

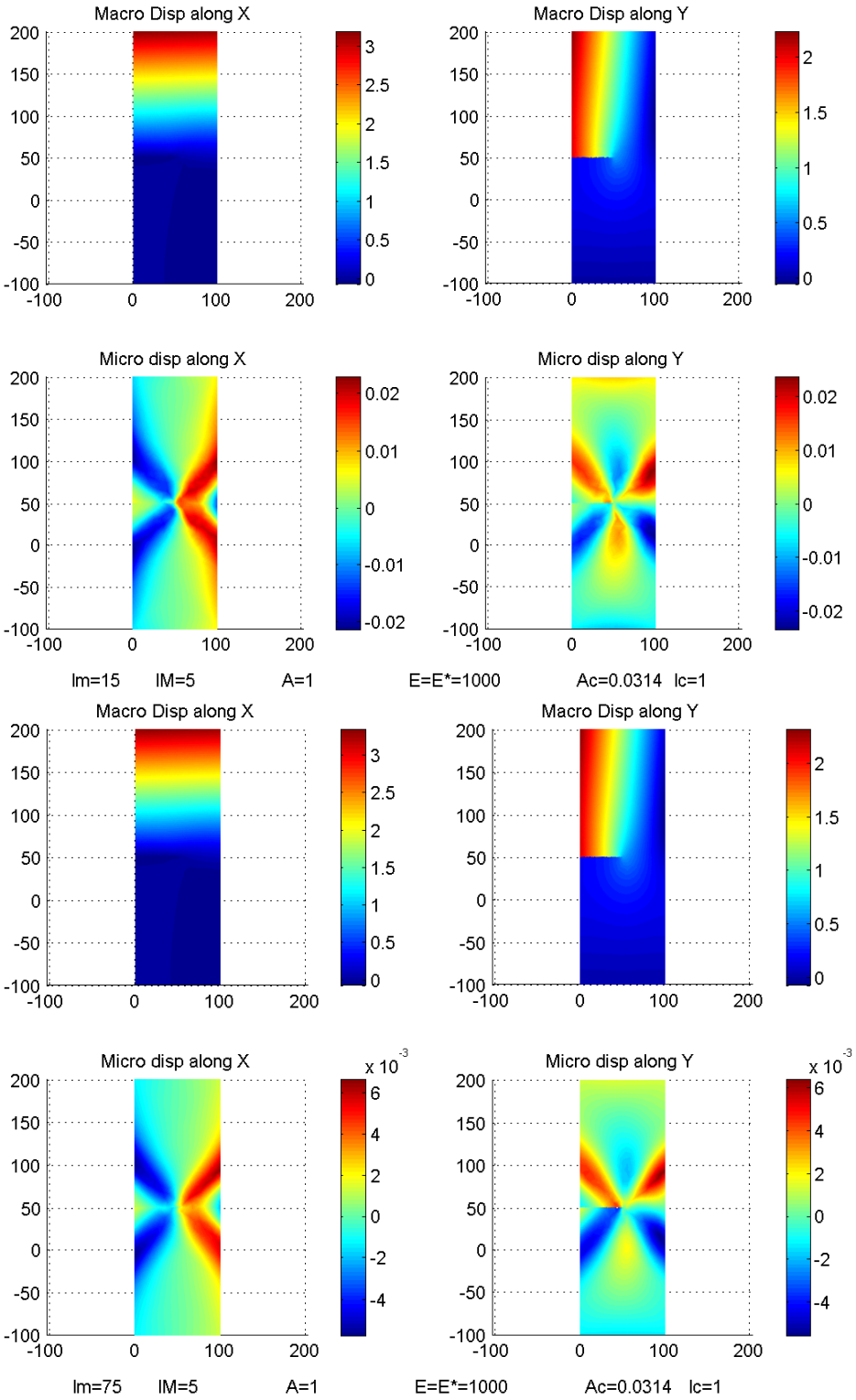

Figure 20. Strip of Figure 19 with dimension 100X300 mm for $l_m = 15$ mm (four top pictures) and $l_m = 75$ mm (four bottom pictures). The numerical solution is given in terms of macro displacement $\mathbf{u}$ and micro displacement d along the X axis (horizontal) and Y axis (vertical)

2. As regards dynamical problems involving even substructural inertia, at least in the elastic case, the program about variational integrators, developed by J. E. Marsden and co-workers (see e.g. [130], [106], [70]), would deserve to be extended to cover multifield theories. In developing the issue, once more the geometrical properties of $\mathcal{M}$ play a crucial role.

3. The analysis of the evolution of structured sharp discontinuity surfaces in complex bodies implies a (perhaps non-trivial) generalization of extended finite element method (XFEM). Such a kind of evolution is ruled by a (rather extended) generalization of the motion by curvature (see equation (271)).

4. The same generalization of XFEM would be useful to analyze cases of the influence of the material substructure on the growth of macroscopic cracks in situations more complicated than the one analyzed here.

5. All problems dealing with irreversible substructural changes deserve to be investigated. We mention, in passing, that some available formulations of strain gradient plasticity are based strictly on the multifield setting.

6. Finally, all items above imply the need of convergence results for the relevant numerical schemes.

ACKNOWLEDGEMENT

PMM acknowledges the support of the Italian National Group of Mathematical Physics (GNFM-INDAM). FLS expresses his gratitute to the Board of ECCOMAS for selecting him as recipient of the 2003 ECCOMAS prize for the best Ph.D. thesis in computational mechanics.

REFERENCES

1 Aero, E.L. and Kuvshinskii, E.V. (1960). Fundamental equations of the theory of elastic media with rotationally interacting particles. *Fizika Tverdogo Tela*, **2**, 1399–1409.

2 Antman, S.S. (1972). The theory of rods. in *Handbuch der Physic Via/2, C. Truesdell ed.*, Springer Verlag, Berlin, 641–703.

3 Antman, S.S. (1995). *Nonlinear problems of elasticity.* Springer Verlag, Berlin, 1995.

4 Augusti, G. and Mariano, P.M. (1999). Stochastic evolution of microcracks in continua, *Comp. Meth. Appl. Mech. Eng.*, **168**, 155–171.

5 Babuska, I. and Melenk, J.M. (1997). The partition of unity method. *Int. J. Num. Meth. Eng.*, **40**, 727–758.

6 Baňas, L. and Slodička, M., (2005). Space discretization for the Landau-Lifshitz-Gilbert equation. *Comp. Meth. Appl. Mech. Eng.*, **194**, 467–477.

7 Belytschko, T. and Black, T. (1999). Elastic crack growth in finite elements with minimal remeshing. *Int. J. Num. Meth. Eng.*, **45**, 601–620.

8 Bernardini, B. and Pence, T.J. (2004). A multifield theory for the modeling of the macroscopic behavior of shape memory materials. in *Advances in multifield theories for continua with substructure*, G. Capriz and P. M. Mariano (Eds.), Birkhäuser, Boston, 199–242.

9 Biscari, P. (2002). Curvature effects on the surface viscosity of nematic liquid crystals. *Eur. J. Mech. B Fluids*, **21**, 739–750.

10 Brezis, H. and Li, Y. (2001). Topology and Sobolev spaces. *J. Funct. Anal.*, **183**, 321–369.

11 Brown, W.F. Jr. (1963). *Micromagnetics*, Wiley.

12 Budiansky, B. and O'Connell, R.J. (1976). Elastic moduli of a cracked solid. *Int. J. Solids Structures*, **12**, 81–97.

13 Capriz, G. (1980). Bodies with microstructure. I. *Riv. Mat. Univ. Parma*, **5**, 673–691.

14 Capriz, G., (1984). Continua with microstructures. (in Italian) *Boll. Un. Mat. Ital. A*, **3**, 181–195.

15 Capriz, G. (1985). Continua with latent microstructure. *Arch. Rational Mech. Anal.*, **90**, 43–56.

16 Capriz, G. (1985a). Introductory remarks to the dynamics of continua with microstructure. in *Mathematical models and methods in mechanics*, 71–95, Banach Center Publ., **15**, PWN, Warsaw.

17 Capriz, G. (1989). *Continua with microstructure*, Springer Verlag, Berlin.

18 Capriz, G. (1994). Smectic liquid crystals as continua with latent microstructure. *Meccanica*, **30**, 621–627.

19 Capriz, G. (2003). Elementary preamble to a theory of granular gases. *Rend. Sem. Mat. Univ. Padova*, **110**, 179–198.

20 Capriz, G. and Biscari, P. (1994). Special solutions in a generalized theory of nematics. *Rend. Mat.*, **14**, 291–307.

21 Capriz, G. and Mariano, P.M. (2003). Symmetries and Hamiltonian formalism for complex materials. *J. Elasticity*, **72**, 57–70.

22 Capriz, G. and Mariano, P.M. (2004). Balance at a junction among coherent interfaces in materials with substructure. in *Advances in multifield theories for continua with substructure*, G. Capriz and P.M. Mariano (Eds.), Birkhäuser, Boston, 243–263.

23 Capriz, G. and Mazzini, G. (1998). Invariance and balance in continuum mechanics. in *Nonlinear analysis and continuum mechanics* (Ferrara, 1992), 27–35, Springer, New York.

24 Capriz, G. and Mullenger, G. (2004). Dynamics of granular fluids. *Rend. Sem. Mat. Univ. Padova,* **111**, 247–264.

25 Capriz, G. and Podio-Guidugli, P. (1976). Discrete and continuous bodies with affine structure. *Ann. Math. Pura Appl.*, **115**, 195–217.

26 Capriz, G. and Podio-Guidugli, P. (1977). Formal structure and classification of theories of oriented materials. *Ann. Math. Pura Appl.*, **111**, 17–39.

27 Capriz, G. and Podio-Guidugli, P. (1981). Materials with spherical structure. *Arch. Rational Mech. Anal.*, **75**, 269–279.

28 Capriz, G. and Podio-Guidugli, P. (1983). Structured continua from a Lagrangian point of view. *Ann. Mat. Pura Appl.*, **135**, 1–25.

29 Capriz, G., Podio-Guidugli, P. and Williams, W. (1982). On balance equations for materials with affine structure. *Meccanica*, **17**, 80–84.

30 Capriz, G. and Virga, E.G. (1990). Interactions in general continua with microstructure. *Arch. Rational Mech. Anal.*, **109**, 323–342.

31 Capriz, G. and Virga, E.G. (1994). On singular surfaces in the dynamics of continua with microstructure. *Quart. Appl. Math.*, **52**, 509–517.

32 Carstensen, C. and Praetorius, D. (2005). Effective simulation of a macroscopic model for stationary micromagnetics. *Comp. Meth. Appl. Mech. Eng.*, **194**, 531–548.

33 Chessa, J. and Belytschko, T. (2003). On construction of blending elements for locally enriched methods. *Int. J. Num. Meth. Eng.*, **57**, 1015–1038.

34 Chirita, S. and Aron, M. (1999). Aspects of Saint-Venant's principle in the dynamical theory of linear micropolar elasticity. *Math. Mech. Solids*, **4**, 17–34.

35 Choksi, R., Kohn, R.V. and Otto, F. (2004). Energy minimization and flux domain structure in the intermediate state of a type-I superconductor. *J. Nonlinear Sci.*, **14**, 119–171.

36 Ciarlet, P. (1988). *Mathematical elasticity. Vol. I. Three-dimensional elasticity*, North-Holland Publishing Co., Amsterdam.

37 Ciarlet, P.G. (1991). *Basic error estimates for elliptic problems. Handbook of numerical analysis, Vol. II.* 17–351, North-Holland, Amsterdam.

38 Coleman, B.D. and Gurtin, M.E. (1967). Thermodynamics with internal state variables. *J. Chem. Phys.*, **47**, 597–613.

39 Coleman, B.D. and Noll, W. (1963). The thermodynamics of elastic materials with heat conduction and viscosity. *Arch. Rational Mech. Anal.*, **13**, 245–261.

40 Coleman, B.D. and Owen, D.R. (1974). A mathematical foundation for thermodynamics. *Arch. Rational Mech. Anal.*, **54**, 1–104.

41 Colli, P., Frémond, M. and Visintin, A. (1990). Thermo-mechanical evolution of shape memory alloys. *Quart. Appl. Math.*, **48**, 31–47.

42 Cosserat E. and Cosserat F. (1909). *Sur la theorie des corps deformables.* Dunod, Paris.

43 Cowin, S.C. (1985). The viscoelastic behavior of linear elastic materials with voids. *J. Elasticity*, **15**, 185–191.

44 Cowin, S.C. and Nunziato, J.W. (1983). Linear elastic materials with voids. *J. Elasticity*, **13**, 125–147.

45 Davì, F. (2001). On domain switching in deformable ferroelectrics, seen as continua with microstructure. *Z. Angew. Math. Phys.*, **52**, 966–989.

46 Davì, F. and Mariano, P.M. (2001). Evolution of domain walls in ferroelectric solids. *J. Mech. Phys. Solids*, **49**, 1701–1726.

47 Davì, F. and Rizzoni, R. (2004). On twinning and domain switching in ferroelectric Pb(Zr1-x Tix)O3. I. Twins and domain walls. *J. Mech. Phys. Solids,* **52**, 113–144.

48 De Angelis, E., Casciola, C.M., Mariano, P.M. and Piva, R. (2004). Microstructure and turbulence in dilute polymer solutions. in *Advances in multifield theories for continua with substructure*, G. Capriz and P. M. Mariano (Eds.), Birkhäuser, Boston, 127–148.

49 de Fabriitis, C. and Mariano, P.M. (2005). Geometry of interactions in complex bodies. *J. Geom. Phys.*, **54**, 301–323.

50 De Gennes, P.-G. and Prost, J. (1993). *The physics of liquid crystals*, Oxford University Press, Oxford.

51 De Simone, A., Kohn, R.V., Müller, S. and Otto, F. (2002). A reduced theory for thin-film micromagnetics. *Comm. Pure Appl. Math.*, **55**, 1408–1460.

52 Del Piero, G. (2003). A class of fit regions and a universe of shapes for continuum mechanics. *J. Elasticity*, **70**, 175–195.

53 Del Piero, G. and Owen, R.D. (2000). *Structured deformations*. Quaderni dell'Istituto di Alta Matematica, Florence.

54 Dietsche, A., Steinmann, P. and Willam, K. (1993). Micropolar elasto-plasticity and its role in localization analysis. *Int. J. Plasticity*, **9**, 813–831.

55 Dolbow J., Moës N. and Belytschko T. (2001). An extended finite element method for modeling crack growth with frictional contact. *Comp. Meth. Appl. Mech. Eng.*, **190**, 6825–6846.

56 Doyle, T.C. and Ericksen, J.L. (1956). Nonlinear elasticity. *Adv. Appl. Mech.*, **4**, 53–115.

57 Dunn, J.E. and Serrin, J. (1985). On the thermomechanics of interstitial working. *Arch. Rational Mech. Anal.*, **88**, 95–133.

58 E, W. (1997). Nonlinear continuum theory of smectic-A liquid crystals. *Arch. Rational Mech. Anal.*, **137**, 159–175.

59 Epstein, M. and de Leon, M. (1998). Geometrical theory of uniform Cosserat media. *J. Geom. Phys.*, **26**, 127–170.

60 Ericksen, J.L. (1960). Theory of anisotropic fluids. *Trans. Soc. Rheol.*, **4**, 29–39.

61 Ericksen, J.L. (1961). Conservation laws for liquid crystals. *Trans. Soc. Rheol.*, **5**, 23–34.

62 Ericksen, J.L. (1962a). Kinematics of macromolecules. *Arch. Rational Mech. Anal.*, **9**, 1–8.

63 Ericksen, J.L. (1962b). Hydrostatic theory of liquid crystals. *Arch. Rational Mech. Anal.*, **9**, 371–378.

64 Eriksen, J.L. (1977). Special topics in elastostacis. *Adv. Appl. Mech.*, **17**, 189–244.

65 Ericksen, J.L. (1991). Liquid crystals with variable degree of orientation. *Arch. Rational Mech. Anal.*, **113**, 97–120.

66 Ericksen, J.L. and Truesdell, C.A. (1958). Exact theory of stress and strain in rods and shells. *Arch. Rational Mech. Anal.*, **1**, 295–323.

67 Eringen, C.A. (1973). On nonlocal microfluid mechanics. *Int. J. Eng. Sci.*, **11**, 291–306.

68 Eringen, A.C. (Ed.) (1975). *Continuum physics. Vol II. Continuum mechanics of single-substance bodies*. Academic Press, New York-London.

69 Eringen, A.C. (1999). *Microcontinuum field theories. I. Foundations and solids*. Springer-Verlag, New York.

70 Fetecau, R.C., Marsden, J.E., Ortiz, M. and West, M. (2003). Nonsmooth Lagrangian mechanics and variational collision integrators. *SIAM J. Dyn. Syst.*, **2**, 381–416.

71 Fleming, M., Chu, Y.A., Moran, B. and Belytschko, T. (1997). Enriched element-free galerkin methods for crack tip fields. *Int. J. Num. Meth. Eng.*, **40**, 1483–1504.

72 Fox, D.D. and Simo, J.C. (1992). A nonlinear geometrically exact shell model incorporating independent (drill) rotations. *Comp. Meth. Appl. Mech. Eng.*, **98**, 329–343.

73 Frémond, M. (1987). Matériaux à mémoire de forme. *C. R. Acad. Sci. Paris*, **304**, 239–244.

74 Frémond, M. (2000). *Non-smooth thermomechanics*. Springer-Verlag, Berlin.

75 Frémond, M. and Nedjar, B. (1996). Damage, gradient of damage and principle of virtual power.*Int. J. Solids Structures*, **33**, 1083–1103.

76 Fulton, C.C. and Gao, H. (2001). Microstructural modeling of ferroelectric fracture. *Acta Materialia*, **49**, 2039–2054.

77 García-Cervera, C.J., Gimbutas, Z. and E, W. (2003). Accurate numerical methods for micromagnetics simulations with general geometries, *J. Comput. Phys.*, **184**, 37—52.

78 Germain, P. (1973). The method of virtual power in continuum mechanics, Part 2: microstructure. *SIAM J. Appl. Math.*, **25**, 556–575.

79 Goodman, M.A. and Cowin, S.C. (1972). A continuum theory of granular materials. *Arch. Rational Mech. Anal.,* **44**, 249–266.

80 Gordon, A. (1986). Interface motions in ferroelectrics. *Physica B*, **138**, 239-243.

81 Gordon, A. (1991). Propagation of solitary stress waves at first-order ferroelectric phase transitions. *Phys. Lett. A,* **154**, 79–80.

82 Gordon, A. (2001). Finite-size effects in dynamics of paraelectric-ferroelectric interfaces induced by latent heat transfer. *Phys. Lett. A*, **281**, 357–362.

83 Gravouil, A., Moës, N. and Belytschko, T. (2002). Non-planar 3D crack growth by the extended finite element and level sets Part II: Level set update. *Int. J. Num. Meth. Eng.*, **53**, 2569–2586.

84 Green, A.E. and Laws, N. (1966). A general theory of rods. *Proc. Roy. Soc. Lond. A*, **293**, 145–155.

85 Green, A.E. and Naghdi, P.M. (1995). A unified procedure for construction of theories of deformable media. II. Generalized Continua. *Proc. Royal Soc. London A*, **448**, 357–377.

86 Green, A.E., Naghdi, P.M. and Wainwright, W.L. (1965). A general theory of a Cosserat surface. *Arch. Rational Mech. Anal.*, **20**, 287–308.

87 Grioli, G. (1960). Elasticità asimmetrica. *Ann. Mat. Pura Appl.*, **50**, 389–417.

88 Grioli, G. (2003). Microstructures as a refinement of Cauchy theory. Problems of physical concreteness. *Cont. Mech. Thermodyn.*, **15**, 441–450.

89 Gurtin, M.E. (1965). Thermodynamics and the possibility of spatial interactions in elastic materials. *Arch. Rational Mech. Anal.*, **19**, 339–352.

90 Gurtin, M.E. (1995). The nature of configurational forces. *Arch. Rational Mech. Anal.*, **131**, 67–100.

91 Gurtin, M.E. (1996). Generalized Ginzburg-Landau and Cahn-Hilliard equations based on a microforce balance. *Physica D*, **92**, 178–192.

92 Gurtin, M.E. (1997). Dynamical theories of electromagnetism and superconductivity based on gauge invariance and energy. *Arch. Rational Mech. Anal.*, **137**, 49–97.

93 Gurtin, M.E. and Struthers, A. (1990). Multiphase thermomechanics with interfacial structure. III. Evolving phase boundaries in the presence of bulk deformation. *Arch. Rational Mech. Anal.*, **112**, 97–160.

94 Hall, E.O. (1951). The deformation and aging of mild steel. *Proc. Phys. Soc. B*, **64**, 747–753.

95 Hashin, Z. (1988). The differential scheme and its applications to cracked materials. *J. Mech. Phys. Solids,* **36**, 719–734.

96 Huang, Y., Hu, K.X. and Chandra, A. (1994). A generalized self-consistent mechanics method for microcracked solids. *J. Mech. Phys. Solids*, **42**, 1273–1291.

97 Holm, D.D. (2002). Euler-Poincaré dynamics of perfect complex fluids. in *Geometry, Mechanics and Dynamics*, 113-167, Springer, New York.

98 Hu, C., Wang, R. and Ding, D.-H. (2000). Symmetry groups, physical property tensors, elasticity and dislocations in quasicrystals. *Rep. Prog. Phys.*, **63**, 1–39.

99 Iesan, D. (1987). Saint-Venant's problem. *Lecture Notes in Mathematics*, Springer-Verlag, Berlin.

100 Iesan, D. (2002). On the theory of heat conduction in micromorphic continua. *Internat. J. Engrg. Sci.*, **40**, 1859–1878.

101 James, R.D. and Rizzoni, R. (2000). Pressurized shape memory thin films. *J. Elasticity,* **59**, 399–436.

102 Krajcinovic, D. (1996). *Damage mechanics*, North-Holland, Amsterdam.

103 Krajcinovic, D. and van Mier, J. (Eds.) (2000). *Damage and fracture in disordered materials*. Springer, Wien.

104 Landau, L.D. and Lifshitz, E.M. (1968). *Course of theoretical physics. Vol. 5: Statistical physics*. Pergamon Press, Oxford-Edinburgh-New York.

105 Leslie, F.M. (1968). Some constitutive equations for liquid crystals. *Arch. Rational Mech. Anal.*, **28**, 265–28.

106 Lew, A., Marsden, J.E., Ortiz, M. and West, M. (2003). Asynchronous variational integrators. *Arch. Rational Mech. Anal.*, **167**, 85–146.

107 Likos, C.N. (2001). Effective interactions in soft condensed matter physics. *Phys. Rep.*, **348**, 267–439.

108 Mariano, P.M. (1995). Fracture in structured continua. *Int. J. Damage Mech.*, **4**, 283–289.

109 Mariano, P.M. (1999). Some remarks on the variational decription of microcracked bodies. *Int. J. Non-Linear Mech.*, **34**, 633–642.

110 Mariano, P.M. (2000). Configurational forces in continua with microstructure. *Z. angew. Math. Phys. ZAMP*, **51**, 752–791.

111 Mariano, P.M. (2000). Premises to a multifield approach to stochastic damage evolution. In *Damage and Fracture in Disordered Materials*, D. Krajcinovic and J. van Mier (Eds.), Springer-Verlag, Berlin, 217–263.

112 Mariano, P.M. (2001). Coherent interfaces with junctions in continua with microstructure. *Int. J. Solids Structures*, **38**, 1243–1267.

113 Mariano, P.M. (2001). Multifield theories in mechanics of solids. *Adv. Appl. Mech.*, **38**, 1–93.

114 Mariano, P.M. (2002). A note on Ceradini-Capurso-Maier's theorem in plasticity. *Int. J. Plasticity*, **18**, 1749–1773.

115 Mariano, P.M. (2003). Cancellation of vorticity in steady-state non-isentropic flows of complex fluids. *J. Phys. A: Math. Gen.*, **36**, 9961–9972.

116 Mariano, P.M. (2005). Influence of material substructure on crack propagation: a unified treatment. *Proc. Royal Soc. London A*, **461**, 371–395.

117 Mariano, P.M. (2005). Migration of substructures in complex fluids. *L. Phys. A*, **38**, 6823–6839.

118 Mariano, P.M. (2005). Mechanics of quasiperiodic alloys. *J. Nonlinear Sci.*, in print.

119 Mariano, P.M. (2005). *Elements of multifield theories of complex bodies*. Birkhauser, Boston, (in preparation).

120 Mariano, P.M. and Augusti, G. (1998). Multifield description of microcracked continua. A local model. *Math. Mech. Solids*, **3**, 237–254.

121 Mariano, P.M. and Bernardini, D. (1998). Flow rules for porous elastic-plastic materials. *Mech. Res. Comm.*, **25**, 443–448.

122 Mariano, P.M., Casciola, C.M. and De Angelis, E. (2004). Substructural interactions and transport in polymer flows. *Int. J. Non-Linear Mech.*, **39**, 457–465.

123 Mariano, P.M., Gioffrè, M., Stazi, F.L. and Augusti, G. (2004). Elastic microcracked bodies with random properties. *Prob. Eng. Mech.*, **19**, 127–143.

124 Mariano, P.M. and Stazi, F.L. (2001). Strain localization in elastic microcracked bodies. *Comp. Meth. Appl. Mech. Eng.*, **190**, 5657–5677.

125 Mariano, P.M. and Stazi, F.L. (2004). Strain localization due to crack-microcrack interactions: X-FEM for a multifield approach. *Comp. Meth. Appl. Mech. Eng.*, **193**, 5035–5062.

126 Mariano, P.M., Stazi, F.L. and Augusti, G. (2004). Phason effects around a crack in Al-Pb-Mn quasicrystals: stochastic aspects of the phonon-phason coupling. *Comp. Stru.*, **82**, 971–983.

127 Mariano, P.M. and Trovalusci, P. (1999). Constitutive relations for elastic microcracked bodies: from a lattice model to a multifield continuum description, *Int. J. of Damage Mech.,* **8**, 153–173.

128 Markov, K.Z. (1995). On a microstructural model of damage in solids, *Int. J. Engng Sci.*, **33**, 139–150.

129 Marsden, J.E. and Hughes, T.J.R. (1994). *Mathematical foundations of elasticity*, Prentice Hall, Dover edition.

130 Marsden, J.E. and West, M. (2001). Discrete mechanics and variational integrators, *Acta Numerica*, **10**, 357–514.

131 McLean, D. (1967). Dislocation contribution to the flow stress of polycristalline iron, *Can. J. Phys.*, **45**, 973–982.

132 Mermin, N.D. (1979). The topological theory of defects in ordered media, *Rev. Mod. Physics*, **51**, 591–648.

133 Michel, L. (1980). Symmetry defects and brocken symmetry configuration hidden symmetry, *Rev. Mod. Phys.*, **52**, 617–651.

134 Mielke, A. (2002). Analysis of energetic models for rate-independent materials, *Proc. Int. Congress Mathematicians*, *Vol III*, Higher Ed. Press, Beijing, 817–828.

135 Mielke, A. (2004). Deriving new evolution equations for microstructures via relaxation of variational incremental problems, *Comp. Meth. Appl. Mech. Eng.*, **193**, 5095–5127.

136 Mielke, A., Theil, F. and Levitas, V.I. (2002). A variational formulation of rate-independent phase transformations using an extremum principle, *Arch. Rational Mech. Anal.*, **162**, 137–177.

137 Mindlin, R.D. (1964). Micro-structure in linear elasticity, *Arch. Rational Mech. Anal.*, **16**, 51–78.

138 Moës, N., Gravouil, A. and Belytschko, T. (2001). Non-planar 3D crack growth by the extended finite element and level sets Part I: Mechanical model, *Int. J. Num. Meth. Eng.*, **53**, 2549–2568.

139 Moran, B. and Shih, C.F. (1987). A general treatment of crack tip contour integrals, *Int. J. Fracture*, **35**, 295–310.

140 Mori, T. and Tanaka, K. (1973). Average stress in matrix and average elastic energy of materials with misfitting inclusions, *Acta Metall.*, **21**, 571–574.

141 Mosconi, M. (2002). Mixed variational formulations for continua with microstructure, *Int. J. Solids Structures*, **39**, 4181–4195.

142 Musesti, A. (2004). The balance equations of continuum mechanics in geometric measure theory, (in Italian) *Boll. Unione Mat. Ital. Sez. B*, **7**, 305–317.

143 Nash, J.F. (1954). C^1 isometric imbeddings, *Ann. Math.*, **60**, 383–396.

144 Nash, J.F. (1956). The imbedding problem for Riemannian manifold, *Ann. Math.*, **63**, 20-63.

145 Nix, W.D. (1988). Mechanical properties of thin films, *Metall. Trans. A*, **20**, 2217–2245.

146 Noll, W. (1973). Lectures on the foundations of continuum mechanics and thermodynamics, *Arch. Rational Mech. Anal.*, **52**, 62–69.

147 Nowaki, W. (1986). *Theory of asymmetric elasticity*, Pergamon Press, New York.

148 Nunziato, J.W. and Cowin, S.C. (1979). A nonlinear theory of elastic materials with voids, *Arch. Rational Mech. Anal.*, **72**, 175–201.

149 Nunziato, J.W. and Walsh, E.K. (1978). On the influence of void compaction and material non-uniformity on the propagation of one-dimensional acceleration waves in granular materials, *Arch. Rational Mech. Anal.*, **64**, 299–316.

150 Pedregal, P. (1993). Laminates and microstructure, *European J. Appl. Math.,* **4**, 121–149.

151 Penrose, O. and Fife, P.C. (1990). Thermodynamically consistent models of phase field type for the kinetics of phase transitions, *Physica D***, 43**, 44–62.

152 Petch, N.J. (1953). The cleavage strength of polycrystals, *J. Iron Steel Inst. London*, **174**, 25–28.

153 Povstenko, Y.Z. (1994). Stress functions for continua with couple stresses, *J. Elasticity*, **36**, 99–116.

154 Qin, Q.-H., Mai, Y.-W. and Yu, S.-W. (1998). Effective moduli for thermopiezoelectric materials with microcracks, *Int. J. Fracture*, **91**, 359–371.

155 Rubin, M.B. and Benveniste, Y. (2000). A Cosserat shell model for interphases in elastic media, *J. Mech. Phys. Solids*, **52**, 1023–1052.

156 Segev, R. (1994). A geometrical framework for the static of materials with microstructure, *Math. Mod. Meth. Appl. Sci.,* **4**, 871–897.

157 Segev, R. (2004). Fluxes and flux-conjugated stresses, in *Advances in Multifield Theories of Continua with Substructure*, G. Capriz and P. M. Mariano (Ed.), Birkhäuser, Boston, 149–163.

158 Shu, Y.C. and Bhattacharya, K. (2001). Domain patterns and macroscopic behavior of ferroelectric materials, *Phil Mag. B*, **81**, 2021–2054.

159 Shu, J.Y. and Fleck, N.A. (1999). Strain gradient crystal plasticity: size dependent deformation of bicrystals, *J. Mech. Phys. Solids*, **47**, 297–324.

160 Šilhavý, M. (1978). A condition equivalent to the existence of non-equilibrium entropy and temperature for materials with internal variables. *Arch. Rational Mech. Anal.*, **68**, 299–332.

161 Šilhavý, M. (1985). Phase transitions in non-simple bodies, *Arch. Rational Mech. Anal.*, **88**, 135–161.

162 Šilhavý, M. (1991). Cauchy's stress theorem and tensor fields with divergences in L^p, *Arch. Rational Mech. Anal.,* **116**, 223–255.

163 Šilhavý, M. (1997). *The mechanics and thermodynamics of continuous media*, Springer Verlag, Berlin, 1997.

164 Simo, J.C. and Fox, D.D. (1989). On a stress resultant geometrically exact shell model. Part I: Formulation and optimal parametrization, *Comp. Meth. Appl. Mech. Eng.*, **72**, 267–304.

165 Simo, J.C., Fox, D.D. and Hughes, T.J.R. (1992). Formulations of finite elasticity with independent rotations, *Comp. Meth. Appl. Mech. Eng.*, **95**, 277–288.

166 Simo, J.C., Fox, D.D. and Rifai, M.S. (1989). On a stress resultant geometrically exact shell model II. The linear theory: computational aspects, *Comp. Meth. Appl. Mech. Eng.*, **73**, 53–92.

167 Simo, J.C., Fox, D.D. and Rifai, M.S. (1990). On a stress resultant geometrically exact shell model III. Computational aspect of the nonlinear theory, *Comp. Meth. Appl. Mech. Eng.*, **79**, 21–70.

168 Simo, J.C., Marsden, J.E. and Krishnaprasad, P.S. (1988). The Hamiltonian structure of nonlinear elasticity: the material and convective representations of solids, rods and plates, *Arch. Rational Mech. Anal.*, **104**, 125–183.

169 Stackgold, I. (1950). The Cauchy relations in a molecular theory of elasticity, *Quart. Appl. Math.*, **8**, 169–186.

170 Stazi, F.L. (2003). Finite element methods for cracked and microcracked bodies, *Ph.D. Thesis,* Universitá di Roma "La Sapienza", Roma (Italy) (avalaible at http://www.cimne.com/eccomas/html/awd1.htm).

171 Stazi, F.L., (2004). Consequences of inavariance under changes of observers in a multifield model of microcracked bodies, *Meccanica*, **39**, 389–393.

172 Stazi, F.L., (2004). Finite element methods for cracked and microcracked bodies, *Proceedings of the European Congress on Computational Methods in Applied Sciences and Engineering (ECCOMAS 2004)*, Jyväskylä, 24–28 July.

173 Stazi, F.L., Budyn, E., Chessa, J. and Belytschko, T. (2002). *A*n Extended Finite Elment Method with Higher-Order Element for Crack Problems with Curvature, *Computational Mechanics*, **31**, 38–48.

174 Steinmann, P. (1994). A micropolar theory of finite deformation and finite rotation multiplicative elastoplasticity, *Int. J. Solids Str.*, **31**, 1063–1084.

175 Stewart, J.R. and Hughes, T.J.R. (1998). A tutorial in elementary finite element error analysis: a systematic presentation of a priori and a posteriori error estimates, *Comp. Meth. Appl. Mech. Eng.*, **158** (1998), 1–22.

176 Stolarska, M., Chopp, D.L., Moës, N. and Belytschko, T. (2001). Modelling crack growth by level sets and the extended finite element method, *Int. J. Num. Meth. Eng.*, **51**, 943-960.

177 Sukumar, N., Moës, N., Moran, B. and Belytschko, T. (2000). Extended finite element method for three-dimensional crack modeling, *Int. J. Num. Meth. Eng.,* **48** (11), 1549–1570.

178 Tiersten, H.F. (1964). Coupled magnetomechanical equations for magnetically saturated insulators, *J. Math. Phys.*, **5**, 1298–1318.

179 Truesdell, C.A. and Noll, W. (2004). *The non-linear field theories of mechanics.* Third edition. Springer-Verlag, Berlin.

180 Truesdell, C.A. and Toupin, R.A. (1960). Classical field theories of mechanics, in *Handbuch der Physics*, Springer Verlag, Berlin.

181 Voigt, W. (1887). Studien über die Elasticitätsverhältuisse der Krystalle, *Abh. Ges. Wiss. Göttingen*, **34**.

182 Voigt, W. (1894). Über Medien ohne innere Kräfte und ein durch gelieferte mechanische Dentung der Maxwell-Hertzschen Gleichungen, *Gött. Abh.*, 72–79.

183 Wang, X.-P., García-Cervera, C.J. and E, W. (2001). A Gauss-Seidel projection method for micromagnetics simulations, *J. Comput. Phy.*, **171**, 357–372.

184 Wei, Y. and Hutchinson, J.W. (1997). Steady-state crack growth and work of fracture for solids characterized by strain gradient plasticity, *J. Mech. Phys. Solids*, **45**, 1253–1273.

185 Whitney, H. (1936). Differentiable manifolds, *Ann. Math.*, **37**, 645–680.

186 Zhang, W. and Bhattacharya, K. (2005). A computational model of ferroelectric domains. Part I: model formulation and domain switching, *Acta Materalia*, **53**, 185–198.

187 Zhang, W. and Bhattacharya, K. (2005). A computational model of ferroelectric domains. Part I: model formulation and domain switching, *Acta Materalia*, **53**, 199–209.

188 Zi, G. and Belytschko, T. (2003). New crack-tip elements for XFEM and applications to cohesive cracks, *Int. J. Num. Meth. Eng.*, **57**, 2221–2240.

Please address your comments or questions on this paper to:
International Center for Numerical Methods in Engineering
Edificio C-1, Campus Norte UPC
Grand Capitán s/n
08034 Barcelona, Spain
Phone: 34-93-4016035; Fax: 34-93-4016517
E-mail: onate@cimne.upc.edu